Modern Corrugated Horn Antennas

Memoria de la tesis Doctoral realizada por:

Jorge Teniente Vallinas

Y dirigida por:

Dr. Carlos del Río Bocio

Para optar al grado de:

Doctor Ingeniero en Telecomunicación

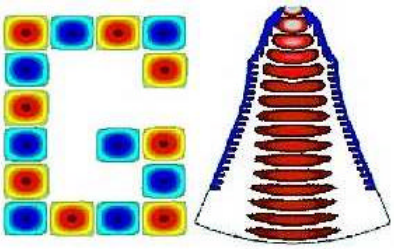

Grupo de Antenas

Departamento de Ingeniería Eléctrica y Electrónica

Universidad Pública de Navarra

Pamplona, Julio de 2003

A Marian, por haberme alegrado
la vida y haberme aguantado
en los momentos difíciles

V Premios Rosina Ribalta
Convocatoria 2002 – 2003

A los mejores proyectos de tesis doctoral en el ámbito de las Tecnologías de la Información y de las Comunicaciones

Este trabajo ha sido galardonado con el **segundo premio** de la **V edición** de los premios **Rosina Ribalta** de la **Fundación EPSON IBÉRICA** al segundo mejor proyecto de tesis doctoral en el ámbito de las Tecnologías de la Información y de las Comunicaciones. Año 2002-2003

This work won the **second prize** of the **V edition** of the **Rosina Ribalta award** given by the **EPSON IBÉRICA Foundation** to the second best Ph. D thesis project about Information an Communications Technology. Year 2002-2003

Agradecimientos

Por fin ha llegado la hora de escribir estas ansiadas líneas que a continuación se suceden. Escribir los agradecimientos es probablemente una de las partes más difíciles en la realización de una tesis doctoral, por un lado porque son normalmente muy personales y por otro lado porque además siempre se sabe que serán las líneas primeramente leídas cuando entregue esta tesis doctoral a mis compañeros y gente allegada porque en el fondo todos somos un poco chismosos.

Para mi encontrarme escribiendo los agradecimientos supone poner prácticamente fin a una etapa que me ha venido preocupando durante los últimos meses ya que son las últimas líneas que escribo de esta tesis antes de depositarla en el registro, ello me llena de alegría ya que ahora volveré a tener tiempo para estar con mi novia e ir a pescar a mosca, ya que las tengo un poco olvidadas a las dos.

Durante estos seis años de realización de la tesis en primer lugar quiero agradecer y muy especialmente a mi director de tesis, el Dr. Carlos del Río con el que he compartido principalmente los devenires de la tesis, con quien he acudido a multitud de congresos y quien siempre ha dado la cara por mí y ha procurado defender mis intereses. Además no me puedo olvidar de mencionar también especialmente al Dr. Ramón Gonzalo, el cual fue mi director de proyecto fin de carrera en el año 1997 y que ahora durante la tesis se ha convertido además de un asesor, en un compañero que sabe ponerme las pilas cuando es necesario.

Durante estos seis años he realizado dos estancias en el extranjero, la primera en Holanda que resulto ser inolvidable por la cantidad de gente estupenda que conocí y por que a pesar de que no podía practicar mi afición favorita (la pesca a mosca) me dio lástima a volver. En ese transcurso de

tiempo no me puedo olvidar especialmente de mi tutor allí, el Dr. Javier Martí el cual me enseñó muchas cosas sobre la medida de antenas y me dejo libertad a la hora de controlar el CATR del que el era responsable. También guardo un especial recuerdo del Dr. Peter de Maagt y su nutrido grupo internacional con el que me reunía todos los días a la hora de comer y en donde aprendí a soltarme hablando inglés de una vez por todas, gracias Peter. En cuanto a mis compañeros de fiestas y juergas en Holanda, merecen mención especial; Eduardo, David Lemus, Santiago Vázquez, Ramón Torres, Iñigo Sarriés, Daniel, Iñigo Ederra, Elvira, Pablo, Santiago Soley y otros muchos mas de los que ya ni me acuerdo de su nombre, perdonad mi omisión los no mencionados si algún día leéis esto y no os sentís identificados.

A mi vuelta a España retomando de nuevo la tesis doctoral en antenas corrugadas después de mi periplo holandés en el campo de la medida de antenas merece la pena recordar especialmente a Gemma y Cristina con quienes tan buenos ratos de asueto pase y para las cuales siempre había una sonrisa en la boca que compartir con los demás; sin olvidar claro está al resto de compañeros del laboratorio, los que pasaron y los que ahora están.

Además merecen mención muy especial por llevarlos muy dentro, la gente de la Asociación Navarra de Pescadores a Mosca y del comité local de AEMS-Ríos con vida de Navarra por ayudarme a reencontrarme con mi afición favorita y compartir con ellos tantas y tantas jornadas de pesca, de tertulias sobre pesca y de conservación ríos y gestión de pesca.

También quiero de recordar aquí como no a mis amigos de Lodosa que tan fenomenalmente me acogieron de vuelta a mi querida tierra. Y con quienes he compartido una fuerte amistad arraigada desde la infancia y como no a mi familia que siempre me ha apoyado a seguir adelante con los estudios.

En mi recta final de la tesis doctoral recuerdo especialmente a mi hermana Leyre con la que he compartido casi dos años de casa hasta que recientemente se ha casado con su novio de toda la vida Oscar. Enhorabuena tata.

No se me debe olvidar una mención especial a mi compañero de despacho de siempre, Iñigo Ederra que fue además compañero en mis estancias en Holanda e Inglaterra, el cual nunca se ha quejado de mis tonterías y que sabe aguantarme estoicamente.

En el verano del 2002 realicé una nueva estancia en el extranjero concretamente en Inglaterra seleccionado para trabajar en el proyecto StarTiger y merece la pena que mencione en primer lugar al jefe del proyecto, el Dr. Chris Mann que siempre sabe transmitir entusiasmo a pesar de que las cosas ya pinten muy negras y es capaz de hacer trabajar a todo el grupo hasta altas horas de la madrugada siempre que aún quede un mínimo resquicio de éxito, va por ti Chris. También debo mencionar al resto de mis compañeros de proyecto y especialmente a James, Frank, Dario e Iñigo otra vez más.

He de agradecer con estas líneas también a Noelia el haberme prestado un diseño suyo de una antena choke-gaussiana para ilustrar esta tesis y por haber continuado la investigación de antenas corrugadas de perfil gaussiano donde yo la deje aparcada para disponer de tiempo para la escritura.

Terminando ya, quiero agradecer especialmente a la Fundación Epson-Ibérica por haberme otorgado por este proyecto el segundo premio de la V edición de premios Rosina Ribalta a los mejores proyectos de tesis doctoral en el ámbito de las tecnologías de la información y de las comunicaciones, llego para mí como agua de Mayo en Junio.

Y por ultimo no me podía olvidar como no de la persona más especial, la cual conocí a primeros de Mayo de 2002 y que actualmente es mi novia;

este agradecimiento especial va para Marian, la chiquita que me alegró la vida, que supo aguantar firme mis cuatro meses de separación cuando apenas habíamos empezado a conocernos y que ha sabido aguantar mis cambios de carácter cuando las premuras de tiempo obligaban a trabajar demasiado en pos de terminar este manuscrito. Así pues que estas líneas le demuestren lo que yo la quiero.

Resumen

La presente tesis doctoral ha tenido como propósito sentar las bases de diseño de las antenas corrugadas de última generación que se vienen desarrollando desde 1995 en el seno del Grupo de Antenas de la Universidad Pública de Navarra.

Este tipo de antenas, ahora mundialmente conocidas como antenas corrugadas Gaussianas o más recientemente con el término “corrugated GPHA’s” donde el término GPHA hace referencia a las siglas en inglés “Gaussian Profiled Horn Antennas” que significa Antenas de Bocina de Perfil Gaussiano; son en la actualidad la mejor solución posible para conseguir patrones de radiación de muy altas prestaciones.

Concretamente, las antenas corrugadas de perfil gaussiano superan al resto de antenas de bocina corrugadas en dos aspectos:

- Es posible diseñar antenas con lóbulos laterales muchísimo más bajos que con cualquier otro tipo de perfil corrugado.
- Son, en general, más cortas que el resto de antenas corrugadas debido a que sus prestaciones son mejores.

Por todo ello, actualmente son la opción elegida por multitud de grupos de investigación a nivel mundial para realizar las antenas de bocina corrugadas que requieren sus proyectos.

Antenas de este tipo ya han sido embarcadas en satélites como Hispasat 1C e Hispasat 1D, van a ser utilizadas para el instrumento aerotransportado de la ESA llamado Marschals, serán utilizadas en el futuro satélite Planck de la ESA y actualmente una nueva versión muy prometedora esta siendo comercializada por la empresa inglesa Flann Microwave, Ltd.

Abstract

This Ph. D. manuscript has the main purpose of summarizing the design techniques of the new technology corrugated horn antennas developed since 1995 in the Antenna Group of the Public University of Navarra.

This type of world-wide accepted antennas, known as corrugated Gaussian Profiled Horn Antennas, (GPHA's); are now-a-days the best possible solution to obtain radiation patterns of very high restrictive requirements.

Corrugated GPHA's are better than the rest of corrugated horn antennas in two particular aspects:

- They present much lower sidelobes than any other corrugated profile
- They are usually shorter than the rest of corrugated profiles because their performance qualities are superior.

Therefore, this antennas are usually the preferred choice of many research groups around the world to develop corrugated horns for their research projects.

Antennas of this type are at present on board of Hispasat 1C and Hispasat 1D satellites, are going to be used in the ESA funded Marschals airborne system, will be used in a near future in the ESA's Planck satellite and now-a-days a new version of a corrugated GPHA is being commercialised by the British company Flann Microwave, Ltd.

Table of Contents

Chapter 1

Introduction

In this introductory chapter, a perspective of the state of the art evolution for corrugated horn antenna technology is presented. In addition, an outline of the structure of this thesis is given.

1.1 Background

There are three main reasons for the existence of corrugated horn antennas. Firstly, they exhibit radiation pattern symmetry, which offers the potential for producing reflector antennas with high gain and low spillover; secondly, they radiate with very low crosspolarisation, which is essential in dual polarisation systems and finally, they offer a wide bandwidth response.

Now-a-days, in the age of the communications, horn antennas take a very important role in the development of the actual and future communications systems with high requirements in their radiations patterns. In fact, corrugated feeds are the best feeds ever developed.

Ten to twenty years ago, corrugated horn antennas were restricted to be used in high performance applications, like being on board of satellites, earth station radiotelescope horns, antenna measurement chambers and very few more applications. They were restricted to those applications for two main reasons: difficulties in the design and difficulties in the manufacture process of a corrugated feed.

At present, the communication systems require really high performance antennas; sidelobe and crosspolar levels should be reduced in

the radiation pattern as well as the size of the antenna. Low crosspolar levels are inherent to the corrugated horn antenna technology and this parameter has been conveniently improved during the last decades with the use of corrugated feeds. But sidelobe level of corrugated horns has got stuck and no improvements have been made till the last five years. Probably, the improvement in sidelobe level has not been really necessary up to now. The incredible quantity of new communication systems that interact between them has made necessary to reduce the mutual interferences through sidelobes. In fact, the major benefits from the extremely low sidelobe interference characteristics are to reduce both operational costs and also the susceptibility to jamming or eavesdropping in military and secure applications.

The manufacture process for corrugated feeds has been improved during the last years due to the massive use of numerical milling machines and the improvement made in computer technology to control those machines. Additionally, sometimes to implement mm-wave and submm-wave corrugated horns, expensive electroforming techniques are needed, specially where thin corrugations, small size and precision are required. Electroforming techniques have the disadvantage of the necessity to manufacture a mandrel for each antenna that will be destroyed afterwards becoming a very expensive manufacture method.

Regarding to the global dimensions of corrugated horns, we can observe that its radiation aperture is almost determined for a given directivity; although a horn antenna can be shortened in its length. Shorter antenna profiles are really the preferred ones for practically all applications, satellites launching reduction of weight, lighter posts for base station

antennas, and additionally they should be as well easier and cheaper to manufacture.

Now-a-days, likely global market applications for corrugated feeds are: compact parabola feeds, covert surveillance, secure communications, base station power saving, reduced interference... So corrugated feeds will no more be restricted nearly exclusively to expensive satellite market.

A huge research has been made in the last years by several groups around the world in optimising corrugated horn antenna profiles, using advanced optimisation programs with the aid of the increasing speed of computers. Each group has its own profiles and reaches its own conclusions, but mainly, the profiles chosen for the most high performance applications are the ones suggested and developed by the Antenna Group of the Public University of Navarra a few years ago. The corrugated Gaussian Profiled Horn Antennas (GPHA's) are at the moment at the highest level of performance among any other corrugated horn antenna.

In this manuscript a modern method to design high performance GPHA's is explained and really good results are being obtained from it. Achievements as making an antenna for HISPASAT 1C and HISPASAT 1D satellites or entering the market with a company as Flann Microwave Ltd. in the last few months with a brand new antenna (http://www.flann.com) could be considered as an absolute success. Other studies have been performed for high requirements applications; the MARSCHALS and the PLANCK instruments and many others applied by other research groups (CSIRO, Queen Mary College, Jet Propulsion Laboratory...) used the technology proposed in the nineties by the Antenna Group of the Public University of Navarra. We hope this research will be expanded a lot more in a near future with the brand new profile types presented at the end of this manuscript.

1.2 Organisation of chapters

This chapter has introduced the reader to the work performed during this doctorate Thesis, providing some historical background to corrugated horn antenna technology and outlining the motivation for the research presented. The mayor novelties of the work performed have been also explained.

Chapter 2 presents the principles of corrugated horn antenna theory. An overview of how corrugations affect the electromagnetic field linked to a modal theory inside a corrugated waveguide is presented. Additionally, some aspects of the paraxial free space radiation by means of gaussian modes is covered.

The classical conical corrugated horn antenna design method is recollected completely in chapter 3. An example of a conical corrugated horn antenna design is developed to evaluate its characteristics and compare it with other designs to be studied in the subsequent chapters.

Once the classical conical corrugated horn antennas have been covered, in chapter 4 the new profiles proposed by the Antenna Group of the Public University of Navarra are explained. This chapter covers the Gaussian Profiled Horn Antenna (GPHA) definition, performance and design. A corrugated GPHA design is developed as well for comparison with the previous chapter conical corrugated horn antenna design.

The objective of chapter 5 is to implement the specific device (TE_{11} to HE_{11} mode converter) to feed correctly the corrugated GPHA developed in the previous chapter. Three different ways to perform this device are explained carefully. Another possibilities under research are briefly explained.

In chapter 6, the information presented in chapters 4 and 5 is joined to implement the complete design using corrugated GPHA's. The design method will combine the three different ways to implement the input device of a corrugated GPHA. An example of a 22 dB directivity horn antenna design is also developed to make comparisons in electromagnetic behaviour and size. Besides, other new possibilities to feed a corrugated GPHA are briefly covered (under research at present). At the end of chapter 6, a bandwidth comparison, the design characteristics of the corrugation parameters and some tricks and rules that will help the designer are also presented.

Several applications developed during the six year research of this thesis are presented in chapter 7. In those applications the reader can check the way this research has been performed discovering the most important aspects of this type of corrugated horn.

Chapter 8 presents the main conclusions of this thesis and the guidelines for a future and promising research.

Chapter 2

Corrugated horn antenna theory

Corrugated horns have become now-a-days the preferred choice of feed antenna for use in high restrictive applications. This is because of their superior radiation performance and in particular their high copolar pattern symmetry and low crosspolarisation.

This chapter starts with the principles of the electrical behaviour of the electrical fields inside a corrugated waveguide. The hybrid mode basis as a tool to help in the analysis of corrugated horns and the relation between waveguide modes and free space gaussian modes are explained to understand the behaviour of the different types of corrugated horn antennas that are going to be covered in this thesis.

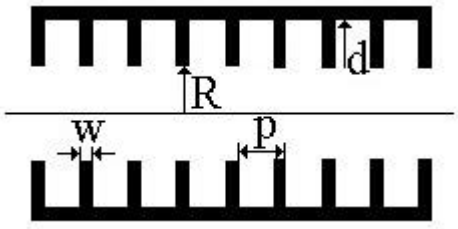

Figure 2.1. Corrugated waveguide

2.1 Principles of operation of corrugated horns

The operation principle of corrugated horns can be physically explained by considering the way in which the corrugated wall affects the field distribution inside a corrugated waveguide (fig. 2.1). As it will be demonstrated, the corrugations change the fields travelling through the

waveguide to produce the desirable radiating properties of axial beam symmetry, low sidelobes and low crosspolarization [1].

A linear electric field for low crosspolar level will be desirable but it cannot be obtained with smooth waveguides that only support pure transverse electric (*TE*) or a pure transverse-magnetic (*TM*) modes. These modes have the aperture electric field lines curved (fig. 2.2). Therefore a multimode horn should be designed. In [2], a special horn design to obtain an appropriate mode mixture by the addition of TE_{11} and TM_{11} modes in a particular proportion and phase is presented, but its bandwidth is very narrow.

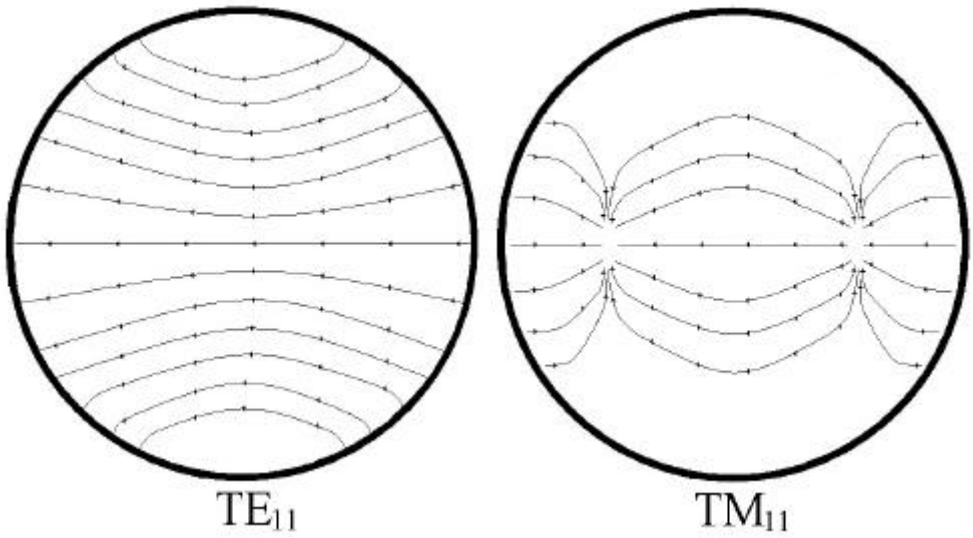

Figure 2.2. TE_{11} and TM_{11} aperture electric fields

Theoretically, as it will be shown later, the hybrid modes HE_{1n} present at the aperture of a circular waveguide perfectly linear electric field lines. The dominant hybrid mode in corrugated waveguide (HE_{11}) has the following aperture electric fields, [1,3,4,5]:

$$\left.\begin{aligned} E_x &= A_1 \cdot J_0\left(\frac{2.405}{R}\cdot r\right) - \frac{(X-Y)}{k\cdot R}\cdot A_2 \cdot J_2\left(\frac{2.405}{R}\cdot r\right)\cdot\cos(2\cdot f) \\ E_y &= \frac{(X-Y)}{k\cdot R}\cdot A_2 \cdot J_2\left(\frac{2.405}{R}\cdot r\right)\cdot\sin(2\cdot f) \end{aligned}\right\} \qquad (2.1)$$

where $J_0(k\cdot r)$ y $J_2(k\cdot r)$ are Bessel functions of the first kind, *k* is the free space wavenumber, A_1 and A_2 are the amplitude coefficients and *X* and *Y* are the impedance and admittance at the boundary $r = R$ given by

$$\left.\begin{aligned} X &= -j\cdot {E_f}/{H_z}\cdot {1}/{Z_0} \\ Y &= j\cdot {H_f}/{E_z}\cdot {1}/{Z_0} \end{aligned}\right\} \qquad (2.2)$$

where Z_0 is the impedance of free space.

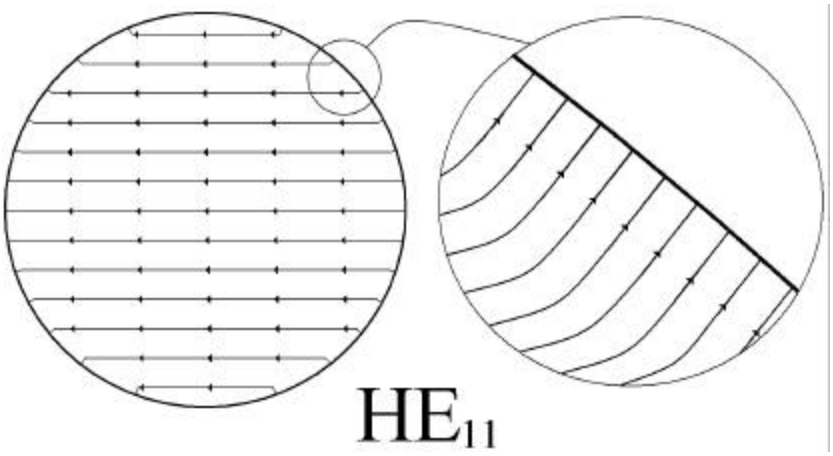

Figure 2.3. HE_{11} aperture electric field of a circular corrugated horn

From equation 2.1 it is seen that, if the term $(X-Y)$ vanishes, the aperture field is independent of the angular variable f and $E_y = 0$, so no crosspolarized field exists.

The condition of zero crosspolarized field $(X-Y)=0$ can be obtained if *X* and *Y* are equal values or if *X* and *Y* are both equal to *zero*. This second

case is called *balanced hybrid condition*. If there are enough corrugations per wavelength, the azimuthal electric field (E_f) will be equal to zero in $r = R$ and then $X = 0$. On the other hand, if the corrugation ridge (*w*) is narrow and quarter wavelength deep ($d = l/4$), they will act as short transmission lines where the short circuit at the end is transferred to an open circuit at the corrugation boundary $r = R$. This ensures that there will not be axial currents generated by H_f, so this too will be zero and then $Y = 0$.

The above description is only a simple physical explanation as to why the corrugated walls produce an approximately linearly polarized aperture field, see figure 2.3.

Because of the fact that the corrugation depth is frequency dependant, the balanced hybrid only happens at a single frequency and zero crosspolarization will be dominated by this aspect. At other frequencies apart from f_0 there will be a crosspolarized component. However, equation 2.1 shows that the crosspolar term decreases as $k \cdot R$ increases, so the larger the diameter of the horn, the wider will be the bandwidth for a given crosspolar level.

The above explanation has described the behaviour for an open-ended waveguide, but almost all horns have a finite flare angle. Then the radiation patterns are partly controlled by the additional factor of the antenna profile. This factor is a function of two parameters: the diameter of the horn and the flare angle; so that factor will increase for a short horn with a wide flare angle and a long horn with a narrow flare angle. As this factor increases, the radiation pattern becomes more and more determined by this opening factor value and less and less by the aperture fields. In the development of this thesis, only tightly controlled aperture angle of the horn antennas is going to

be considered. Then, the radiation of the horn designs will be completely controlled by the aperture fields.

2.2 Hybrid modes

To define properly the field inside a circular waveguide the most known basis used is the *TE* and *TM* family of modes which are direct solution of the wave equation inside a smooth circular waveguide [6]. But if the waveguide is corrugated it could be also useful to define the field inside the waveguide by the family of hybrid modes *HE* and *EH*. So in fact we can choose to define the field inside the corrugated horn antennas in terms of *TE* and *TM* modes or in terms of *HE* and *EH* modes.

Along this manuscript we will use both families to define the fields, and we will use in each particular case the family which better explains the behaviour we want to remark.

2.2.1 Simple mathematical definition of hybrid modes

Transverse electric and magnetic modes (*TE* and *TM*) are usually well known in waveguide theory. On the other hand, hybrid modes (those modes which doesn't present pure transverse components along the waveguide) are not so well known. It is interesting to aid in the knowledge of corrugated horn antennas to deepen in the understanding of hybrid modes of a corrugated waveguide. So in this section, a brief physical explanation of the properties of hybrid modes is going to be developed.

If we assume *balanced hybrid condition*, hybrid modes can be defined with the following simplified equations:

HE_{mn} modes

$$E_x(r,f) = \frac{\sqrt{2 \cdot Z_0}}{R \cdot \sqrt{p}} \cdot \frac{J_{m-1}(\frac{c_{m,n} \cdot r}{R})}{J'_{m-1}(c_{m,n})} \cdot \cos\left[(m-1) \cdot f\right]$$
$$E_y(r,f) = \frac{\sqrt{2 \cdot Z_0}}{R \cdot \sqrt{p}} \cdot \frac{J_{m-1}(\frac{c_{m,n} \cdot r}{R})}{J'_{m-1}(c_{m,n})} \cdot \sin\left[(m-1) \cdot f\right] \quad (2.4)$$

EH_{mn} modes

$$E_x(r,f) = \frac{\sqrt{2 \cdot Z_0}}{R \cdot \sqrt{p}} \cdot \frac{J_{m+1}(\frac{c_{m,n} \cdot r}{R})}{J'_{m-1}(c_{m,n})} \cdot \cos\left[(m+1) \cdot f\right]$$
$$E_y(r,f) = \frac{\sqrt{2 \cdot Z_0}}{R \cdot \sqrt{p}} \cdot \frac{J_{m+1}(\frac{c_{m,n} \cdot r}{R})}{J'_{m-1}(c_{m,n})} \cdot \sin\left[(m+1) \cdot f\right] \quad (2.5)$$

where $c_{m,n}$ are the roots of the Bessel functions ($J_{m-1}(x) = 0$ for *HE* modes and $J_{m+1}(x) = 0$ for *EH* modes), R is the waveguide radius, m and n the radial and azimuthal indexes of the modes and Z_0 is the impedance of free space.

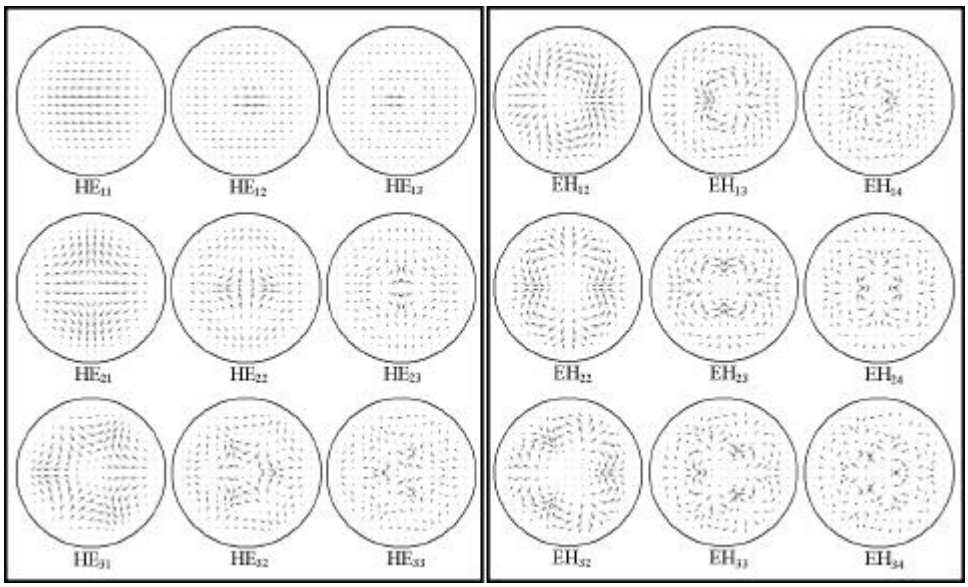

Figure 2.4. HE_{mn} and EH_{mn} aperture electric fields (linear scale)

From equations 2.4 and 2.5, the main property we can extract is for $m=1$, the HE_{1n} modes are linearly polarized, ($E_y = 0$ see equation 2.4), however the EH_{1n} modes have a high crosspolar component, ($E_y \neq 0$ see equation 2.5).

The aperture electric field of the first HE_{mn} and EH_{mn} modes is represented in fig. 2.4, the crosspolar component of EH_{1n} can be checked.

Also in fig. 2.5, the aperture power of the first HE_{mn} and EH_{mn} modes is represented.

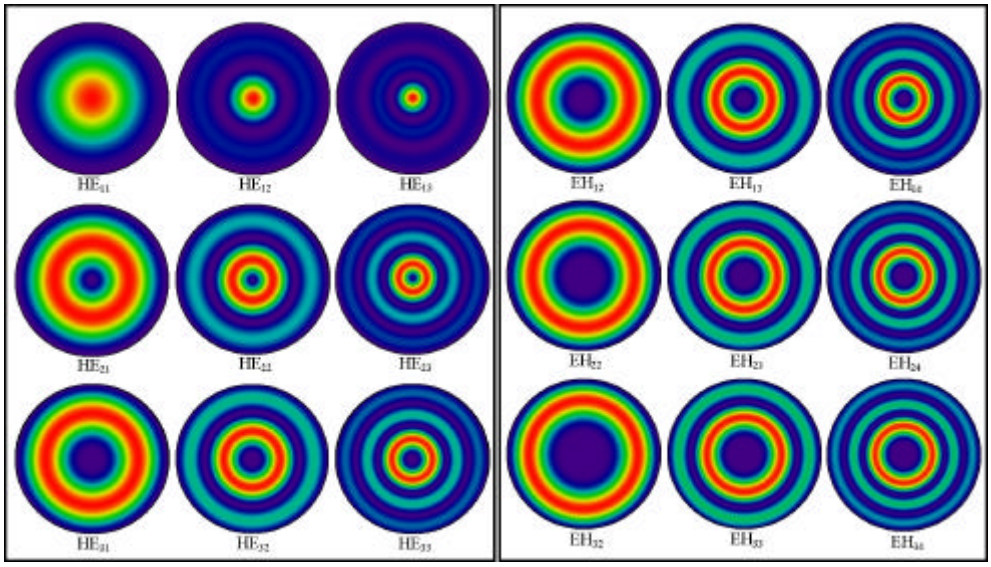

Figure 2.5. HE_{mn} and EH_{mn} aperture power (linear scale)

The important modes in the present study will be those with *m=1*, HE_{1n} and EH_{1n}, because the mode used to feed a corrugated horn antenna is always the TE_{11} and the corrugations are symmetrical variations of radius so they only generate modes with variation of the second index, *n*.

2.2.2 The fundamental mode of a corrugated waveguide, HE_{11} mode

The HE_{11} mode is the fundamental mode of a corrugated waveguide and presents linear electric field at the aperture, (fig. 2.2). From equation 2.4, this mode is defined only by a unique axial component, (equation 2.6).

$$E_x(r,f) = \frac{\sqrt{2 \cdot Z_0}}{R \cdot \sqrt{p}} \cdot \frac{J_0\left(\frac{c_{1,1} \cdot r}{R}\right)}{J_0^{'}(c_{1,1})} \qquad E_y(r,f) = 0 \tag{2.6}$$

where $c_{1,1}$ is the root of the Bessel function $J_0(x) = 0$ and in this particular case, for the HE_{11} mode is $c_{1,1} = 2.404826$. Equation 2.6 can be obtained from a particularization of equation 2.4 or from equation 2.1 assuming *X-Y=0* (balanced hybrid condition).

TE modes	TE_{11} {84.496% 0º	TE_{12} {0.082% 180º	TE_{13} {$3.58 \cdot 10^{-3}$% 180º	TE_{14} {$4.94 \cdot 10^{-4}$% 180º
TM modes	TM_{11} {14.606% 0º	TM_{12} {0.613% 0º	TM_{13} {0.121% 0º	TM_{14} {0.039% 0º

Table 2.1. HE_{11} mode decomposition in terms of TE_{1n} and TM_{1n} modes

The mode can be expressed as a combination of TE and TM modes, as a generating basis that they are. Commonly, in the bibliography [1], the HE_{11} mode is supposed to be a combination of *85 %* of TE_{11} and *15 %* of TM_{11} with the adequate phase shift between them. But in fact, this mode mixture is not perfect, (*99.19 %* efficient with HE_{11} mode), the perfect mode mixture in terms of smooth waveguide modes, supposing *balanced hybrid condition* can be seen in table 2.1.

To check the validity of the mode mixture given in table 2.1 with respect to the *85 %* of TE_{11} and *15 %* of TM_{11} mode mixture commonly

accepted; a simple experiment has been performed. Both mode mixtures have been introduced into an oversized corrugated waveguide $32 \cdot l$ long with corrugation depth $l/4$ and enough corrugation periods per wavelength. This example has been analysed with a mode matching and generalized scattering matrix code and the results of the behaviour of the different modes inside the corrugated waveguide can be seen in figure 2.6.

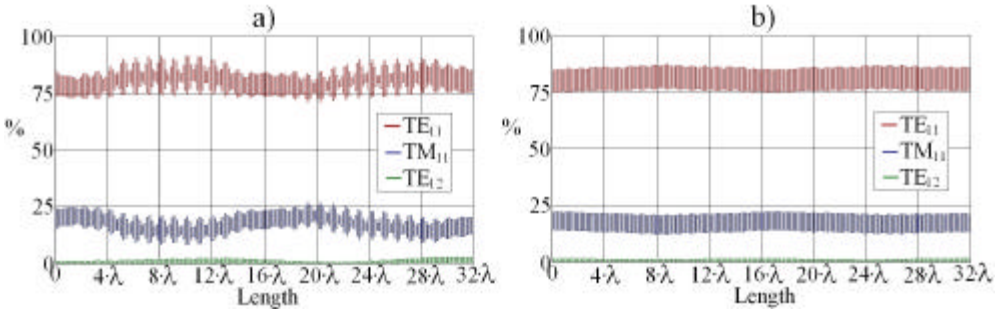

Figure 2.6. a) 85 % TE_{11} and 15 % TM_{11} mode mixture inside a corrugated waveguide
b) Exact HE_{11} mode mixture (table 2.1) inside a corrugated waveguide

One important assumption or property of any field structure that we refer it as a mode is that it will be an eigen solution of the Maxwell Equations inside the structure. From figure 2.6b it can be seen that the mode mixture of table 2.1 maintains itself better inside the corrugated waveguide than the common mode mixture of 85-15 (fig. 2.6a), so that the mode mixture of table 2.1 is much more efficient to define a HE11 hybrid mode, fundamental mode of that corrugated waveguide studied.

2.2.3 Radiation properties of the HE_{11} mode of a corrugated waveguide

It is also important to know the radiation properties of hybrid modes to understand the behaviour of corrugated horn antennas. In fig. 2.8, the radiation diagrams of the first HE_{1n} and EH_{1n} modes is represented. In that figure we can see, for example, the effect on the crosspolar component if a

EH_{1n} mode is excited inside a corrugated horn. Or also from the same figure, the excellent radiation properties of the HE_{11} with nearly null crosspolar component and with a radiation diagram with quite low sidelobes can be observed.

The HE_{11} fundamental corrugated waveguide hybrid mode is then an excellent mode for radiation purposes. For a common corrugated horn with oversized aperture, the radiated crosspolarized level will be very low, the aperture illumination efficiency will be high and the sidelobe level will be also quite low, (fig. 2.7).

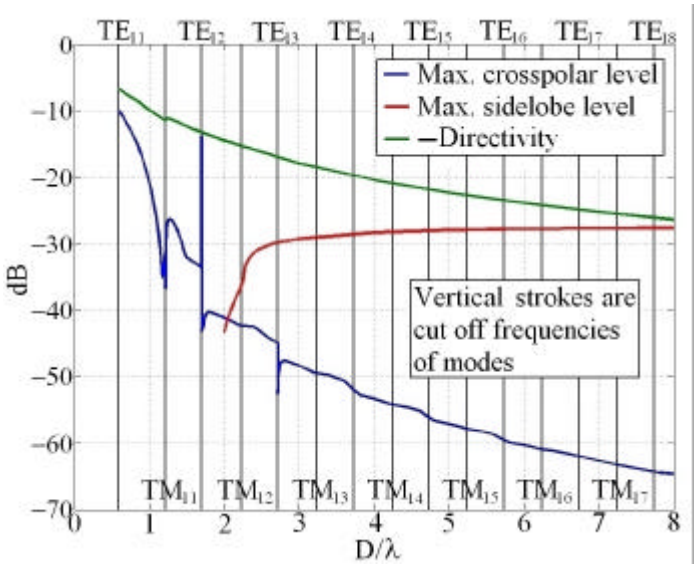

Figure 2.7. Radiation properties of the HE_{11} hybrid mode against aperture diameter (D)

From figure 2.7 we can extract several radiation properties of the HE_{11} hybrid mode:

- It can seen that as aperture diameter (D_{apert}) increases, and more smooth waveguide modes appear in propagation, the crosspolarized component decreases, as it was predicted for equation 2.1, as well as directivity and sidelobe level increase.

- For big apertures (which implies big directivities (*>20 dB*)), there is a *sidelobe level limit*. For a corrugated horn antenna with a pure HE_{11} mode at its aperture and an achieved directivity bigger than *20 dB*, is not possible to lower the sidelobe level more than *-28 dB*. The theoretical sidelobe level limit for huge directivities is *–27.5 dB*.

- Sidelobe levels below *–35 dB* can be obtained for aperture values below $D=2.25\cdot l$, but the maximum achievable directivity for this case is *15.4 dB*.

- For low level radiated crosspolarized component (*<-40 dB*), at least three smooth waveguide modes must be present, (TE_{11}, TM_{11} and TE_{12}) so a horn aperture diameter of at least $D=1.7\cdot l$ is needed[1].

Also from fig. 2.7, it can be seen that theoretically, the frequency that implies exactly $D=1.697\cdot l$ will have a big amount of crosspolarized component. This is due to that diameter is just the cut-off diameter for TE_{12} smooth waveguide mode. Furthermore, at the cut off frequencies of smooth waveguide modes, crosspolarization spikes can be seen.

As a final conclusion of the radiation properties of the HE_{11} hybrid mode, it can be said that this mode is an excellent mode to be excited at the aperture of a corrugated waveguide, and it offers low crosspolar levels and quite low sidelobe levels. However, if very low sidelobes are required for a high restrictive antenna, and its necessary to maintain low crosspolar levels,

---

[1] Furthermore, with a horn aperture diameter similar to $D=1.2\cdot l$ (between $1.13\cdot l$ and $1.22\cdot l$) just where the TE_{11} mode is alone at the aperture and the TM_{11} mode is just below cut-off, a quite good crosspolarized component (*<-30 dB*) can be obtained but only for a very small bandwidth [1] and also with directivities below *11.5 dB*.

we need several higher order HE_{1n} modes to be present at the aperture of the horn (see fig. 2.8) with appropriate amplitude and phase shift between them.

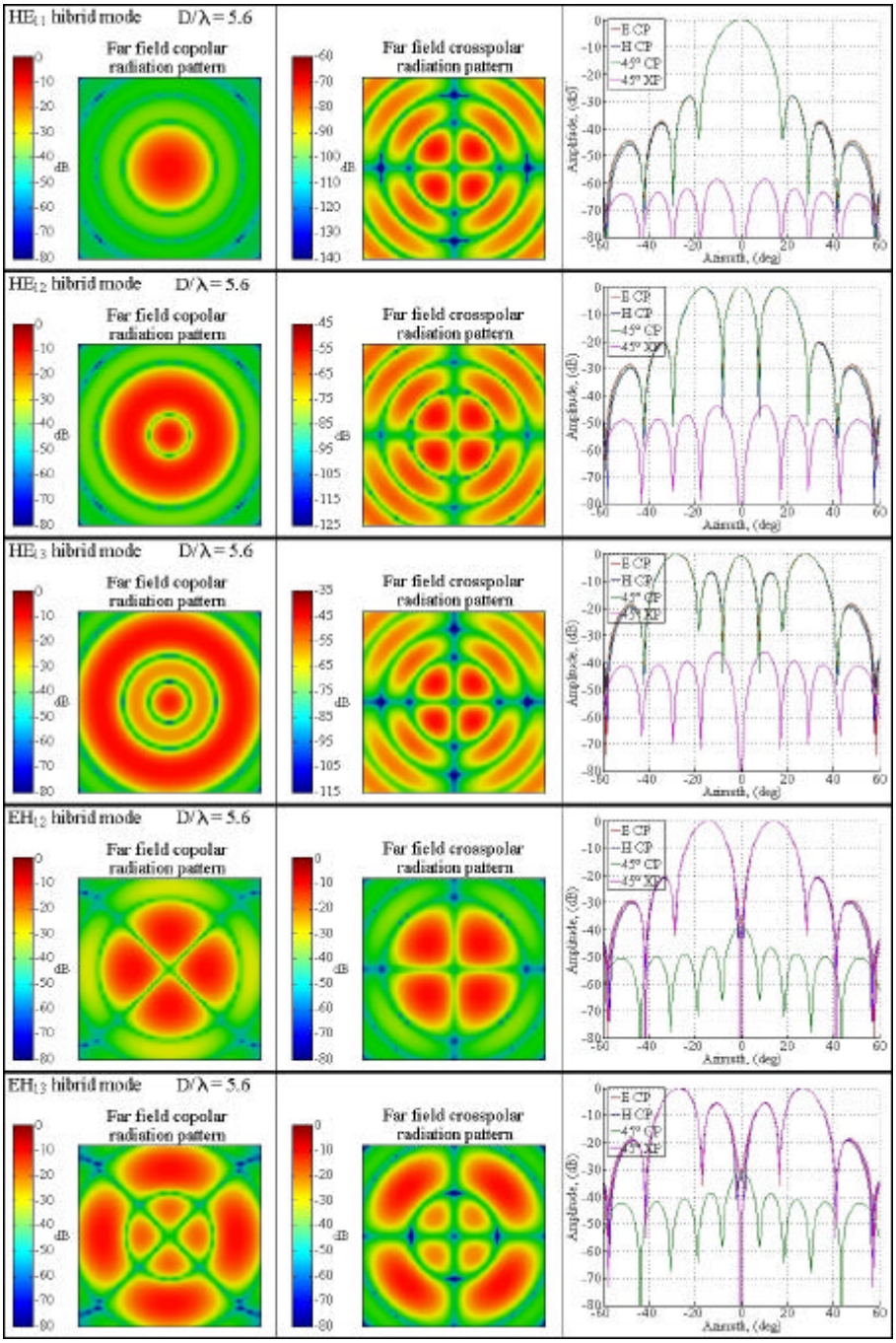

Figure 2.8. Radiation properties of several HE_{1n} and EH_{1n} modes

2.3 Paraxial free space modes (Gaussian modes) and their relation to waveguide modes.

It is well known that one of the best ways to define a free space radiation from an antenna is by means of the paraxial free space modes, the gaussian modes, which are a solution of the paraxial free space equation. A complete theory about properties of gaussian modes can be found on appendix I.

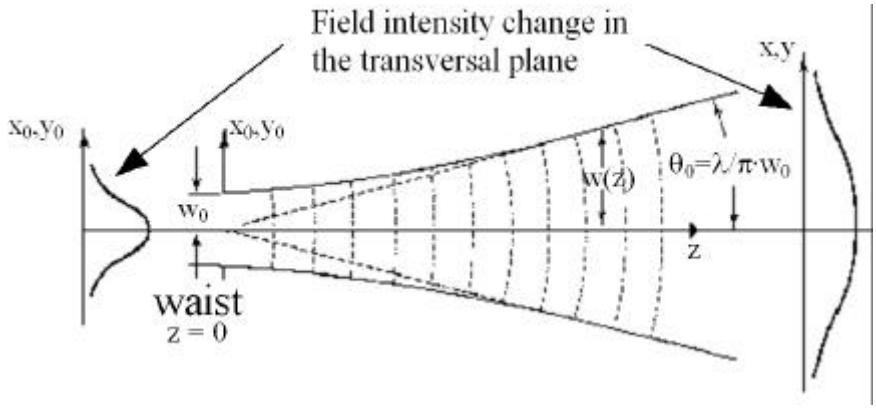

Figure 2.9. Propagation of a fundamental gaussian beam mode

The main mode for our corrugated horn radiation purposes is the fundamental gaussian mode. This mode has null crosspolarisation and null sidelobes. Its electric field propagation formula can be seen in equation 2.7:

$$E(r,j,z) = \frac{w_0}{w(z)} \cdot e^{\frac{-r^2}{w^2(z)}} \cdot e^{-j\frac{kr^2}{2 \cdot R(z)}} \cdot e^{-j(kz - z(z))} \qquad (2.7)$$

where $r^2 = x^2 + y^2$ and $w(z)$ is the beamwidth where there is a field decay of $1/e$ respect to the maximum, (see figure 2.9). In $z = 0$, the function $w(z)$, (see equation 2.8), has a minimum known as beamwaist and called w_0.

$$w(z) = w_0 \cdot \sqrt{1 + \left(\frac{2 \cdot z}{k \cdot w_0}\right)^2} \qquad (2.8)$$

It is important also to remark the similarity between the fundamental gaussian mode of a certain w_0 and the HE_{11} mode at a certain diameter aperture. As it can be seen in figure 2.10, we can nearly excite a fundamental gaussian with the HE_{11} hybrid mode.

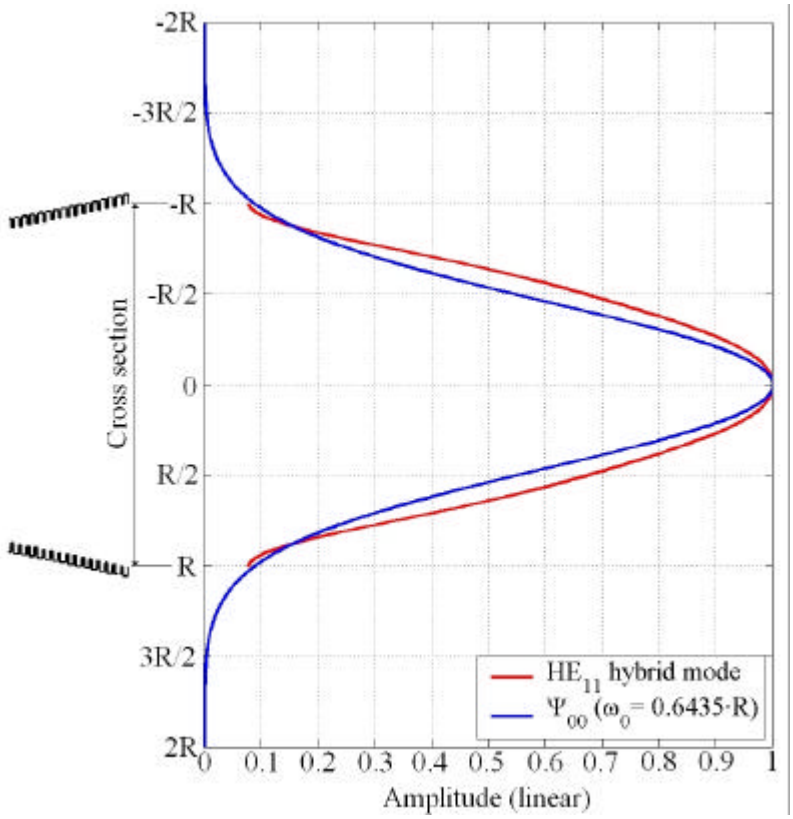

Figure 2.10. Comparison between an HE_{11} hybrid mode at the aperture of a horn antenna and its most similar fundamental gaussian beam mode

To make a proper comparison between the gaussian mode family and waveguide modes a mathematical correlation between them has been made (see appendix II). Then, the fundamental gaussian beam mode has been decomposed in terms of smooth waveguide modes (TE_{mn} and TM_{mn}) and also in terms of corrugated waveguide hybrid modes (HE_{mn} and EH_{mn}) at a certain horn aperture radius (R) with respect to the beamwaist (w_0) of the gaussian beam at that horn aperture.

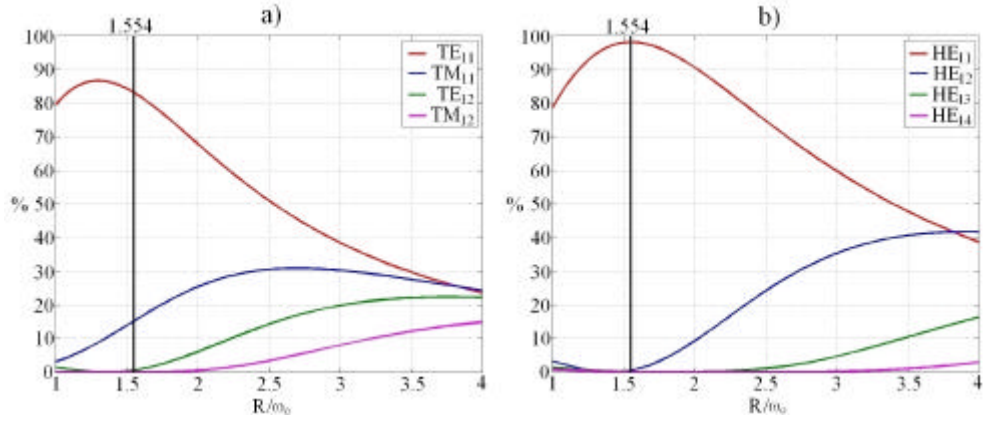

Figure 2.11. a) Fundamental gaussian mode decomposition in terms of TE and TM
b) Fundamental gaussian mode decomposition in terms of HE and EH

From figure 2.11 we can see that the fundamental gaussian mode can be expressed completely as a combination of TE_{1n} and TM_{1n} smooth waveguide modes and also as a combination of HE_{1n} hybrid modes.

At this point, it should be noted that HE_{11} mode has been always known as a gaussian-like mode because its field is nearly a pure gaussian, in fact it is up to *98.1 %* efficient with a fundamental gaussian beam of $R/w_0=1.554$ ($w_0/R=0.6435$) (see figures 2.10 and 2.11b). To obtain at the aperture of a corrugated horn antenna a high efficient fundamental gaussian beam mode (this implies lower sidelobes), more hybrid modes must be present at the horn aperture as it was said in section 2.2. This aspect will be covered in the following chapters, [7,8].

2.4 References.

[1] A.D. Olver, P.J.B. Clarricoats, A.A. Kishk and L. Shafai, “Microwave Horns and Feeds”, *IEE Electromagnetic waves series 39*, The Institution of Electrical Engineers, 1994.

[2] P.D. Potter, “A new horn antenna with suppressed sidelobes and equal beamwidths”, *Microwave Journal*, 1963, 6, pp. 71-78.

[3] Clarricoats, P.J.B. and Olver, A.D., “Corrugated Horns for Microwave Antennas”, *IEE Electromagnetic waves series 39,* The Institution of Electrical Engineers, 1984.

[4] Clarricoats, P.J.B., Saha, P.K. and Tech. M, “Propagation and Radiation behaviour of corrugated feeds”, *IEE Proceedings*, September 1971, Vol. 118, Nº 9.

[5] Zhang, X., “Design of Conical Corrugated Feed-Horns for Wide-Band High-Frequency Applications”, *IEEE Transactions on Microwave Theory and Techniques*, August 1993, vol. 41, n. 8.

[6] S. Ramo, J.R. Whinnery, T. van Duzer, “Fields and Waves in Communication Electronics”, *John Wiley & Sons, Inc.*1994.

[7] Del Río C., “Diseño de guías de onda cuasi-ópticas para modos gaussianos de orden superior”, Ph. D. dissertation, Escuela Técnica Superior de Ingenieros Industriales y de Ingenieros en Telecomunicación, *Public University of Navarra, (UPNA)*, November 1996

[8] Carlos del Río, Ramón Gonzalo, Mario Sorolla and Manfred Thumm, “Antenas de Bocina Conversoras de Modos de Guía de Onda a Estructuras Gaussianas”, *Spanish Patent N. P.9501922 Public University of Navarra, (UPNA)*, September 1995.

Chapter 3

Conical corrugated horn antennas

The design of circular horn antennas has been based, for a long time, in the control of the guide mode mixture to excite an HE_{11} circular corrugated waveguide mode. It is well known from the previous chapter that this hybrid mode can be made up of approximately a combination of 85% TE_{11} and 15% TM_{11} smooth circular waveguide modes with an appropriate relative phasing between them. The starting field distribution is usually the TE_{11} mode of the circular waveguide under monomode operation, and by means of a proper step or taper in the horn radius, the right amount of TM_{11} (amplitude and phase) is excited (Potter type horns) [1,2,3].

This technique, firstly used in non-oversized horns, was later extended to oversized ones, using long and smooth conical tapers after the step, which provided the appropriate mode mixture at the aperture (85%-15%). To get this mixture with nice radiating features, two main parameters have to be considered: the output diameter and the horn length. Since the coupling coefficient between waveguide modes is directly related to the waveguide slope change, for a given output radius that fixes the desired beamwidth, the change in horn length allows the designer to select the appropriate phasing in the 85% of TE_{11} and 15% of TM_{11} mode mixture obtaining the appropriate sidelobe and crosspolarization minimum levels. Therefore, the only parameter to adjust is the taper length. This type of horn antennas were extensively used in the past decades and were known as Potter type horns,

[1]. Its drawback was the reduced bandwidth a design of this type could cover.

Another technique is based on corrugated circular waveguides and takes profit of the fact that this mode mixture corresponds to the fundamental mode of a circular corrugated waveguide, the HE_{11} mode. This technique reported in [2,3,4,5] involves a gradual matching of the smooth circular guide to another corrugated one wherein the corrugation depth is smoothly tapered from $\lambda/2$ to $\lambda/4$.

These two outlined techniques are combined in the so-called conical corrugated horn antennas with a matching device at their input port. In principle, corrugated horn antennas presents a wider frequency response than Potter type horns. Their design parameters are basically: corrugation parameters (period, duty cycle, depth, shape, etc...); length and profile of the $\lambda/2$-to-$\lambda/4$ impedance matching device; and the horn geometry in order to optimise the global performance of the horn.

Directivity, gain, sidelobe and crosspolarization levels are important design parameters for many applications involving horn antennas. Additional design parameters, relevant to satellite applications are length and weight, which need to be minimized, [6,7].

During the last 20 years, many of the applications involving high performance horn antennas have been equipped with conical corrugated horn antennas.

Conical corrugated horn antennas are one of the best possibilities to accomplish very high radiation pattern requirements; but during the last decade another shorter and better profiles for corrugated horn antennas have aroused. Nevertheless, a brief review of the way of designing conical

corrugated horn antennas has been summarized in the following paragraphs. This simple design method will help in the understanding of modern corrugated horn antenna design for the rest of this thesis.

In this chapter, only moderate directivity antennas (above 15 dB) for high performance applications will be covered.

3.1 Conical corrugated horn antenna design

Among the specifications detailed for the design of a corrugated horn antenna, there is an specially important parameter, the directivity needed for the design, or more specifically, the edge taper of the radiation pattern at a certain angle (copolar beamwidth).

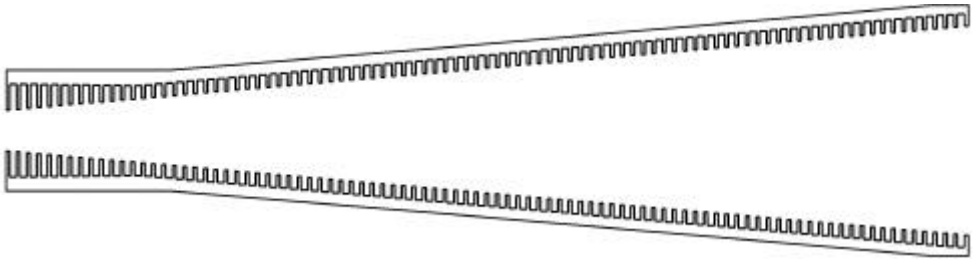

Figure 3.1. Conical corrugated horn antenna

So, once we have defined the directivity of the design and assumed at the aperture an HE_{11} mode (85% TE_{11} + 15% TM_{11} approximately), the output radius of the conical corrugated horn antenna is nearly fixed from a physical point of view.

For normal conical corrugated horn antenna design, there are several diagrams for –3 dB and –10 dB half beamwidth that define the copolar pattern in terms of the profile angle and the aperture diameter, [3]. A version of these diagrams has been depicted in figures 3.2a and 3.2b. On the other

hand, if our design parameter is the directivity we can select the aperture diameter of the antenna with the aid of figure 3.3a.

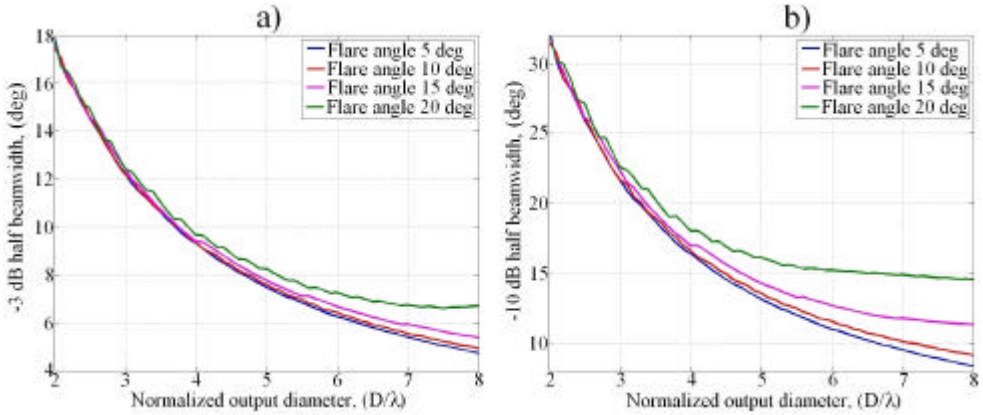

Figure 3.2. a) –3 dB design curve for conical corrugated horn antennas
b) –10 dB design curve for conical corrugated horn antennas

Usually, for moderate to high directivities (>18 dB) and high performance, the profile angle will be below 20 degrees. As we decrease this angle, the antenna becomes longer for a given directivity, but its radiation pattern becomes more perfect. The profile angle is usually defined by the maximum sidelobe level and beam purity allowed for the design, (see figures 3.3b and 3.4).

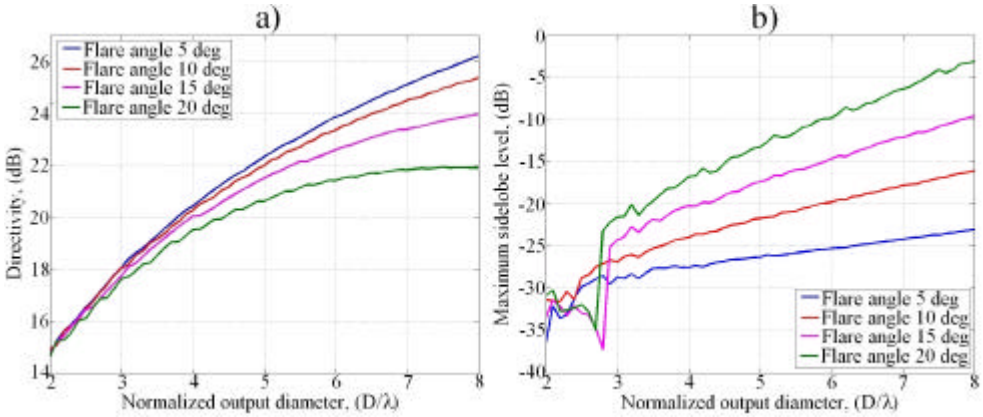

Figure 3.3. a) Directivity design curves for conical corrugated horns antennas
b) Max. sidelobe level design curves for conical corrugated horns

Conical corrugated horn antennas for flare angles below 20 degrees usually tend to maintain the purity of the fundamental corrugated waveguide mode, HE_{11}, to a proper diameter to obtain the desired copolar beamwidth pattern, (see fig. 3.4b).

As we pointed out in chapter 2, the HE_{11} mode is an excellent mode for radiation features, because it is 98.1% efficient to a fundamental gaussian beam and has a very low crosspolarized component. In a conical corrugated horn antenna, a quite pure HE_{11} mode is generated after the impedance transformer between the throat and the flare angle regions. If the angle of the antenna is not very high, (below 20 degrees), this mode is smoothly tapered to a bigger diameter. It presents higher efficiencies for small taper angles, (see fig. 3.4b) .

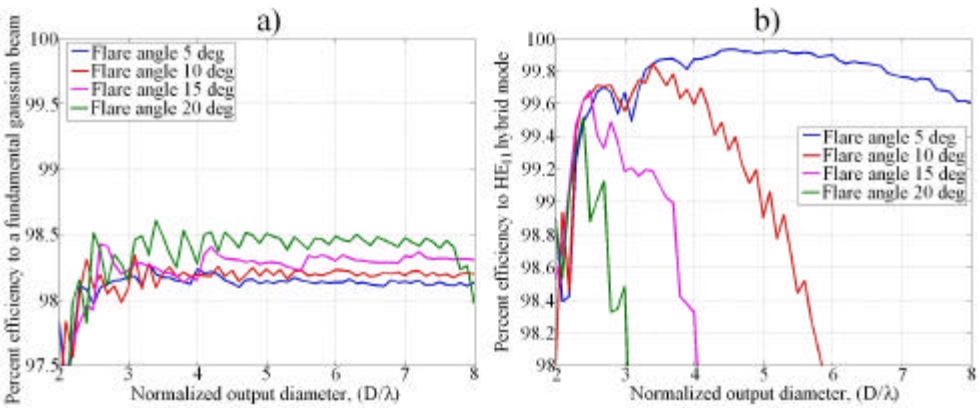

Figure 3.4. a) Effic. of conical corrugated horns to a fundamental gaussian beam
b) Efficiency of conical corrugated horns to a HE_{11} hybrid mode

As smoother is the tapering of the HE_{11} mode to the aperture (lower profile angle) of the antenna as more pure will be its power at the output against other spurious modes like HE_{1n} or EH_{1n}, (see figs. 3.4b and 3.3b). So for high performance antennas the flare angle must be reduced, so the length will then increase.

But, the efficiency to the fundamental free space mode (fundamental gaussian) is not very high for a conical corrugated horn antenna (around 98.1 % efficient to a fundamental gaussian beam for a pure HE_{11} hybrid mode), see figure 3.4a. Then, the sidelobe level for a conical corrugated horn antenna with moderate directivities (above 20 dB) cannot be lowered below –30 dB, (see figure 3.3b and figure 2.7).

In figure 3.3b, a picture of sidelobe level against flare angle and output diameter is depicted. Shoulders are considered as sidelobes in that figure because they broaden the radiation pattern.

In figure 3.5 a picture of the phase center position inside a conical corrugated horn antenna against flare angle is depicted. Phase center moves closer to the aperture of the antenna as flare angle decreases, that means that output aperture diameter is more efficiently illuminated, so directivity increases a little for smaller flare angles as can be seen in figure 3.3a.

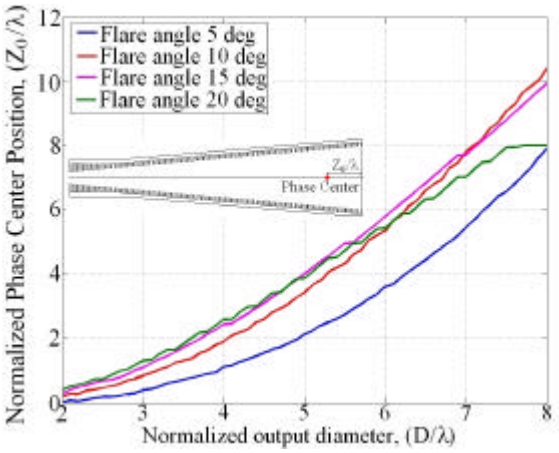

Figure 3.5. Phase center position in a conical corrugated horn antenna against flare angle of the profile

Phase center position is a very important horn antenna design parameter because it allocates the source for the free space radiation, (the

beamwaist of the gaussian mode propagation or the point where the phase fronts are planar), see appendix I.

Big flare angle conical corrugated horn antennas (15 and 20 deg) present shoulders that broaden the radiation pattern whereas small flare angle ones present a quite pure radiation pattern till the first sidelobe, (see fig. 3.6). So, the antenna with lower profile angle will be of higher performance in spillover radiation and with a smaller aperture diameter, although it will be longer.

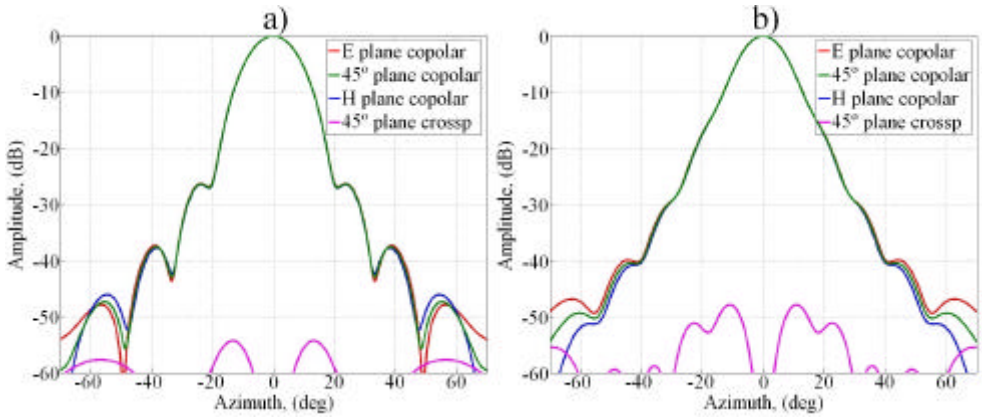

Figure 3.6. Comparison of the effect in the radiation pattern between two different flare angles for the same directivity antenna.
a) 5 degrees flare angle b) 15 degrees flare angle

3.1.1 Corrugation parameters design

After the election of this two parameters (aperture diameter and profile angle), corrugation geometry must be chosen. To define corrugation geometry, the antenna must be divided in two parts, the throat region and the flare angle region. The corrugation geometry at the throat region will define the input impedance of the antenna, (and then the resultant return loss), and the corrugation geometry along the flare angle will define the crosspolar patterns.

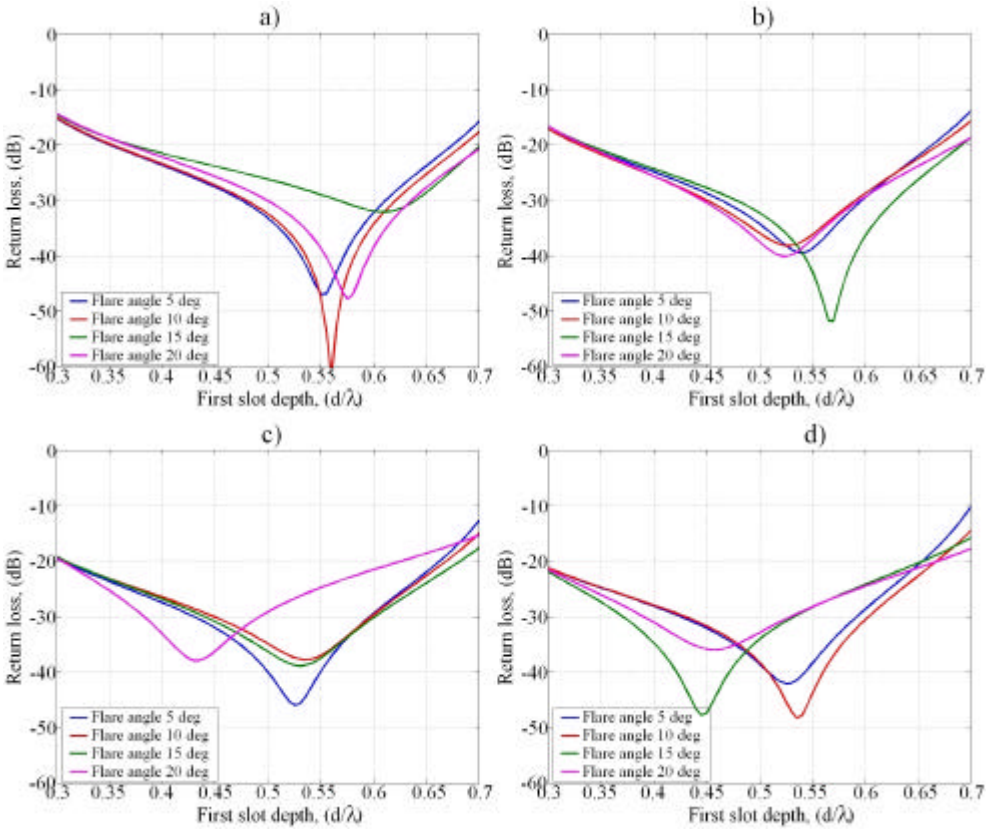

Figure 3.7. Return loss of TE_{11} mode at the throat of different profile angles of conical corrugated horns against first slot depth
a) Throat radius of 0.39·l b) Throat radius of 0.414·l
c) Throat radius of 0.446·l d) Throat radius of 0.477·l

Usually, for a normal corrugated horn antenna, the input mode at the throat region will be the TE_{11} smooth circular waveguide mode, this mode defines approximately the input radius of the corrugated horn antenna profile. For minimum return loss of this mode, corrugation depth at the throat region must be around λ/2, (see figure 3.7).

After an analysis of figure 3.7, we can conclude that depending on the value of the input radius and the angle of the conical corrugated profile, the best possible value of the first corrugation depth can change and be slightly

different of λ/2, in fact as it can be seen the best possible value for small profile angles is usually slightly above λ/2.

As it has been shown in the previous chapter, for corrugated structures, for minimum crosspolarization, (balanced hybrid condition), corrugation depth must be around λ/4. Therefore, along our corrugated horn antenna, in order to satisfy both conditions, good impedance matching at the throat and low crosspolar levels, a tapered change in corrugation depth between the throat region and the flare angle region is then necessary.

A new parameter controlling the compromise between matching and radiation features appears, the length of this λ/2 to λ/4 input waveguide transformer.

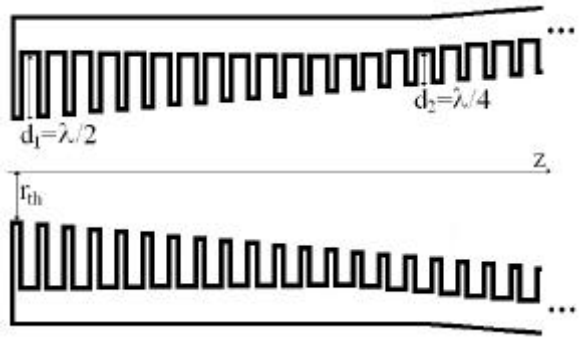

Figure 3.8. Detail of a l/2 to l/4 impedance transformer at the throat of a corrugated horn antenna

If the return loss must be improved, a longer transformer should be necessary, but if the crosspolar level is the critical specification a shorter impedance transformer could be chosen. In general, the length of this transformer will be defined as the length from the throat to the point where TM_{11} mode start to be propagating at the inner antenna part of the corrugation. A linear taper for the transformation between λ/2 and λ/4 is usually chosen, (see figure 3.8).

The number of corrugations per wavelength (p) must be usually above three at the lowest frequency of the necessary bandwidth, but it is not usually necessary to use more than five corrugations per wavelength, as it will be seen in appendix II. This parameter complicates a lot the manufacturing process for the antenna if many corrugations per wavelength are needed and the frequency of operation is high (i.e. millimeter waves), and can also be counterproductive for return loss at lower band frequencies.

Corrugation slot width (w) is usually chosen thinner than half corrugation period, but it is usually not necessary to reach really thin widths for a good performance, and this also provides an easier manufacturing process.

3.2 Design of a 22 dB conical corrugated horn antenna

As a practical example of how to design a conical corrugated horn antenna, let's say that we want to design a 22 dB directivity conical corrugated horn antenna with sidelobes lower than –25 dB and as low return loss and crosspolar level as possible in the most compact profile.

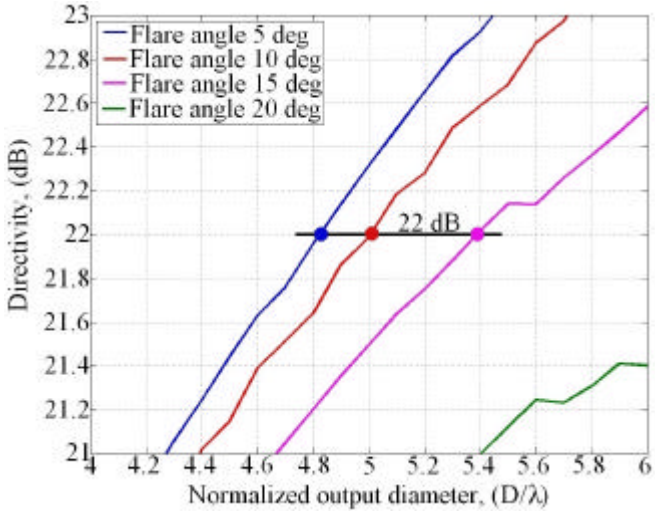

Figure 3.9. Directivity design curves for conical corrugated horns antennas

To design this antenna, we make a zoom of figure 3.3a in figure 3.9. From this figure we see that we can design a 5 degrees profile angle antenna with a 4.8·λ aperture diameter or a 10 degrees profile angle antenna with a 5·λ aperture diameter or a 15 degrees profile angle antenna with a 5.4·λ aperture diameter. Having a look at figure 3.3b we can fill a table with this parameters as well as sidelobe level and required length for each of the profile angles, (see table 3.1).

Profile angle (deg)	**Directivity, (dB)**	**Input radius**	**Aperture diameter**	**Length**	**Phase center**	**Sidelobe level, (dB)**
5 deg	22 dB	0.39·λ	4.8·λ	23·λ	1.85·λ	-26.5 dB
10 deg	22 dB	0.39·λ	5·λ	12·λ	3.42·λ	-21.7 dB

Table 3.1. 22 dB conical corrugated horn antenna design parameters

Selecting an input radius such as the one in figure 3.4a[1], (r_{throat}=0.39·λ), and having a look at table 3.1; we can select approximately a profile angle of 6 degrees or perhaps 7 degrees to achieve the –25 dB sidelobe level requirement.

Analyzing carefully the antenna the result leads to an antenna of 6.6 deg taper profile with the first corrugation depth of 0.52·λ decreasing linearly with an impedance transformer of 1.9·λ long to a corrugation depth for the rest of the antenna of 0.25·λ, see figure 3.10. The corrugation parameters have been selected as p=λ/5 and w=p/3.

The resultant length of the profile is 17.8·λ. It is really a quite long antenna for 22 dB directivity. This length cannot be shortened if we must

[1] An input radius of 0.39·λ is one of the monomode input radius most widely used for waveguide standards. λ is considered to be the wavelength in the middle of the band.

have the sidelobe level at –25 dB or less by any method if we maintain the conical corrugated profile.

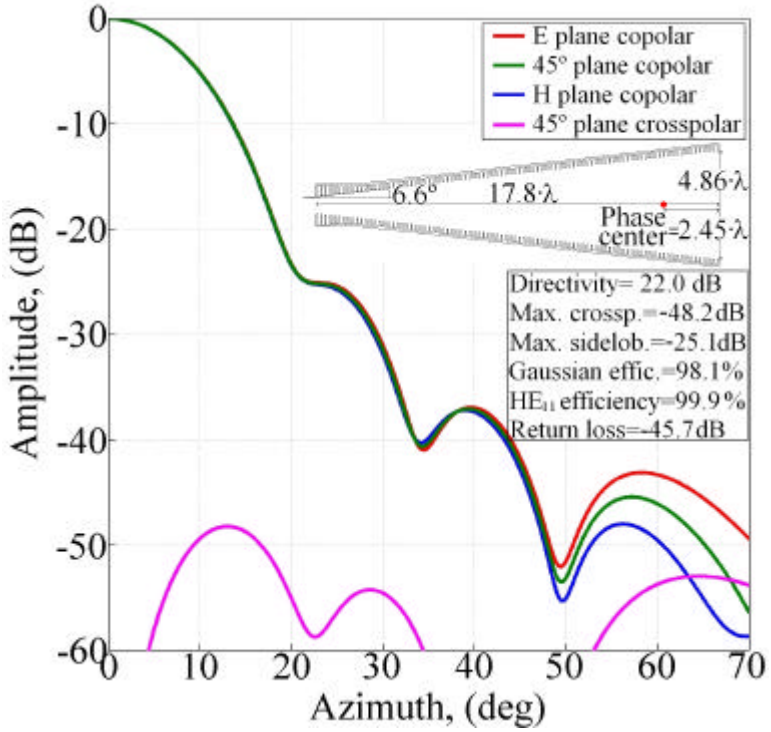

Figure 3.10. Conical corrugated horn antenna design for 22 dB directivity and -25 dB maximum sidelobe level

What would happen if we need to design a 22 dB directivity antenna but with the sidelobe level below for example -35 dB? The answer using a conical corrugated horn will be simple: a conical corrugated horn antenna with a directivity above 16 dB can never have a sidelobe level below -35 dB, (see figure 2.7) and exactly at 22 dB directivity a sidelobe level below –28 dB is also impossible. But there are other possibilities to solve this problem: we could use other corrugated horn profile to improve the sidelobe level and reduce the length. At this point is where we designed and patented in the year 1995 the gaussian profiled horn antenna, (GPHA) [8]. But this will be the topic covered in the next chapter.

3.3 References.

[1] Potter, P. D., "A New Horn Antenna with Suppressed Sidelobes and Equal Beamwidths", *Microwave Journal*, vol. VI, June 1963, pp. 71-78.

[2] Clarricoats, P.J.B. and Olver, A.D., "Corrugated Horns for Microwave Antennas", *IEE Electromagnetics Waves Series 18*, Chap. 5, 6 and 7, Peter Peregrinus, 1984.

[3] A.D. Olver, P.J.B. Clarricoats, A.A. Kishk and L. Shafai, "Microwave Horns and Feeds", *IEE Electromagnetic waves series 39*, The Institution of Electrical Engineers, 1994.

[4] G.L. James, "Analysis and design of TE_{11} to HE_{11} corrugated cylindrical waveguide mode converters", *IEEE Transactions on Microwave Theory and Techniques*, Vol. MTT-29, pp. 1059-1066, 1981.

[5] B. Maca, Thomas, G.L. James and K.J. Greene, "Design of high-performance wideband corrugated horns for Cassegrain antennas", *IEEE Transactions on Antennas and Propagation*, Vol. AP-34, pp. 750-757, 1986.

[6] G.L. James, "Design of wide-band compact corrugated horns", *IEEE Transactions on Antennas and Propagation*, Vol. AP-32, pp. 1134-1138, 1984.

[7] C. Granet, T.S. Bird and G.L. James, "Compact low-sidelobe corrugated horn for global earth coverage", *Proceedings of the IEEE Antennas and Propagation International Symposium and URSI Radio Science Meeting*, Orlando, Florida, 11-16 July 1999, pp. 712-715.

[8] Carlos Del Río, Ramón Gonzalo, Mario Sorolla and Manfred Thumm, "Antenas de Bocina Conversoras de Modos de Guía de Onda a

Estructuras Gaussianas", *Spanish Patent. N. P.9501922 Public University of Navarra, (UPNA)*, September 1995.

Chapter 4

Corrugated Gaussian Profiled Horn Antenna design

Gaussian Profiled Horn Antennas (GPHA's) were firstly proposed in the year 1995 during the research developed in [1,2]. Those GPHA's were smooth waveguide horns that optimized the conversion between the smooth circular waveguide mode TE_{01} (at the input of the antenna) to the gaussian mode Ψ_{01} (at the aperture of the antenna) with a really nice conversion efficiency (above 99%). As gaussian modes are the solution of the paraxial wave equation for free space (see appendix I) every radiation which is propagated in free space can be decomposed in terms of gaussian modes[1].

By using these horn antennas, the matching between the waveguide and the free space is almost perfect, being the most "natural" way to match the two media. From a waveguide mode or mode mixture, what the GPHA's do is to excite a very similar transversal field distribution with Gaussian propagating features.

Most of the applications in telecommunication, telecontrol and telemetric systems deal with the fundamental gaussian mode Ψ_{00} as the main free space mode of a modern radiation pattern. To obtain a high purity Ψ_{00} mode at the aperture of a horn antenna, the corrugated version of the GPHA's developed in [3] aroused. The introduction of the corrugated GPHA becomes very useful to address the most stringent requirements in

[1] Only the radiation that complies with the paraxial condition which is the case of all the radiation from the antennas we are going to consider in this thesis.

directivity, gain, sidelobe and crosspolarization levels as well as reducing the total length and weight of the resultant profile.

The design procedure for a corrugated GPHA starts like in a conical corrugated horn with a detailed list of specifications; directivity, maximum allowable crosspolar level, sidelobe level, return loss… But unlike for conical corrugated horn antenna design, corrugated GPHA design follows a completely different path, as it will be seen in the following paragraphs.

It will be shown that with these new profiles we can improve important far field radiation pattern features of any existing conical horn, like sidelobe levels, while keeping its other far field characteristics, by adding some part of a GPHA at its end.

4.1 Corrugated Gaussian Profiled Horn Antenna definition

Corrugated GPHA's aroused to implement a perfect match between waveguide modes (mostly HE_{11} mode or similar mode mixtures) and the fundamental free space modes (fundamental gaussian mode, Ψ_{00}). If we have the possibility of obtaining at the aperture of a horn antenna a field that is nearly the transversal field distribution of a fundamental gaussian mode (see figure 4.1), its radiation pattern would be also nearly a fundamental gaussian beam propagation.

Because of the definition of the gaussian beam modes (appendix I), the Ψ_{00} mode doesn't have sidelobes and crosspolarization. This is much better than the radiation of a HE_{11} mode, despite for many applications it could be enough (see figures 2.7 and 3.10).

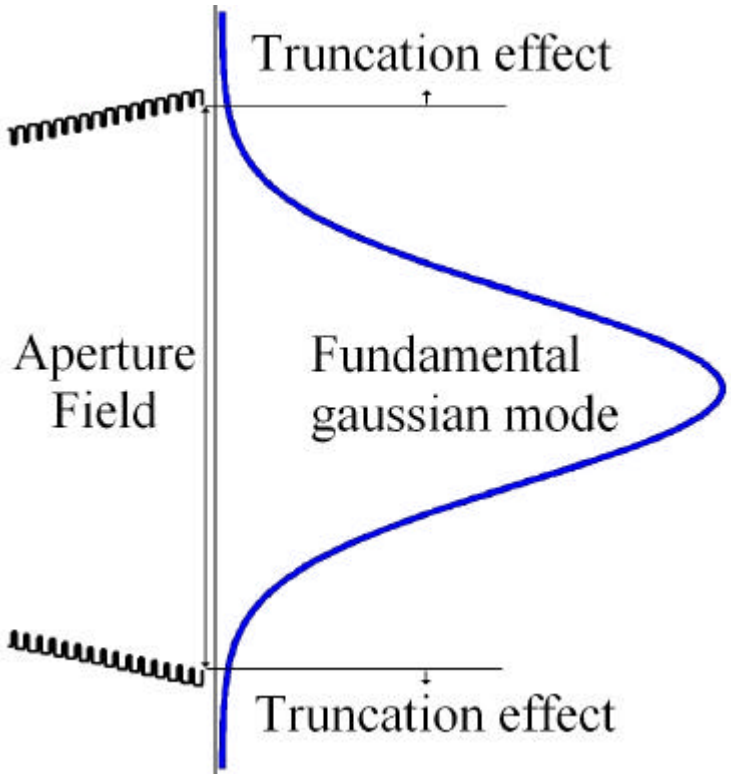

Figure 4.1. Fundamental gaussian mode approximation at the aperture of a corrugated horn antenna

The Gaussian beam modes are a solution of the paraxial wave equation in the free space [3]. Any paraxial radiation from a waveguide can be understood as an infinite summation of Gaussian beam modes, since they are orthogonal and therefore can generate a basis in free space. The conceptual idea involves the generation of any kind of transversal field distribution having Gaussian radiation features. Feeding a GPHA with several appropriate field distributions (i.e., TE_{0m}, HE_{11} circular waveguide modes), we can excite very efficiently a pure Gaussian beam mode.

The profile of a GPHA is defined basically by the expansion formula of the gaussian beam modes. So, the Gaussian beam broadening (decay of fields to 1/e of the central value) is given by:

$$\varpi(z)=\varpi_0 \cdot \sqrt{1+\left(\frac{2\cdot z}{k\cdot \varpi_0^2}\right)^2} \tag{4.1}$$

where ν_0 is the beamwaist at $z=0$ and $k=2p/l$ is the wavenumber in free space. The corresponding waveguide profile which follows the curve for Gaussian equi-amplitude relative surfaces is given by,

$$R(z)=r_0 \cdot \sqrt{1+\left(\frac{2\cdot z}{k\cdot \varpi_0^2}\right)^2}=\frac{D_0}{2}\cdot \sqrt{1+\left(\frac{\lambda\cdot z}{\pi\cdot\alpha^2\cdot\left(D_0/2\right)^2}\right)^2} \tag{4.2}$$

where $r_0=D_0/2$ is the input radius of the corrugated profile and $\nu_0=\alpha\cdot r_0=\alpha\cdot D_0/2$ is the beamwaist value at $z=0$ related with the D_0 through the parameter α. The α parameter controls the aperture angle of the horn for a given frequency and waveguide radius. D_0 is the input diameter. Figure 4.2 shows the relationship between the horn profile (equation 4.2) and the beamwaist propagation imposed by equation 4.1.

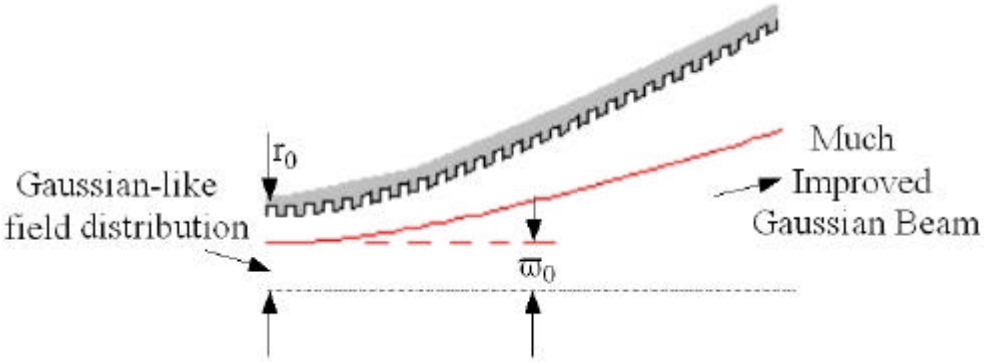

Figure 4.2. Corrugated Gaussian Profiled Horn Antenna, (corrugated GPHA)

The input field distribution to a corrugated GPHA could be anyone with a controlled diffraction. In principle, any waveguide mode or mixture of waveguide modes with low amplitude near the metallic walls is suitable

to feed a corrugated GPHA, but if we want to obtain a high purity fundamental gaussian beam a HE_{11} mode is one of the best solutions. The forward scattered fields will have the same transversal amplitude distribution as the original ones but with Gaussian broadening properties.

For instance, if a smooth circular waveguide excited in its TE_{01} mode is used as input to the GPHA, the forward scattered field will be a hollow beam azimuthally polarized expanding its width as a Gaussian field structure, (Ψ_{01} gaussian mode) [4]. Alternatively, to properly excite the fundamental Gaussian beam, (Ψ_{00} gaussian mode), one should use something like the HE_{11} mode from a corrugated circular waveguide [5,6,7,8,9].

4.2 Gaussian profiled corrugated horn antenna design

The corrugated GPHA to generate gaussian field structures can be applied to any kind of waveguide cross sections. In this thesis, only circular waveguides have been analyzed, but similar conclusions could be obtained for rectangular, square or any arbitrary waveguide cross section [10].

In this chapter, we are going to analyze the *oversized operation* [3,5], wherein the radiation features of almost any horn antenna or TE_{11} to HE_{11} mode converter can be improved by addition of a corrugated GPHA section at its end.

The corrugated GPHA feed mode will be the HE_{11} mode. So we will assume that the horn antenna or antenna converter just behind the corrugated GPHA provide us a quite perfect HE_{11} mode at its end. We could use, for example, a conical corrugated horn antenna or other shorter possibilities that will be covered in the chapter 5 of this thesis.

To design a corrugated GPHA, we have three main design parameters (see equation 4.2); profile length (L), input diameter (D_{in}) and the alpha parameter of the profile (α). In figure 4.3 we can see how this parameters affect to the profile shape.

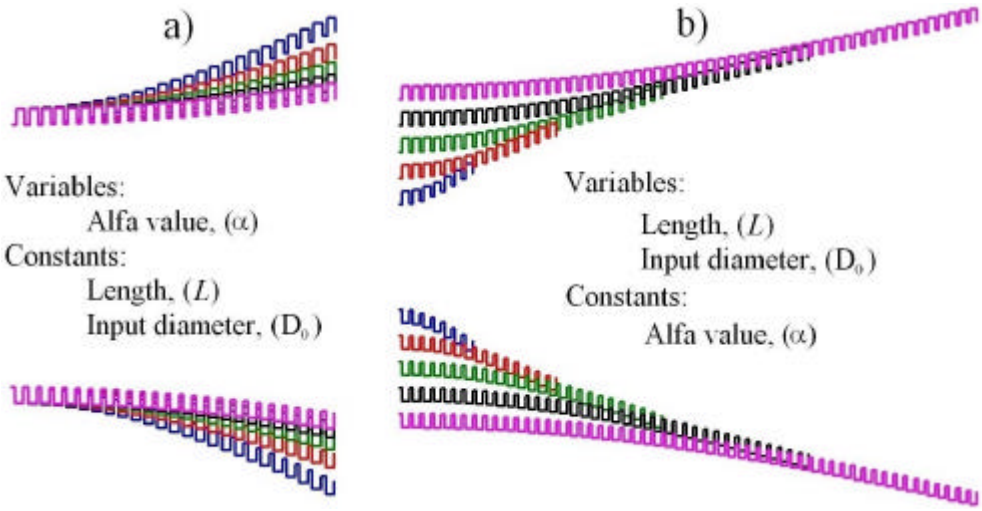

Figure 4.3. Corrugated GPHA main design parameters

To define the beamwidth of the radiation pattern of a corrugated GPHA we must select the value of D_0, not the value of the output aperture diameter (D_{apert}) as in a conical corrugated horn design of chapter 3. Thus, for a given directivity or beamwidth, we could fix quite approximately the value of D_0. Then, there are still two more parameters to play with: the profile length, (L), and the alpha parameter of the profile, (α).

Fixing the length to be enough to extract the main radiation parameters (approximately, $L=[3.5 \cdot D_0/\lambda - 5] \cdot \lambda$) and changing the alpha parameter, we could modify slightly the final directivity of the GPHA section (see figure 4.4).

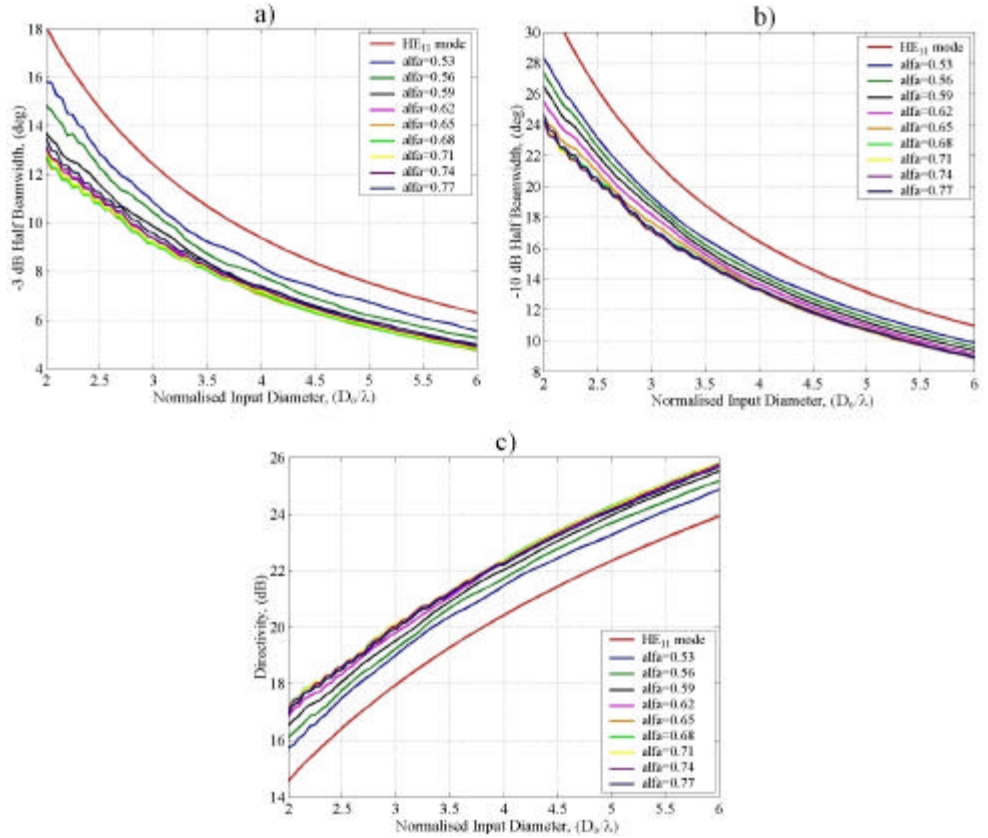

Figure 4.4. Beamwidth definition of the radiation pattern of a corrugated GPHA in terms of a
a) –3 dB half beamwidth curves b) –10 dB half beamwidth curves
c) Directivity curves

In figure 4.4, the –3 dB and –10 dB half beamwidth curves for a corrugated GPHA have been given. We will use for the rest of the thesis only directivity curves to define the beamwidth of corrugated GPHA's because we think it is clearer. For a comparison of a certain beamwidth with directivity, a reference to appendix III is needed where the comparison will be given in some figures assuming a pure fundamental gaussian beam as the radiation mode[2].

[2] This assumption is enough because usually the antennas to be designed in this thesis present pure fundamental gaussian beam decay till at least –25 dB.

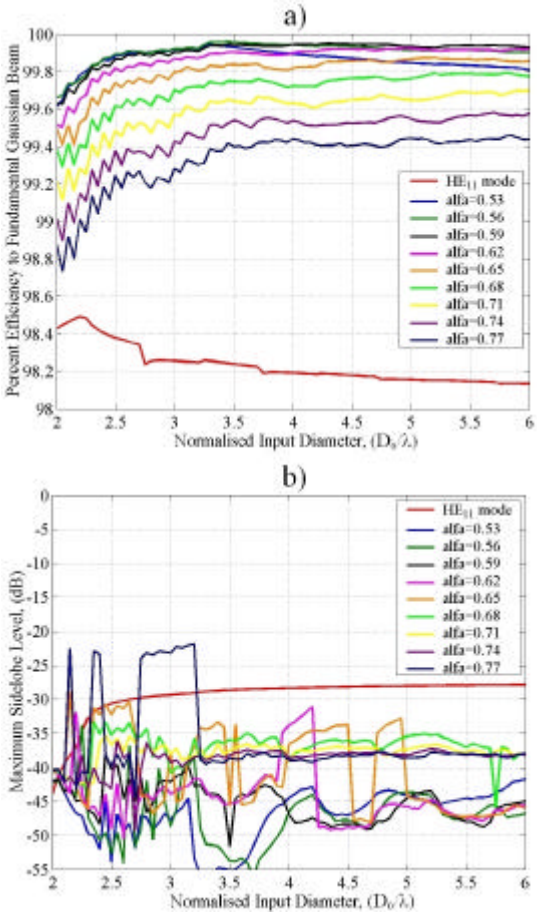

Figure 4.5. a) Corrugated GPHA efficiency to a fundamental gaussian beam in terms of a
b) GPHA maximum sidelobe level in terms of a

We have two possibilities or criteria to define the alpha parameter of the profile, (α): to select the α value that provides the most perfect gaussian beam at the output (this means minimum sidelobes) or to select the α value that is not the best for gaussian beam efficiency but gives a little bit more directive radiation pattern in a smaller output diameter.

The best α value for gaussian beam efficiency is $\alpha=0.59$ and the best α value for maximum directivity is $\alpha=0.68$, see figure 4.5. The main difference is that with $\alpha=0.59$ we can easily get sidelobes below *–45 dB* and

with $\alpha>0.65$ the sidelobes will be around *-35 dB* but with a slightly improvement in directivity, (around *0.2 dB*) and a significant reduction in aperture diameter.

In figure 4.5 we can also see the great improvement in the radiation pattern that a corrugated GPHA provides in comparison with the conical corrugated horn antenna radiation pattern with the HE_{11} mode at its output aperture, (see figures 2.7 and 3.10).

The last parameter we must define to completely design the GPHA is the profile length, *L*. To define the length of a GPHA we have developed an empirical formula with a parameter called *factor of length, f,* see equation 4.3.

$$L = \lambda \cdot \overline{D_0} \cdot \sqrt{f \cdot \left[1 + \left(\overline{D_0}\right)^2\right]} \qquad \overline{D_0} = D_0 / \lambda \tag{4.3}$$

where $\overline{D_0}$ is the normalized input diameter of the GPHA.

The *factor of length, f,* can be any number between *0.01* and *0.3*. The bigger is this number, the longer the antenna would be. If the antenna is very long we can say that we are over-guiding the gaussian beam and the addition of more antenna length is not really improving the beam, so the efficiency can be the same than with a shorter antenna. The best value for very nice gaussian beam efficiency and not excessive length (which means low sidelobes) is *f=0.19* (*f=0.19* has been the *factor of length* selected for figures 4.4 and 4.5 in fact), but values of f between *0.05* and *0.1* are usually enough and are the most currently used giving a short profile with not a big output diameter, see figure 4.6.

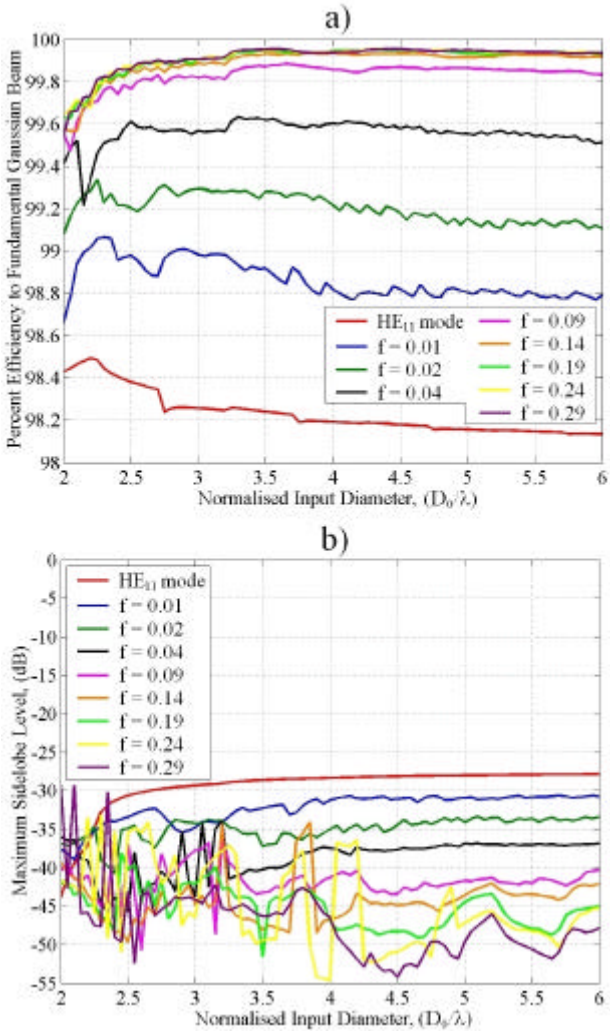

Figure 4.6. a) Corrugated GPHA efficiency to a fundamental gaussian beam in terms of length (L), a=0.59
b) Corrugated GPHA maximum sidelobe level in terms of L, a = 0.59

From figure 4.6b we can see that a small piece of corrugated GPHA of a ridiculous length with $f = 0.01$, can improve quite a lot the radiation pattern of a conical corrugated horn antenna lowering the sidelobe below *-30 dB*. Increasing the length to $f = 0.03$, the sidelobe level would be below *–35 dB*, (to have a reference of the antenna length in terms of the factor of length f see figure 4.7).

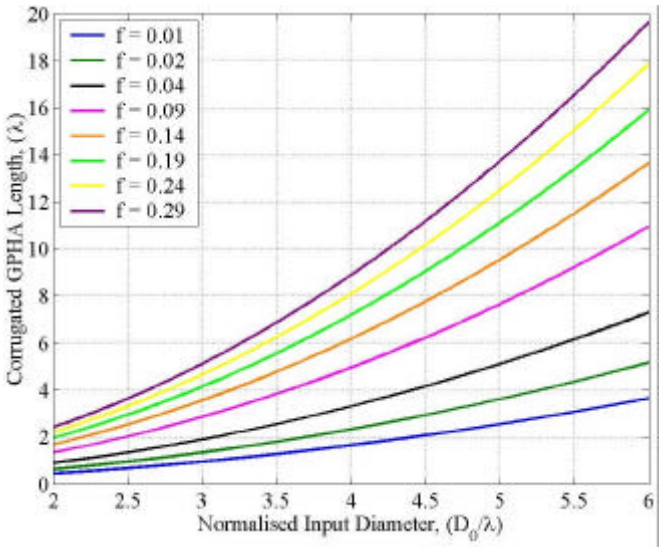

Figure 4.7. Corrugated GPHA length in terms of factor of length, (f)

Additionally, if *f>0.1* the directivity of a corrugated GPHA has an improvement of around *1.5 dB* higher directivity than the conical corrugated horn antenna alone (figure 4.8) but with a wider output aperture diameter indeed.

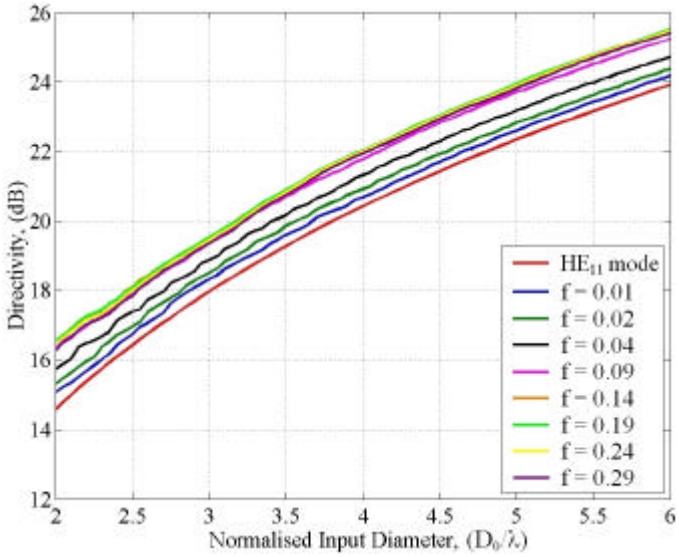

Figure 4.8. Corrugated GPHA directivity in terms of L, a=0.59

Corrugation parameters of a GPHA are just the same as any other corrugated horn antenna, corrugation period, *p* between *l/3* and *l/5* and corrugation tooth width, *w* around *p/2* are usually nice corrugation parameters, see appendix II.

There is only one parameter left in the corrugated GPHA design; what will be the phase center position in a corrugated GPHA?

We know that in a conical corrugated horn antenna, the phase center position if the profile angle is below 10 degrees which is usually normal, will be quite near the radiation aperture. But in a corrugated GPHA, the phase center is more inside the horn antenna than in the conical counterpart. Its position depends a lot on the α value of the corrugated GPHA as it can be seen in figure 4.9. As we will see in the rest of this thesis, to have a phase center position inside the horn antenna gives a better stability of this parameter in a wider bandwidth but provides a worse aperture size to directivity ratio than a conical corrugated horn, that's the price that a better radiation pattern must pay.

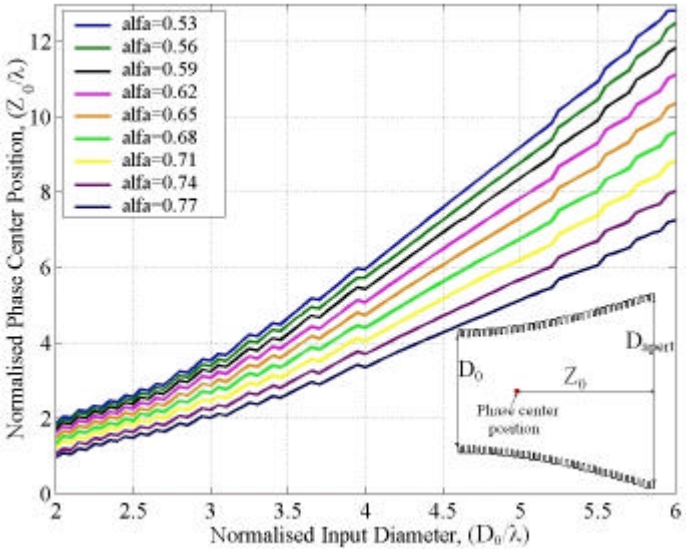

Figure 4.9. GPHA phase center position in terms of a, f = 0.19

From figure 4.9, the bigger is the α value, the nearer the phase center to the antenna aperture will be. So this means that if α is bigger, the antenna opens to free space slower, so the fields inside are guided (not radiated) and the phase center moves to the aperture.

4.3 Gaussian profiled corrugated horn antenna performance

Till now we have assumed that at the input of a corrugated GPHA we have a pure HE_{11} mode but, what would happen if the HE_{11} mode is not so ideal? Will the GPHA still have the nice radiation properties we studied in the last paragraphs?

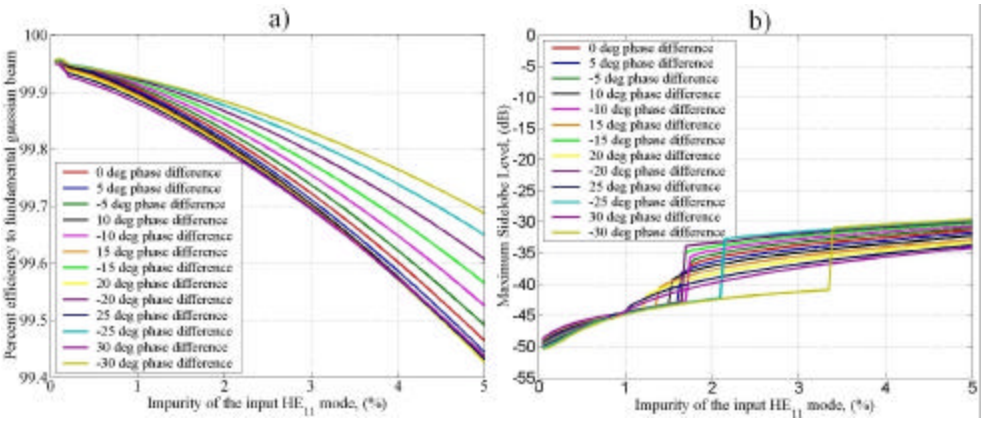

Figure 4.10. GPHA performance (a=0.59, f=0.19) under HE_{11} impurities of HE_{12}
a) Efficiency to a fundamental gaussian beam
b) Max. sidelobe level (shoulders above 10º are considered sidelobes[3])

An study of the impurity allowed for the HE_{11} mode at the input aperture of a corrugated GPHA was made for one of them of $\alpha=0.59$ and $f=0.19$. To define the impurity of a HE_{11} mode is rather difficult, but to have an impression of what happens, we made a sweep of a mixture of HE_{11} and HE_{12} at the input aperture of the GPHA. In fact, the sweep was made

[3] The degree level of a shoulder is defined as the difference in the slope between the no-shoulder estimated slope of the radiation pattern and the resultant slope at the inflexion point of that shoulder

with an impurity of HE_{12} from *0* to *5%* and from *0 deg* phase to ±*30 deg* phase difference with respect to HE_{11} mode, (see figures 4.10 and 4.11).

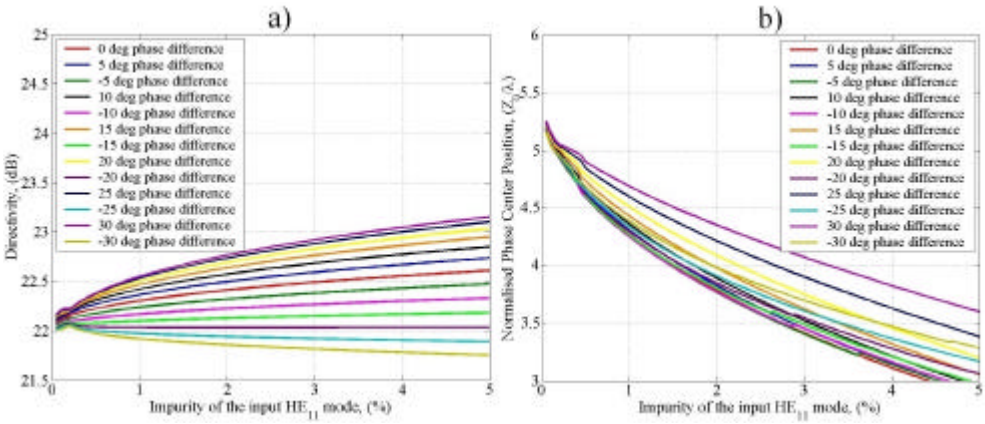

Figure 4.11. GPHA performance (a=0.59, f=0.19) under HE_{11} impurities
a) Directivity
b) Normalized phase center position

The result is that the impurity added to the HE_{11} lowers the efficiency to a fundamental gaussian beam (as it was expected) increasing the sidelobes. An impurity bigger than *1.5%* usually means that the sidelobe level is higher than *–40 dB*, see figure 4.9b. But an impurity of *5%* with a ±*30 deg* phase difference still exhibits a radiation pattern with lower sidelobes than a conical corrugated horn antenna.

In figure 4.11 can be checked also the changes due to impurities in the input HE_{11} mode for parameters such as beamwidth, directivity and phase center position.

4.4 Design of a 22 dB corrugated Gaussian Profiled Horn Antenna

As a practical example of how to design a corrugated GPHA, let's say that we want to design a *22 dB* directivity corrugated GPHA with sidelobes lower than *–35 dB* and as low return loss and crosspolar level as possible in

the most compact profile. The design specifications are the same that the ones in 3.3 section except that we want the sidelobe level *10 dB* lower for the corrugated GPHA.

To design the corrugated GPHA we must have a look to figures 4.6b and 4.8. The best value that gives the most compact design seems to be for $\alpha=0.59$ and $f=0.025$ for an input diameter of $4.49\cdot l$. The corrugation parameters chosen are: $d=l/4$, $p=l/5$ and $w=p/3$. With this values, the corrugated GPHA would be $3.4\cdot l$ long and with an output diameter of $5.22\cdot l$.

The output diameter is a little bit larger than for the conical antenna design in section 3.3, and the total length can not be yet compared because we assume a pure HE_{11} at the input of the corrugated GPHA, and a TE_{11} to HE_{11} transformer should be included for a correct comparison, (see chapter 6 for a comparison). To reduce the output diameter of the GPHA we could use a bigger α value and a little bit longer profile to achieve the same -35 dB sidelobe level. For example an $a=0.64$ with an $f=0.034$ for an input diameter of $4.47\cdot l$. can be used to obtain the *–35 dB* sidelobe level as well, and this design presents a length of $3.8\cdot l$ and an output diameter of $5.17\cdot l$. The difference is small in the output diameter compared to the length increase, so the first design with $a=0.59$ is going to be selected.

In the next chapter (chapter 5) an analysis different models of TE_{11} to HE_{11} mode converters will be studied. A perfect comparison between conical corrugated horn antennas and corrugated GPHA's will be carried out in chapter 6.

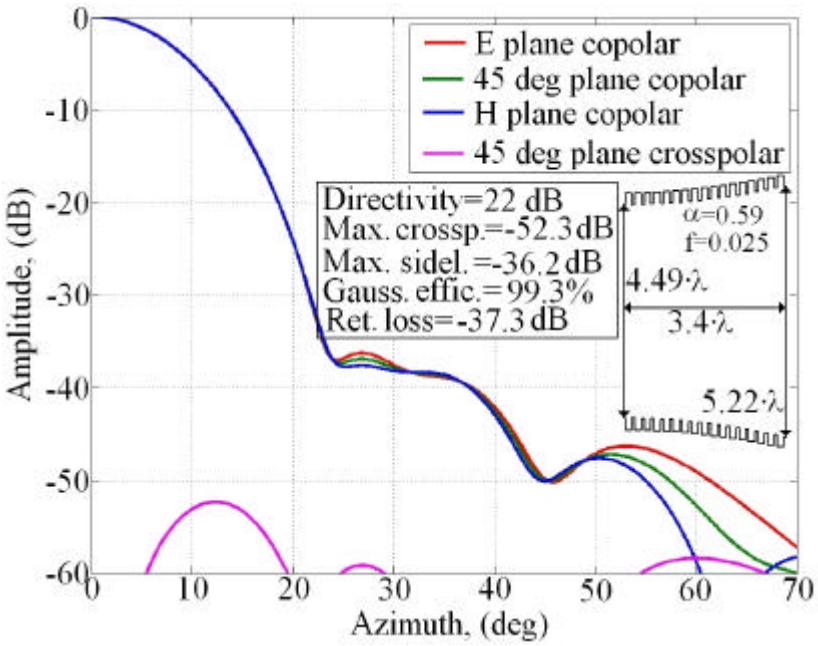

Figure 4.12. Corrugated GPHA design for 22 dB directivity and -35 dB maximum sidelobe level

4.5 Conclusions

A new model of corrugated horn antenna profile (corrugated GPHA) has been explained. This new profile produces very nice radiation patterns with very low sidelobe level and beam purity.

The design method of this corrugated GPHA has been explained to reduce design effort.

This antennas need at the throat a quite nice HE_{11} mode to achieve nice radiation results.

4.6 References.

[1] Del Río C., “Diseño de guías de onda cuasi-ópticas para modos gaussianos de orden superior”, Ph. D. dissertation, Escuela Técnica

Superior de Ingenieros Industriales y de Ingenieros en Telecomunicación, *Public University of Navarra, (UPNA),* 1996

[2] Carlos del Río, Ramón Gonzalo, Mario Sorolla and Manfred Thumm, "Antenas de Bocina Conversoras de Modos de Guía de Onda a Estructuras Gaussianas", *Spanish Patent. N. P.9501922 Public University of Navarra, (UPNA),* September 1995.

[3] Del Río C., Gonzalo R. and Sorolla M., "High Purity Gaussian Beam Excitation by Optimal Horn Antenna", Proc. *Int. Symposium on Antennas and Propagation*, Chiba, Japan, September 1996.

[4] Del Río, C., Gonzalo, R., Sorolla, M. and Thumm,. M., "Optimal Horn Antenna to Excite High Order Gaussian Beam Modes from TE_{0m} Smooth Circular Waveguide Modes*" IEEE Transactions on Antennas and Propagation*, Vol. AP-47, Nº 9, pp. 1440-1448, 1999.

[5] Gonzalo R., Del Río C., Teniente J. and Sorolla M., "Optimal Horn Antenna Design to excite High Purity Gaussian Beam using Overmoded Waveguides", *Proceedings of the 21st International Conference on Infrared and Millimeter Waves*, BTh3, Berlin, July 1996.

[6] Gonzalo R., Del Río C. and Sorolla M., "Generation of the HE_{11} Mode from Monomode Smooth Circular Waveguide", *Proceedings of the 21st. International Conference on Infrared and Millimeter Waves, BTh8,* Berlin, July 1996.

[7] Gonzalo, R., Teniente, J. and Del Río, C., "A novel and efficient corrugated feeder for reflector antennas", *Proceedings of the IEEE Antennas and Propagation International Symposium and URSI Radio Science Meeting*, Montreal, Canada, July 1997.

[8] Gonzalo, R., Marti, J., Teniente, J., del Rio, C. and Sorolla, M., "Measurement of a New Gaussian Profiled Corrugated Horn Antenna for Millimeter Wave Applications" *Proceedings of the IEEE Antennas and Propagation International Symposium and URSI Radio Science Meeting*. Atlanta, United States of America, June 1998.

[9] Gonzalo, R., Teniente, J. and del Río, C., "Improved Radiation Pattern Performance of Gaussian Profiled Horn Antennas", *IEEE Transactions on Antennas and Propagation*, Vol. 50, N. 11, pp. 1505-1513, November 2002.

[10] Gonzalo, R., Teniente, J. and del Río, C., "Generation of the HE_{11} mode in Rectangular Waveguide using Gaussian Techniques", *1999 IEEE AP-S International Symposium and URSI Radio Science Meeting*, 11-15 of July, Orlando, Florida, United States.

Chapter 5

Corrugated TE_{11} to HE_{11} mode converter design

As it was stated in chapter 4, corrugated GPHA's need at the throat a quite pure *HE_{11}* mode to produce nice radiation patterns. This chapter deals with the different method of generating quite pure *HE_{11}* hybrid mode at the aperture of such a converter.

This mode converter usually starts from a smooth circular monomode waveguide propagating the TE_{11} mode and ends at the required aperture diameter to feed the corrugated GPHA models of chapter 4.

In the literature one could find several types of TE_{11} to *HE_{11}* mode converters. One of them is the horn type proposed by Potter [1,2], which using several steps of the internal smooth waveguide radius generate the well known mode mixture of *85% TE_{11}* and *15% TM_{11}*. The needed phase shift between those two modes at the aperture is adjusted with the length of the horn. This type of TE_{11} to *HE_{11}* mode converters have the disadvantage of a reduced bandwidth.

Another type of TE_{11} to *HE_{11}* mode converter could be just a conical corrugated horn antenna (presented in chapter 3 of this thesis). This type of horn antenna or mode converter has a quite wide bandwidth as corresponds to a corrugated feed. Its main disadvantage is that it is quite long, heavy and complex to manufacture.

In this chapter we are going to explain how to design TE_{11} to HE_{11} mode converters by means of the use of gaussian techniques [3,4,5]. Other techniques presented by other authors, [6], will be covered as well. These techniques will lead to shorter profiles with quite nice bandwidth and efficiency.

Finally, a prime focus feed more commonly known as a choked feed, will be reconsidered as mode converter. Their main advantage is their size (really compact) and on the opposite, the main disadvantage is a reduced bandwidth in comparison to a normal corrugated converter.

Each of the possibilities covered in this chapter has advantages and disadvantages, and finally the designer should select with the information collected in this chapter the more convenient design for their purposes.

5.1 Design of a TE_{11} to HE_{11} mode converter using gaussian techniques

This particular technique is quite similar to a pure conical corrugated horn antenna, and the main idea is to create the appropriate mode mixture at the final aperture, mainly as the effect of the corrugations and by means of the slowly opening of the corrugated waveguide profile. As we will shown in the following paragraphs, both techniques use profiles with very slow variations of the waveguide radius with the length, generating really long devices to finally define the HE_{11} with very nice characteristics.

The gaussian propagation formula shows an asymptotic behaviour and the following equation can be obtained:

$$v(z)=v_0\cdot\sqrt{1+\left(2\cdot z/k\cdot v_0^2\right)^2};\quad v(z,z>>0)\cong\frac{2}{k\cdot v_0}\cdot z \tag{5.1}$$

being v_0 the beamwaist at $z=0$ and k the wavenumber.

Similarly, the corresponding waveguide profile which follows the curve for Gaussian equi-amplitude relative surfaces under the same assumptions is the given by:

$$R(z)=r_0\cdot\sqrt{1+\left(2\cdot z/k\cdot v_0^2\right)^2};\ R(z,z>>0)\cong\frac{2}{k\cdot r_0\cdot a^2}\cdot z=\frac{?}{p\cdot r_0\cdot a^2}\cdot z \qquad (5.2)$$

where $v_0 = a\cdot r_0$ and r_0 is the input radius (R_{in}).

Thus, from equation 5.2 a pure gaussian corrugated antenna can be approximated at enough distance by a conical corrugated horn of $\varphi=\tan^{-1}\left(\lambda/\pi\cdot r_0\cdot\alpha^2\right)$ flare angle.

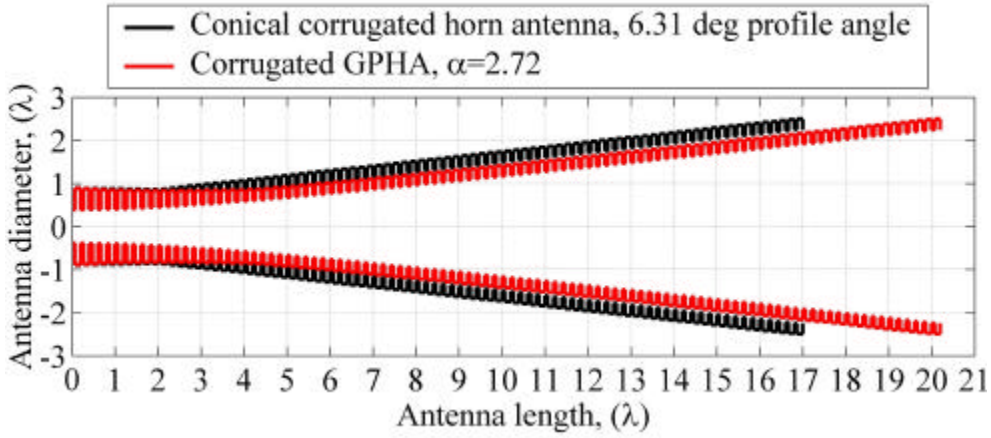

Figure 5.1. Length comparison between a conical corrugated horn antenna and a corrugated GPHA of the same effective aperture angle

In figure 5.1, the comparison of a *6.31 degrees* flare angle conical corrugated horn and a corrugated GPHA of $\alpha=2.72$ is shown. The input (*0.78l*), output diameter (*4.5l*) and the flare angle are selected to be the same for both antennas. The corrugated GPHA starts smoothly, so it will be

longer for the same flare angle, but a better response in return loss and bandwidth is expected.

5.1.1 Gaussian TE_{11} to HE_{11} mode converter performance

In order to study the behaviour of the corrugated GPHA as a TE_{11} to HE_{11} mode converter, we will fix the input radius to 0.39λ (the most typical value of a monomode smooth waveguide), and we will use a impedance transformer as the one defined in chapter 3 decreasing slowly the corrugation depth from $\lambda/2$ to $\lambda/4$ at the beginning of the mode converter.

As it will be seen in the following pictures, the behaviour of the corrugated GPHA as TE_{11} to HE_{11} mode converter is very similar to the behaviour of the corresponding conical corrugated horn antenna. The smooth input part will give the designer some advantages specially in return loss and bandwidth, as we will see later on.

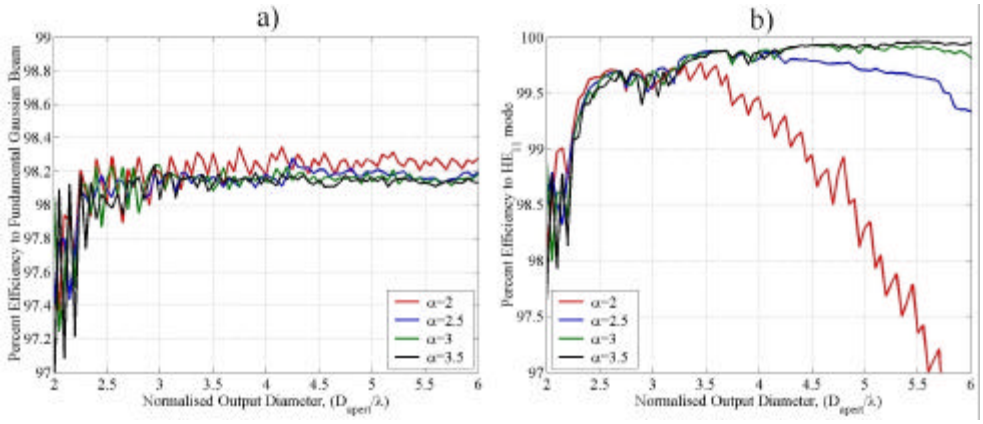

Figure 5.2. a) Efficiency of corrugated GPHA to a fundamental gaussian beam
b) Efficiency of corrugated GPHA to a HE_{11} hybrid mode

In figure 5.2 the conversion efficiency to a fundamental gaussian beam and to a HE_{11} hybrid mode are shown. It can be seen that the corrugated GPHA in this case is a very nice TE_{11} to HE_{11} mode converter, as it was the

conical corrugated horn of chapter 3 (figure 3.4). In fact, as the α parameter is increased, the conversion efficiency goes purer. However if the α parameter is increased the length of the component to reach the same output aperture is radically increased too.

The directivity and maximum sidelobe level design curves are depicted in figure 5.3. In this case, the equivalent figure for comparison of a conical corrugated antenna is the figure 3.3.

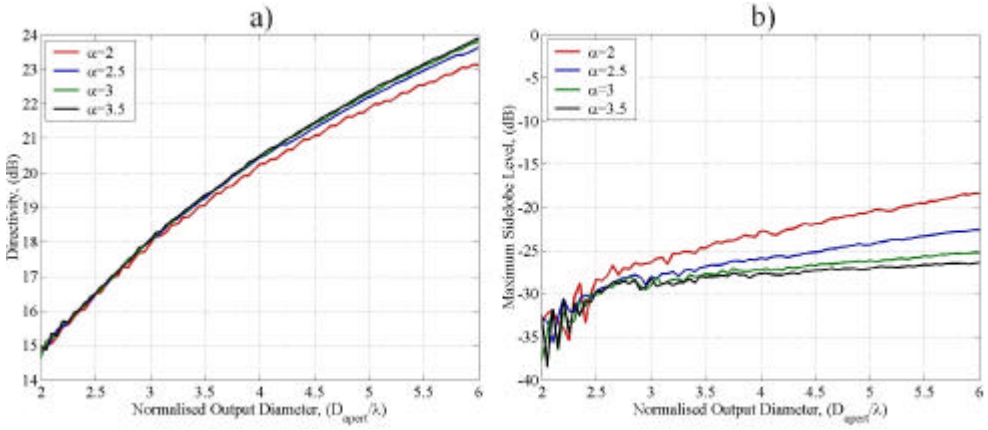

Figure 5.3. a) Directivity design curves for corrugated GPHA
b) Maximum sidelobe level design curves for corrugated GPHA

5.1.2 Corrugated GPHA versus corrugated conical TE_{11} to HE_{11} mode converters

Regarding the conversion efficiency it have been concluded that both techniques give practically identical results. Thus, the question is: What will be the advantage of using a corrugated GPHA instead a conical corrugated mode converter?

In order to be able to answer that question, we should complete the comparative study, including other performance parameters, as the bandwidth and return loss.

We will use two equivalent designs to compare their frequency response: the input diameter is selected to be $0.78 \cdot l$ and the output diameter $5 \cdot l$, the flare angle of the conical corrugated antenna is 5.33^{o} which corresponds with a $a=2.96$ for the corrugated GPHA.

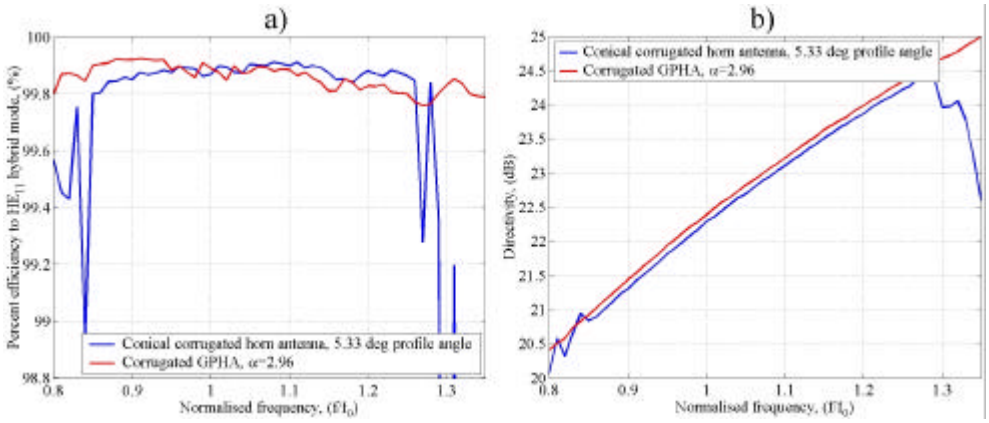

Figure 5.4. a) Bandwidth comparison in percentage efficiency to HE_{11} hybrid mode
b) Bandwidth comparison in directivity

In figures 5.4 and 5.5 we can see effectively that the corrugated GPHA TE_{11} to HE_{11} mode converter has a slightly wider bandwidth.

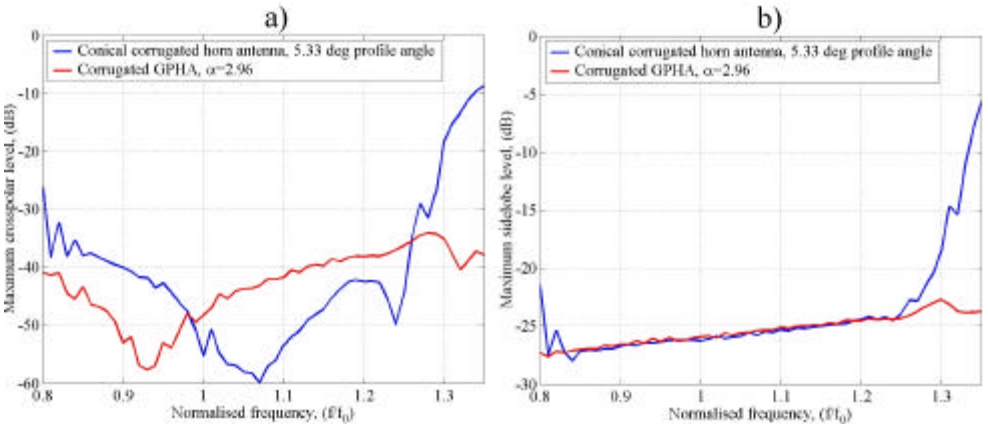

Figure 5.5. a) Bandwidth comparison in maximum crosspolar level
b) Bandwidth comparison in maximum sidelobe level

Also the wider response in return loss obtained for the corrugated GPHA mode converter is shown in figure 5.6.

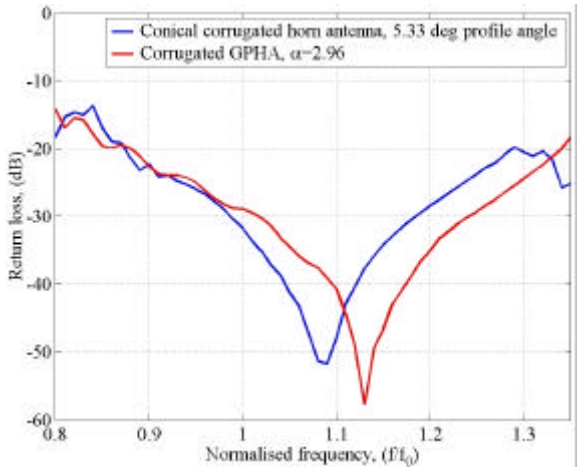

Figure 5.6. Bandwidth comparison in return loss

5.2 Design of a symmetric GPHA TE_{11} to HE_{11} mode converter

The two possibilities of corrugated TE_{11} to HE_{11} mode converters seen until now are very similar and also quite long. Would there be a possibility of designing shorter corrugated TE_{11} to HE_{11} mode converter maintaining the good performance?

The new possibility to be considered is called the symmetric GPHA [7,8] and it consists of two GPHA sections arranged in odd symmetry as depicted in figure 5.8. The new profile, $r(z)$, is given as:

$$f(z)=R_{in}\sqrt{1+\left(\frac{2\cdot z}{k\cdot v_0^2}\right)^2} \quad ; \quad v_0=a\cdot R_{in}$$

$$r(z)=\begin{cases} f(z) & z\le L/2 \\ -f(L-z)+2f\left(L/2\right) & z\ge L/2 \end{cases} \qquad (5.3)$$

being the L the length of the whole device, R_{in} the input radius, k the wavenumber and w_0 the beamwaist.

This new component has the advantage a smooth input and output parts and uses the gaussian propagating formula to increase quickly the profile angle obtaining a bigger diameter in a shorter length. At the second half part, the profile angle is reduced in order to guide the generated HE_{11} towards the aperture. This allows connectivity of the converter to other components.

At the throat, this component also includes an impedance transformer decreasing linearly from λ/2 to λ/4 the corrugation depth as any corrugated horn antenna with a smooth waveguide at the input port.

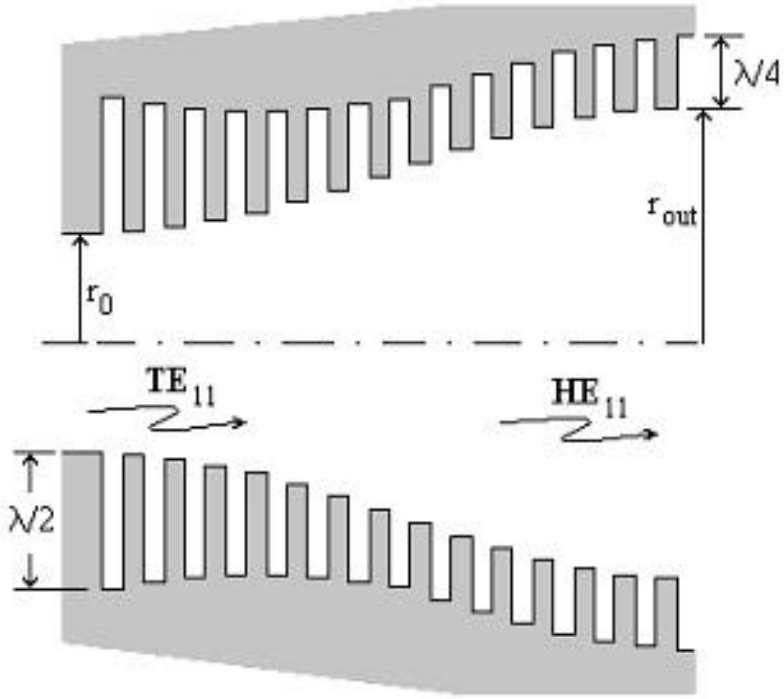

Figure 5.7. Symmetrical corrugated GPHA TE_{11} to HE_{11} mode converter

5.2.1 Symmetrical corrugated GPHA TE_{11} to HE_{11} mode converter performance

Assuming the same input diameter of $0.78 \cdot l$, the conversion efficiency to an HE_{11} mode and a fundamental Gaussian mode are depicted in figure 5.8.

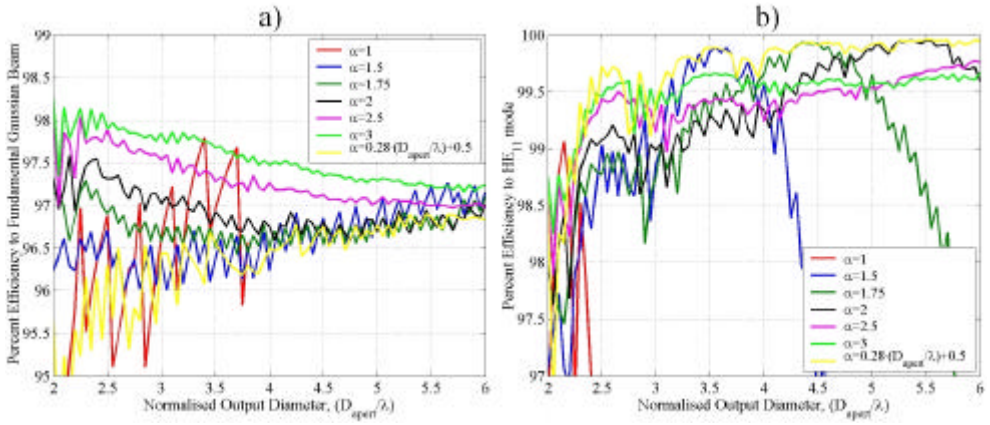

Figure 5.8. a) Efficiency of symmetrical corrugated GPHA to a fundamental gaussian beam
b) Efficiency of symmetrical corrugated GPHA to a HE_{11} hybrid mode

In figure 5.8, the high conversion efficiency of this new symmetrical corrugated GPHA converter is proved. Differently to the direct corrugated GPHA converter, this one doesn't present better efficiency as bigger is α parameter, in fact the best efficiency could be approximated by (empirical formula):

$$a = 0.28 \cdot \overline{D_0} + 0.5 \qquad (5.4)$$

where $\overline{D_0} = D_{apert} / l$ is the normalised output aperture diameter of the component in wavelengths. This optimal α parameter has been depicted as a yellow line in figures 5.8, 5.9 and 5.10.

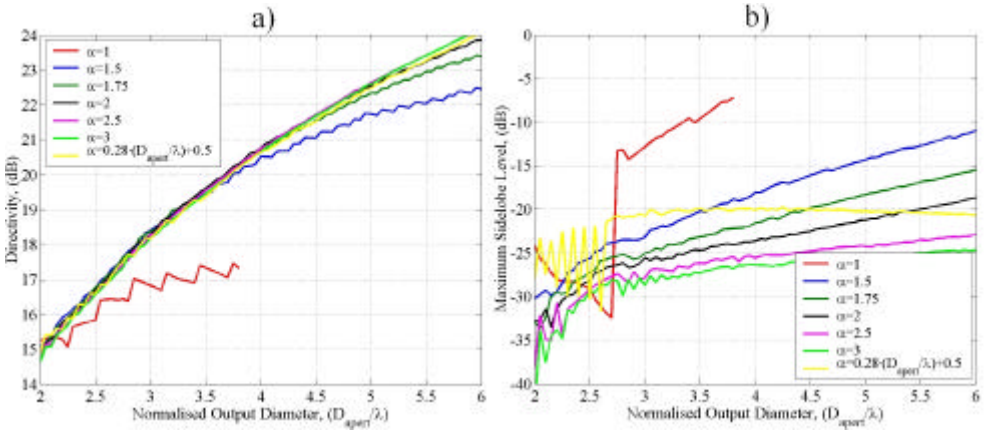

Figure 5.9. a) Directivity design curves for symmetrical corrugated GPHA
b) Maximum sidelobe level design curves for symmetrical corrugated GPHA

In figures 5.9a and 5.10b there is a special detail that makes this converter design slightly different from the other two previous ones:

- For the best possible result maximizing the HE_{11} mode conversion (yellow line), the efficiency to a gaussian beam is around *96.8%* whilst in the other two converters was around *98.2%*.
- The sidelobe level for this optimal case is limited to *–20 dB* while for the other two designs was around *–26 dB*.

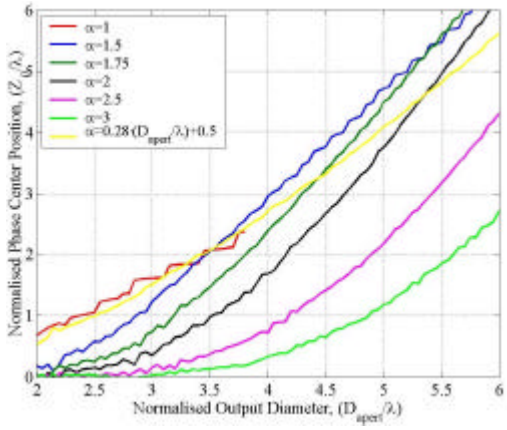

Figure 5.10. a) Normalized phase center position design curves for symmetrical corrugated GPHA

Usually, because of these limitations observed, we shall not use these symmetric GPHA as radiating antennas but as the initial part of a composed horn antenna that includes a pure GPHA section at its end. This type of compositions will be more extensively covered in following chapters.

Nevertheless, the symmetric GPHA is always a possibility to be consider if our design requirements enable us to use them, obtaining considerably short antennas.

5.3 Designing a Corrugated TE_{11} to HE_{11} mode converter

The optimum value of the α parameter has been obtained for the case of symmetric GPHA *TE_{11}-HE_{11}* mode converter to define the most pure *HE_{11}* mode (equation 5.4).

Similarly, we propose two new and empirical formulas to define the parameters of a conical (flare angle) and direct corrugated GPHA (α parameter) *TE_{11}-HE_{11}* mode converters to obtain the higher conversion efficiency to *HE_{11}* mode with the shorter length. The formulas have been extracted with the aid of figures 3.4b and 5.2b, and all of them are a function of the normalized output diameter $\overline{D_0}$.

For a conical corrugated TE_{11} to *HE_{11}* mode converter, the obtained formula can be written as follows:

$$\text{Profile angle } = j = \frac{70}{\overline{D_0}^{1.6}} \quad \text{degrees} \tag{5.5}$$

For a direct corrugated GPHA TE_{11} to *HE_{11}* mode converter the design equation will be:

$$a = \frac{2.57}{p} \cdot \sqrt{\overline{D_0}^{1.6}} \tag{5.6}$$

Equation 5.6 could be obtained from equation 5.5 selecting exactly the same profile angle as in the conical corrugated converter for the end of the component as it was explained in equation 5.2.

Then, with the use of equations 5.4, 5.5 and 5.6, we could define the best mode converter for a given output diameter.

In figure 5.11 the efficiencies to a fundamental gaussian beam and to a HE_{11} mode of each converter are shown. All the converters give conversion efficiencies to an HE_{11} hybrid mode above *99.9%*, for normalized aperture diameters higher than 4. In fact, the efficiency for the three models is nearly the same. Nevertheless, the efficiency to a fundamental gaussian beam is higher in the conical and GPHA models due to the higher sidelobe of the symmetrical GPHA one, (see figure 5.12b).

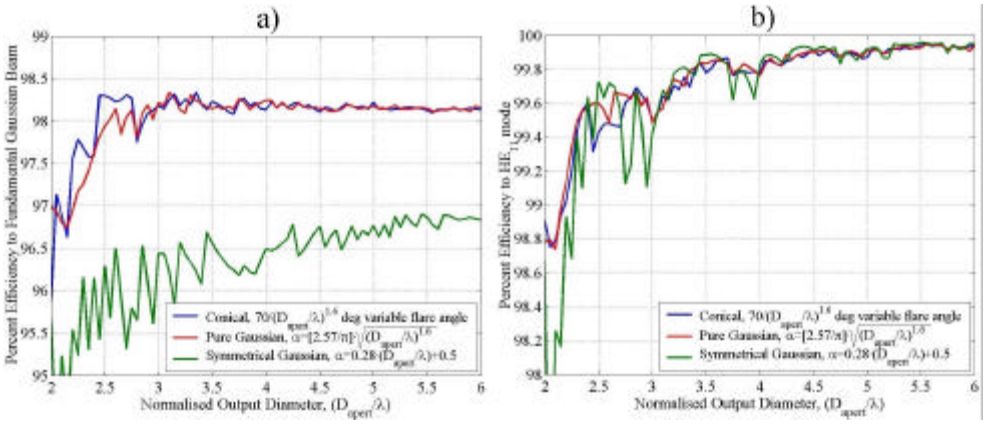

Figure 5.11. a) Efficiency of optimal TE_{11} to HE_{11} corrugated mode converters to a fundamental gaussian beam
b) Efficiency of optimal TE_{11} to HE_{11} corrugated mode converters to a HE_{11} hybrid mode

In figure 5.12a, it could be noticed that the symmetrical GPHA model has a slightly higher directivity for the same output aperture.

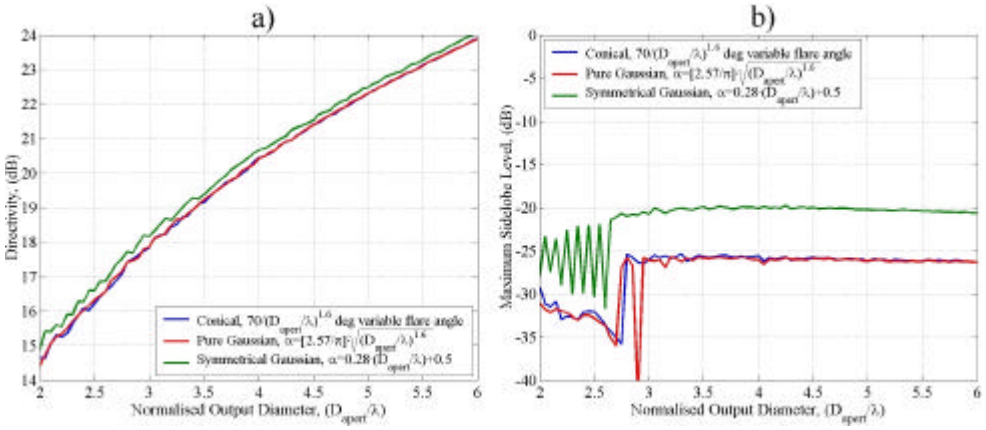

Figure 5.12. a) Directivity design curves for optimal TE_{11} to HE_{11} corrugated mode converters
b) Maximum sidelobe level design curves for optimal TE_{11} to HE_{11} corrugated mode converters

A comparison of the length in the three models is shown in figure 5.13a. From the figures, we can conclude that the symmetrical corrugated GPHA converter will usually be the best choice, except for low aperture diameters, ($\overline{D_0} \leq 3$), where the conical or direct GPHA give better efficiency solutions (see figure 5.11b) in a similar length.

From figure 5.13c, we can see that for large aperture diameters, the length of the symmetrical GPHA can be half of the other two models, so the length improvement is very high.

The mode content of the conical and GPHA corrugated *TE_{11}* to *HE_{11}* mode converters are really similar (figure 5.13b) because the mode mixture at the aperture is practically the same, (*83.3%* of TE_{11}, *14.9%* of TM_{11}, *0.9%* of TE_{12} and *0.7%* of TM_{12}). However, for the symmetrical corrugated GPHA the mode content is slightly different, (*82.2%* of TE_{11}, *12.7%* of TM_{11}, *3.2%* of TE_{12} and *1.5%* of TM_{12}). This could be probably the reason

of the different radiation behaviour of the symmetric GPHA in relation with the other two mode converters.

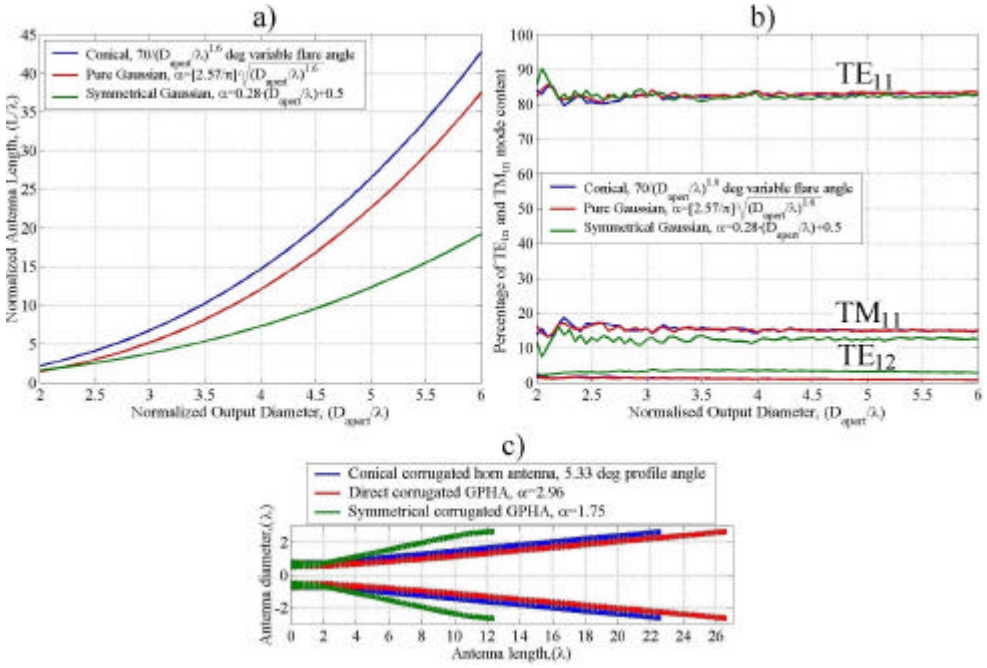

Figure 5.13. a) Length comparison for optimal TE_{11} to HE_{11} corrugated mode converters
b) Percentage of TE_{1n} and TM_{1n} mode content for optimal TE_{11} to HE_{11} corrugated mode converters
c) Length comparison for optimal TE_{11} to HE_{11} corrugated mode converters of $D_{apert}/l=5$

In relation with the bandwidth, the performance are quite similar between the three different techniques, improving with the Gaussian profiles (symmetric and non symmetric) the bandwidth and the return loss due to the smoothed initial part of the horn.

5.4 Corrugated TE_{11} to HE_{11} mode converter bandwidth comparison

To make a complete mode converter comparison between the three different models we have been explaining, it is necessary to inspect on the bandwidth of each mode converter.

For all the three designs, a normalized output diameter of $\overline{D_0}=5$ has been used. For this $\overline{D_0}$, the conical corrugated mode converter presents a profile angle of *5.33 degrees*, the direct GPHA mode converter presents an $\alpha=2.96$ and the symmetrical GPHA an $\alpha=1.9$.

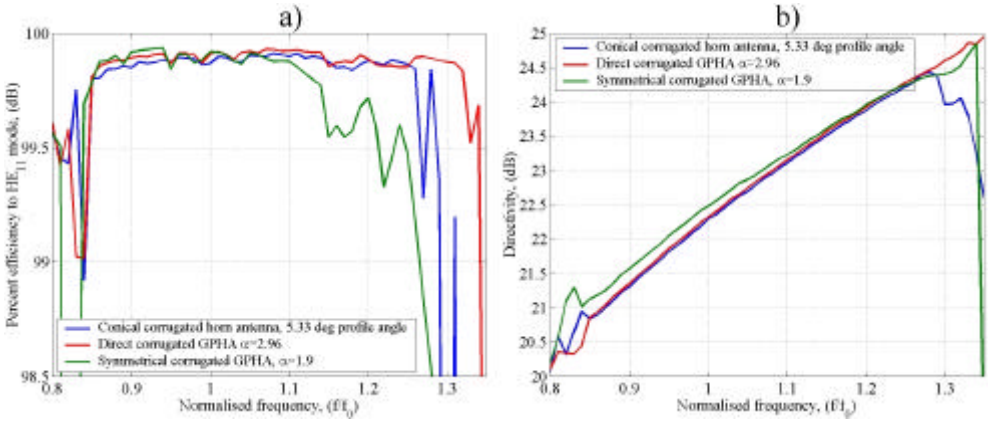

Figure 5.14 a) Bandwidth comparison in percentage efficiency to the HE_{11} hybrid mode
b) Bandwidth comparison in directivity

Figure 5.14a shows that the efficiency to the HE_{11} mode of the symmetrical GPHA converter is not as nice as the other two components in all the bandwidth (*25%* bandwidth with an efficiency above *99.8%*). The direct GPHA presents the best bandwidth efficiency, (*47%* bandwidth with an efficiency above *99.8%*). Conical corrugated converter presents also a wide bandwidth efficiency to HE_{11} (*41%* bandwidth whit an efficiency above *99.8%*).

If we have a look to figure 5.14b where the directivity of each design is plotted. The narrower bandwidth happens for the conical corrugated converter. The main difference in that figure is that the symmetrical converter presents at lower frequencies of the band a higher directivity than the other two.

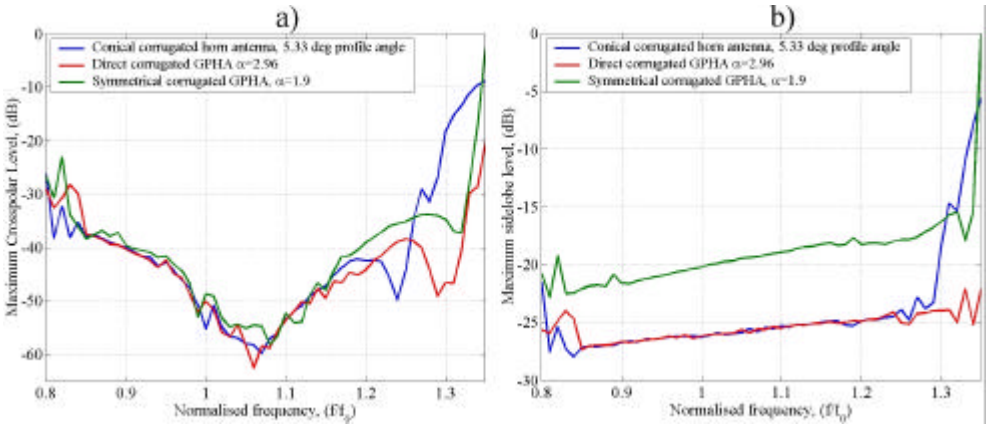

Figure 5.15. a) Bandwidth comparison in maximum crosspolar level
b) Bandwidth comparison in maximum sidelobe level

Figure 5.15a shows the bandwidth comparison in crosspolar level (*l/4* corrugation depth). The three converter models present a similar bandwidth response at lower frequencies of the band. At higher frequencies, the direct GPHA shows a slightly better crosspolar bandwidth followed by the symmetrical GPHA. The sidelobe level can be checked in figure 5.15b. As it was assumed, the symmetrical GPHA has a 5 dB higher sidelobe level response. The direct GPHA has a wider bandwidth response in sidelobe level.

Regarding return loss, figure 5.16, symmetrical GPHA and direct GPHA show a wider bandwidth at the lower part of the frequency band (smoother throat in those two converters), whereas at higher frequencies of the band the conical corrugated mode converter performs better results.

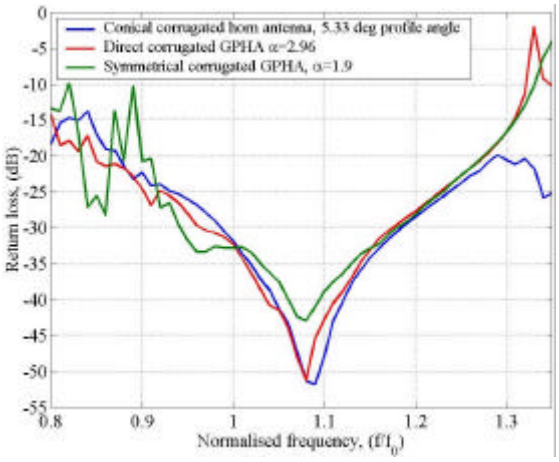

Figure 5.16. Bandwidth comparison in return loss

So, bandwidth performance of these corrugated mode converters is dominated by the direct GPHA mode converter that presents nearly always the wider bandwidth. Nevertheless, every application will lead to the election of one or other mode converter.

5.5 Other types of corrugated TE_{11} to HE_{11} mode converters

5.5.1 Example of a shorter TE_{11} to HE_{11} mode converter [9]

One valid example of other type of TE_{11} to HE_{11} mode converter is the one presented in [9] (figure 5.17a), a rather short length is obtained for such a wide diameter aperture converter. This converter presented in [9] has a length of $17.2 \cdot l$ for a $\overline{D_0}=6.4$ and an input diameter of $0.9 \cdot l$. The symmetrical mode converter presented in the previous sections would have an $\alpha=2.292$ (equation 5.4) for the same input and output diameters resulting in a length of $26.5 \cdot \lambda$.

This new converter [9] works very nice but for a narrower bandwidth (see figure 5.17b). Sometimes a solution like this one could be perfect for several applications.

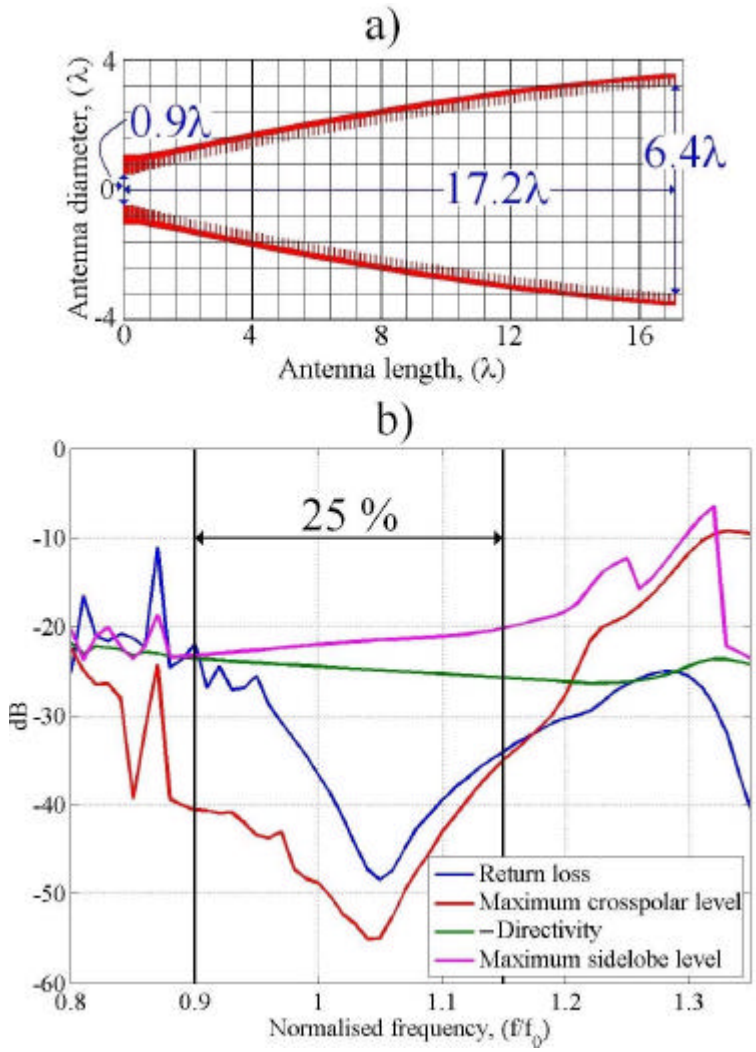

Figure 5.17. a) CSIRO TE_{11} to HE_{11} corrugated mode converter with aperture diameter of 6.4·l
b) Return loss, maximum crosspolar level, -directivity and maximum sidelobe level with the usable bandwidth of this mode converter

In this mode converter, the efficiency to an HE_{11} mode is not a nice as in the other converters (around 98.5%) seen in this chapter (see figure 5.18),

but as we will see in the next chapter, it can be enough for certain applications.

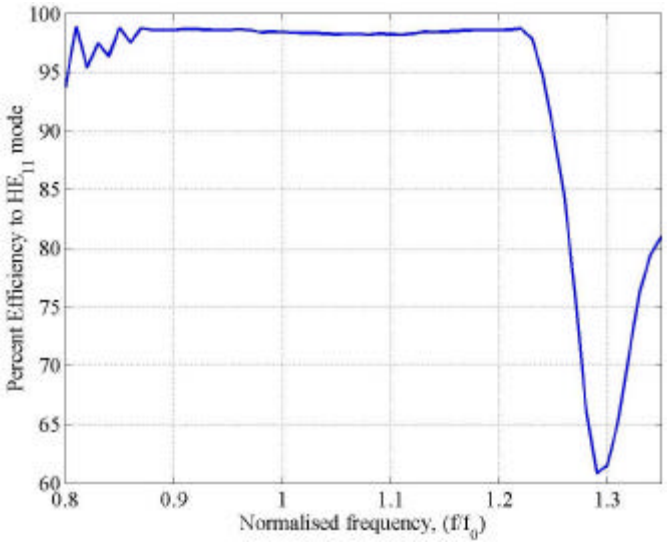

Figure 5.18. Percent efficiency in band to HE_{11} mode of CSIRO converter

5.5.2 Choked TE_{11} to HE_{11} mode converter

Another and very promising *TE_{11}* to *HE_{11}* mode converter is the choked waveguide mode converter.

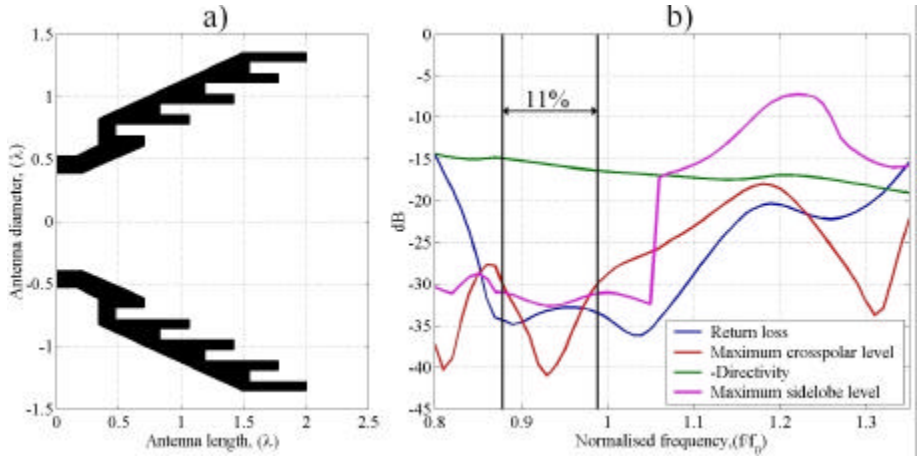

Figure 5.19. a) Choked waveguide TE_{11} to HE_{11} corrugated mode converter, $D_{apert}=2.6 \cdot l$

b) Return loss, maximum crosspolar level, -directivity and maximum sidelobe level with the usable bandwidth of this mode converter

In this case the corrugations are parallel to the electromagnetic waves propagation direction (see figure 5.19a). Really very short devices can be obtained with this technique (see figure 5.19a a TE_{11} to HE_{11} mode converter with $2.6 \cdot l$ aperture diameter and $2 \cdot l$ long and $0.78 \cdot l$ input diameter). The corresponding symmetrical mode converter would present an $\alpha = 1.228$ by means of equation 5.4 with $\overline{D_0} = 2.6$ and a corresponding length of $2.85 \cdot l$.

This compact mode converter has another very nice advantage: it reduces a lot the manufacture process because it doesn't present deep corrugations at the throat as the other corrugated profiles. Usually, these deep $l/2$ corrugations complicate a lot the manufacture for a milling machine.

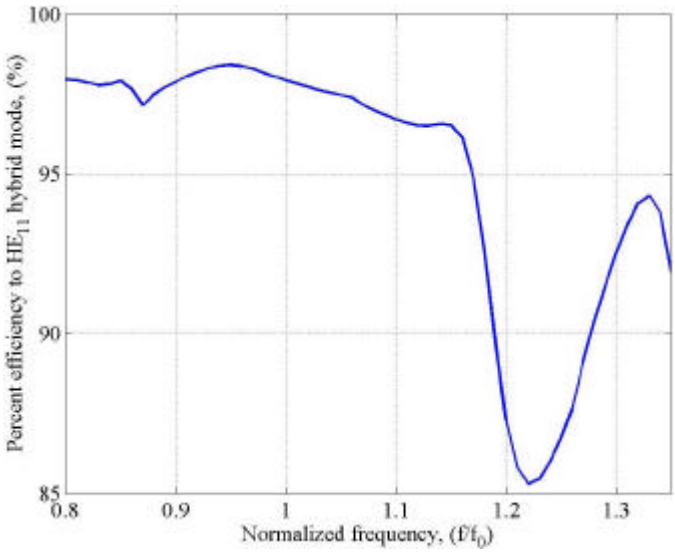

Figure 5.20. Percent efficiency in band to HE_{11} mode of choked converter

The disadvantage of this mode converter is its bandwidth (see figure 5.19b), around *10-15%*. Nevertheless it could be enough for many applications. Also, in this mode converter, the efficiency to an HE_{11} mode is

not very nice (see figure 5.20) as in the converters presented in this chapter (around 98%) but we will see in the next chapter that this one can be really good for several applications.

5.6 Conclusions

The TE_{11} to HE_{11} mode converter state of the art technology has been explained. Several empirical formulas have been defined to aid in the design of the different converters.

If the converter has vertical corrugations, the design will always have approximately the following properties:

- The input diameter corresponds to a monomode smooth waveguide.
- An impedance transformer of enough length that changes linearly the corrugation depth between $\lambda/2$ to $\lambda/4$ must be included at the throat.
- A controlled aperture angle, collecting smoothly the inside fields towards the output aperture.
- As smooth is the taper change of the converter as wide will be the usable bandwidth. Converters of very short length and sharp changes are used for narrow bandwidth requirements only.

Every application can determine the use of one or other design technique.

The use of the choked waveguide converter can reduce really a lot the length if the application has not much bandwidth, and this converter is also very easy to manufacture because of the lack of the $\lambda/2$ to $\lambda/4$ tapered corrugation depth change at the throat.

5.7 References

[1] Potter, P. D., "A New Horn Antenna with Suppressed Sidelobes and Equal Beamwidths", *Microwave Journal*, vol. VI, June 1963, pp. 71-78.

[2] Christophe Granet and Val Dyadyuk, "Compact Potter-Type Horns for a Traffic Management Radar", *AP2000 Millennium Conference on Antennas & Propagation*, 9-14 April 2000, Davos, Switzerland

[3] Gonzalo R., Del Río C. and Sorolla M., "Generation of the HE_{11} Mode from Monomode Smooth Circular Waveguide", Proc. *21st. International Conference on Infrared and Millimeter Waves, BTh8,* Berlin, July 1996.

[4] Gonzalo, R., Teniente, J. and Del Río, C., "Very Short and Efficient Feeder Design from Monomode Waveguide", *1997 IEEE AP-S International Symposium and URSI Radio Science Meeting*, 14-18 of July, Montreal, Canada.

[5] Gonzalo, R., Teniente, J. and del Río, C., "Improved Radiation Pattern Performance of Gaussian Profiled Horn Antennas", *IEEE Transactions on Antennas and Propagation*, Vol. 50, N. 11, pp. 1505-1513, November 2002.

[6] S.G. Hay, S.J. Barker, C. Granet, A.R. Forsyth, T.S. Bird, M.A. Sprey and K.J. Greene, "Multibeam Earth Station Antenna for a European Teleport Application", *2001 IEEE AP-S International Symposium and URSI Radio Science Meeting*, 8-13 of July, Boston, Massachusetts, United States

[7] Gonzalo R., Del Río C. and Sorolla M., "Generation of the HE_{11} Mode from Monomode Smooth Circular Waveguide", Proc. *21st.*

International Conference on Infrared and Millimeter Waves, BTh8, Berlin, Germany, July 1996.

[8] Spanish Patent P.9601636, "Mode converter: from the TE_{11} monomode circular waveguide mode to the HE_{11} corrugated circular waveguide mode", Authors: Carlos Del Río, Ramón Gonzalo, y Mario Sorolla, 11/07/1996.

[9] S.G. Hay, S.J. Barker, C. Granet, A.R. Forsyth, T.S. Bird, M.A. Sprey and K.J. Greene, "Multibeam Earth Station Antenna for a European Teleport Application" *2001 IEEE AP-S International Symposium and URSI Radio Science Meeting*, 8-13 of July, Boston, United States.

Chapter 6

Complete antenna design using corrugated Gaussian Profiled Horn Antennas

This chapter deals with the complete design of a corrugated GPHA. This means that we can design a short and nice corrugated horn antenna with the information contained here; beginning from a monomode input waveguide with the TE_{11} mode inside and obtaining the radiation pattern that we are seeking in a quite compact profile .

The idea of this chapter is provide all the information to help the designer to implement a first design that really meets nearly all the requirements (except length probably). This first design will not the better and shorter one. The experience of the designer with the aid of some *"rules of thumb"*, to be included at the end of this chapter, will help to achieve the final and optimal corrugated GPHA profile that best meets the specifications.

Also this first profile can be used as the initial profile of a corrugated horn antenna optimizing code. This will reduce the computing time quite a lot. We have our own optimizing code [1] to make corrugated GPHA's and the results we obtain from it are really nice.

To obtain the information needed to design the complete corrugated antenna, we will compile the information presented in chapters 4 and 5.

It seems easy to design the complete corrugated GPHA adding the information of those two chapters; firstly designing the TE_{11} to HE_{11} mode

converter with the information of chapter 5 and then adding the corrugated GPHA with the information of chapter 4. By means of stacking those two parts together we would have the complete design; but this chapter will reveal that it is not as easy as seems to be. In fact, the interaction of both parts will change the performance of both. A complete study of the components stacked together will be done in this chapter.

6.1 Complete design of a corrugated GPHA with a conical corrugated input as TE_{11} to HE_{11} mode converter

To design a complete corrugated antenna with a conical corrugated input section finishing with a corrugated GPHA; we must know first which is the directivity at the central frequency for the design that we need. If the requirement is given in terms of beamwidth a quick view of appendix III will directly change this parameter to directivity.

After knowing the directivity, we should select approximately the D_0 or inner diameter ($\overline{D_0} = D_0 / l$ where D_0 is the output diameter of the corrugated conical TE_{11} to HE_{11} mode converter and the input diameter of the corrugated GPHA section). To select this diameter, we could ideally have a look at figure 4.8. But this figure is the first one that changes due to the interaction of the two components stacked together.

In fact, what happens is that the directivity obtained for a given normalised inner diameter, is approximately around 1 dB higher that the directivity curves from figure 4.8.

At this point, we should consider the complete set of mode converter and gaussian section together (figure 6.1) for directivity instead of figure 4.8; assuming that the conical corrugated converter flare angle has been

selected by means of equation 5.5 ($j = 70/\left(\overline{D_0}\right)^{1.6}$ degrees), the input diameter is around $0.78 \cdot l$ and trying with different lengths for the final section (f := 0.05 to 0.3).

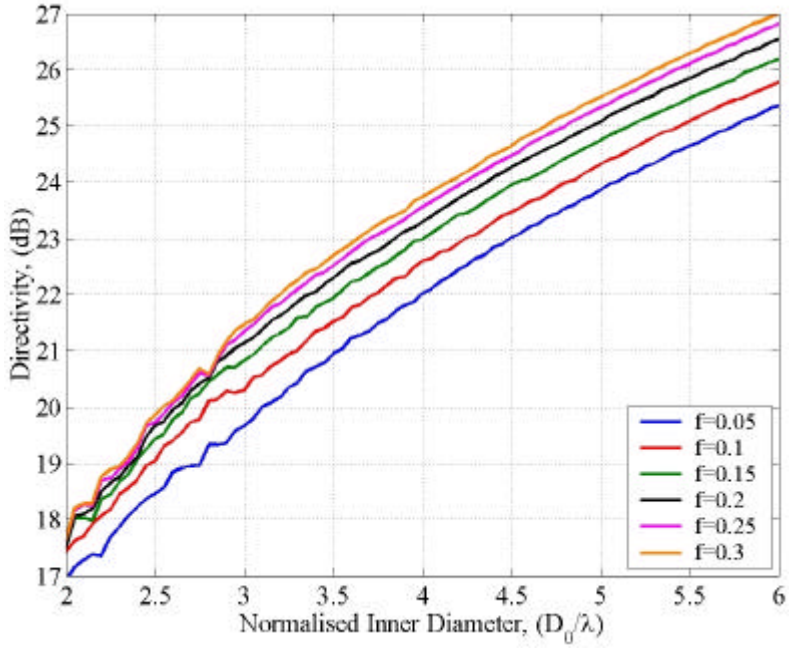

Figure 6.1 Directivity design curves for the combination conical+GPHA

From chapter 4 we select the length in terms of the parameter defined in equation 4.3, *length factor*, (f), according to the maximum allowable sidelobe level for our design, (figure 4.6b). Unfortunately, also this parameter changes for the complete design and we should instead make use of figure 6.2b to select the appropriate value of f. The required length for the second corrugated GPHA section will be longer than the one assumed in chapter 4 for the same sidelobe level.

Also from chapter 4, we knew that α parameter of the corrugated GPHA section was fixed at $\alpha=0.59$ for a better efficiency of the radiated field to a fundamental gaussian beam. However, α parameter for the

complete corrugated antenna must change and it depends on both, the normalized inner diameter, ($\overline{D_0}$), and the length factor, (*f*).

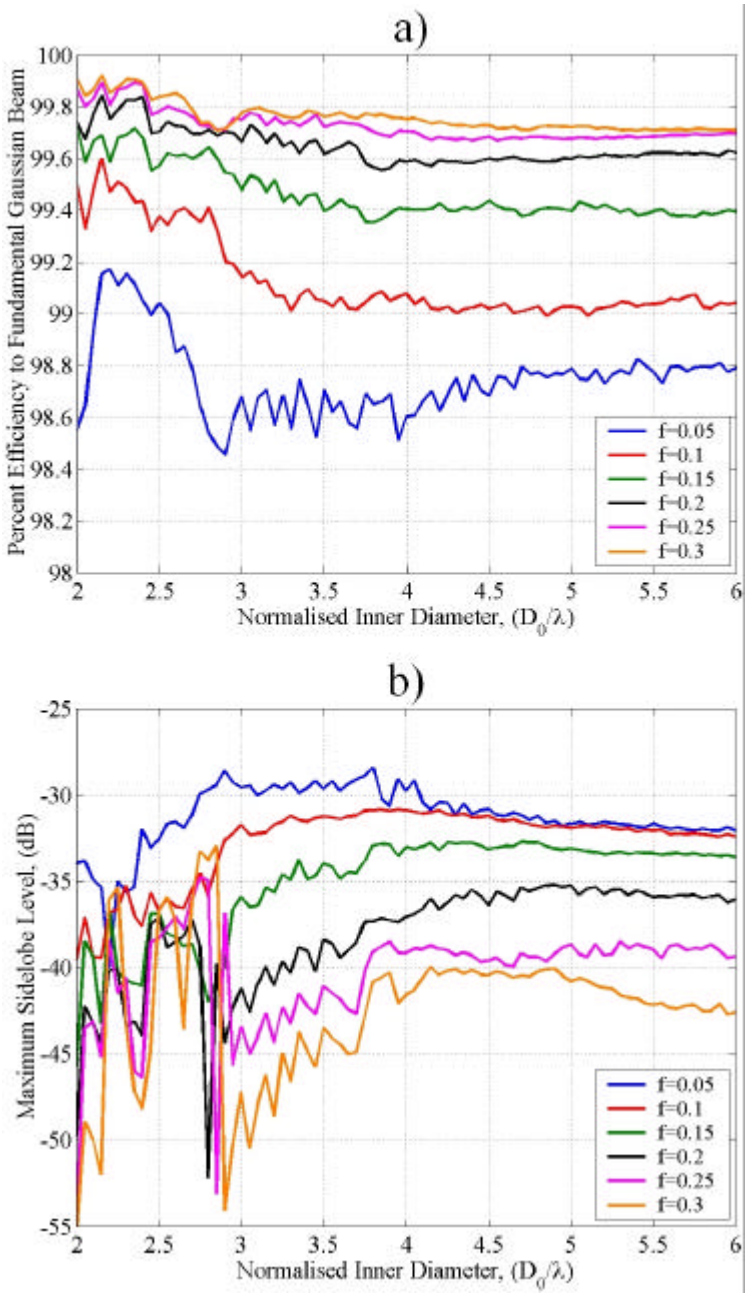

Figure 6.2 a) Efficiency to a fundamental gaussian beam for the combination conical+GPHA
b) Maximum sidelobe level for the combination conical+GPHA

Optimum α parameter is below *0.59* for short corrugated GPHA sections and/or small inner diameters and above *0.59* for long corrugated GPHA sections and/or large inner diameters. A rather complex empirical formula to select the optimum α parameter is given in equation 6.1.

$$a = \left(\frac{1.6 - 2 \cdot f}{100} \right) \cdot \overline{D_0} + \left(\frac{f}{2} \right)^{0.18} - \frac{f}{4} \qquad (6.1)$$

where $\overline{D_0}$ is the normalised inner diameter of the corrugated GPHA section and *f* is the length factor.

To finish the combination conical+GPHA design we should select the corrugation values, and this is the easiest part. As defined in chapters 3 to 5, corrugation period (*p*) should be around *l/5*, corrugation tooth width (*w*) around *p/2* or thinner, corrugation depth around *l/4*, first corrugation depth around *l/2* tapered to *l/4* with an impedance transformer of a length approximately equal to the distance from the throat of the corrugated horn antenna to where the antenna profile reaches an inner diameter where the TM_{11} mode is in propagation.

With the information considered until this point we have enough to fully design the antenna we desire.

As summary, in figure 6.3a, the normalised antenna length against directivity is depicted; this figure shows that as longer we make the second section of the antenna (increasing *f*, the length factor) as shorter the complete profile will be. Additionally, the sidelobe level will decrease increasing *f*, this means that a shorter combination conical+GPHA gives a better radiation pattern, (see figure 6.2b). The disadvantage is that a longer second section corrugated GPHA means a wider output diameter of the

complete antenna (see figure 6.3b) and a compromise between length and output diameter for a given directivity must be reached.

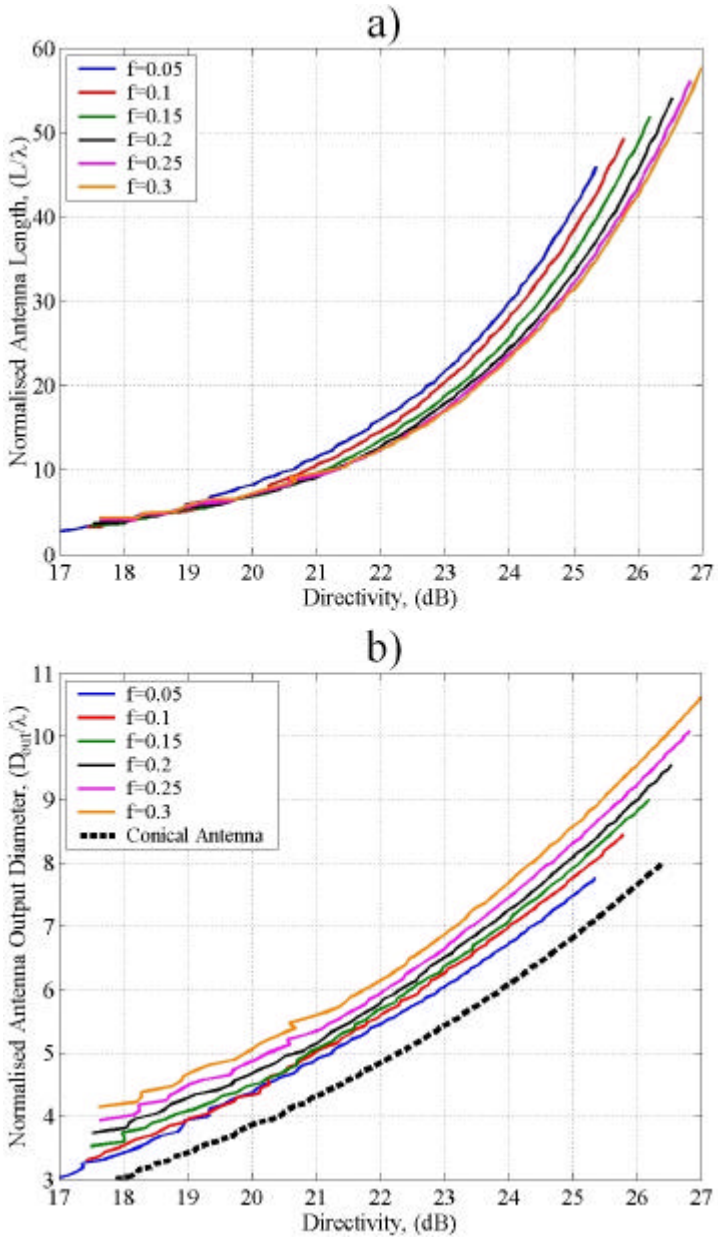

Figure 6.3 a) Normalised antenna length against directivity for the combination conical+GPHA

b) Normalised antenna output diameter against directivity for the combination conical+GPHA (conical corrugated horn antenna output diameter is also depicted for a better comparison)

6.1.1 Design of a 22 dB combination conical+GPHA

As a practical example of how to design a complete corrugated antenna of this kind, and also to compare it with the conical corrugated horn antenna designed in chapter 3; a 22 dB directivity complete antenna will be performed.

With the aid of figures 6.1, 6.2b and 6.3 and using an input diameter of $0.78\cdot\lambda$, we can fill the following table:

Normalised inner diameter,($\overline{D_0}$)	**GPHA factor of length, (f)**	**Sidelobe level, (dB)**	**Normalised antenna length, (l)**	**Normalised antenna output diameter, (l)**
3.99	0.05	-29.6 dB	$15.99\cdot\lambda$	$5.45\cdot\lambda$
3.73	0.1	-31.0 dB	$14.59\cdot\lambda$	$5.60\cdot\lambda$
3.52	0.15	-34.0 dB	$13.53\cdot\lambda$	$5.69\cdot\lambda$
3.36	0.2	-38.9 dB	$12.77\cdot\lambda$	$5.79\cdot\lambda$
3.26	0.25	-42.5 dB	$12.41\cdot\lambda$	$5.94\cdot\lambda$
3.2	0.3	-48.6 dB	$12.48\cdot\lambda$	$6.14\cdot\lambda$

Table 6.1. 22 dB directivity combination conical+ GPHA design parameters

The shortest choice is the one with a corrugated GPHA section of *f=0.25*, but its output diameter is quite large.

The antenna designed in chapter 3 had a side-lobe requirement of -25dB, and as it can be seen from table 6.1, the worst case is better than this (the length for the conical horn was 17.8λ). In order to have some possibility to play with the design parameters we will reconsider the sidelobe requirement down to –35dB.

With a more detailed observation of the figures 6.1, 6.2 and 6.3, for *-35 dB* sidelobe level we will obtain: $\overline{D_0} = 3.47$ and *f=0.165*. The flare

angle for the conical corrugated mode converter (equation 5.5) will be of $70/3.47^{1.6} = 9.56$ *degrees.* Then, the conical corrugated converter will result in a length of $8 \cdot l$, with an input diameter at the throat of $0.78 \cdot l$. The corrugated GPHA part will result in a length of $\lambda \cdot 3.47 \cdot \sqrt{0.165 \cdot \left(1+3.47^2\right)} = 5.1 \cdot ?$ (equation 4.3), and with an $\alpha = 0.641$ (equation 6.1).

The corrugation parameters we are going to use for this antenna design will be: corrugation period ($p = l/5$), corrugation tooth width ($w = p/3$), corrugation depth ($d = l/4$), first corrugation depth $l/2$ linearly tapered to $l/4$ in a length of $1.3 \cdot l$.

The total length of this antenna will be of $13.27 \cdot l$ taking into account the fact that corrugations provide discrete lengths and each section length is defined by an integer number of corrugation periods. The formula for the length of a complete corrugated antenna of two sections will be:

$$Total\ length = ceil(L_{section\ 1}/p) \cdot p + ceil(L_{section\ 2}/p) \cdot p + w \qquad (6.2)$$

where the operator *ceil(x)* rounds x to the nearest integer towards infinity. $L_{section\ 1}$ and $L_{section\ 2}$ are the calculated lengths of the two sections and p, w are the corrugation period and corrugation tooth width respectively.

In figure 6.4 the resultant antenna is depicted as well as its resultant far field radiation pattern.

This antenna design is $4.5 \cdot l$ shorter than the conical corrugated design of chapter 3 and presents *10 dB* lower sidelobe level. On the other hand its output diameter is $0.86 \cdot l$ wider.

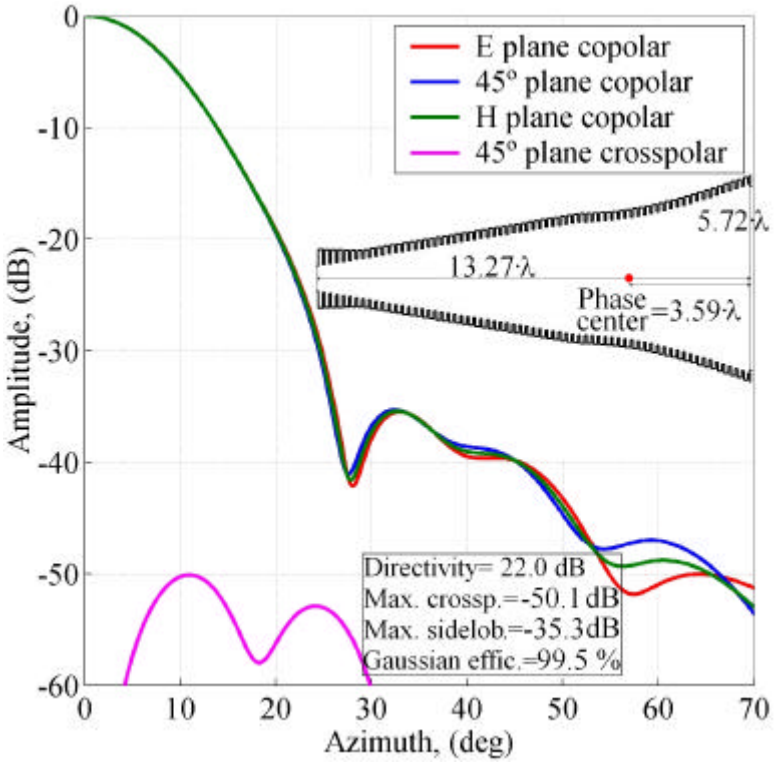

Figure 6.4. Combination of corrugated GPHA with a conical corrugated mode converter input for 22 dB directivity and –35 dB sidelobe level

The reason why GPHA's present wider output diameters for the same directivity is strongly related with the position of its phase centre, in fact as it can be seen in figure 6.4, the phase centre for the combination conical + GPHA design is placed at $3.59 \cdot l$ from the aperture (27% of the total antenna length, in this example), compared to the conical corrugated horn antenna design of figure 3.10 where the phase centre was only a 14% inside of the horn (see figure 3.10).

A phase centre placed far away from the aperture of the horn antenna gives less directivity for a given output diameter (disadvantage) but also gives more stability in the phase centre position along a wider frequency band (advantage).

An optimisation of this example of a combination conical + GPHA is still possible, and a reduction in length of at least 10% should be quite easy to obtain. A method that usually works to optimise the length is to shorten the input converter an lengthen the corrugated GPHA section increasing a little the α value to reduce the output diameter.

6.2 Complete design of a corrugated GPHA with a corrugated GPHA input as TE_{11} to HE_{11} mode converter

The design of a combination of a corrugated GPHA with another corrugated GPHA at its input that serves as TE_{11} to HE_{11} mode converter is not needed to be covered specifically. The results will be just the same as the ones described with conical corrugated mode converter but with a bit longer profile and better bandwidth specially regarding return loss. The formula to be used to design the first section corrugated GPHA mode converter will be the given in equation 5.6, ($a=2.57/p\cdot\sqrt{D_0^{1.6}}$).

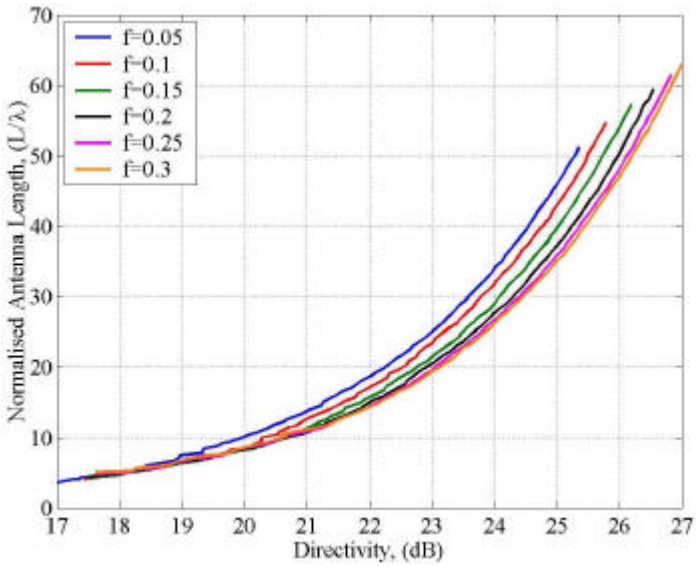

Figure 6.5 Normalised antenna length against directivity for the combination GPHA + GPHA

Figures 6.1, 6.2 and 6.3b can be used directly for the design, the only difference will be that the figure 6.3a (complete antenna length) is directly substituted by figure 6.5.

6.3 Complete design of a corrugated GPHA with a symmetrical corrugated GPHA input as TE_{11} to HE_{11} mode converter

To design a combination of a corrugated GPHA with another symmetrical GPHA at the input, is really similar to the last described designs. The only difference is that the formula selected to define optimum α parameter given in chapter 5, (equation 5.4), doesn't work optimally with this complete design.

The reason is that the symmetrical corrugated GPHA TE_{11} to HE_{11} mode converter presented a sidelobe level around *–20 dB* for that empirical formula. In fact, we obtained the equation 5.4 to achieve the highest possible efficiency to the HE_{11} mode at its aperture and not the lowest sidelobe level.

Then, another formula for the α parameter for the symmetrical corrugated GPHA with lower sidelobe level should be specified.

After a deep and careful study of figure 5.9b, and consider several possibilities, we have found the optimum formula for the symmetrical corrugated GPHA that gives a nice compromise between length and performance of the complete antenna. This formula is expressed in equation 6.3 and achieves a sidelobe level in the symmetrical corrugated GPHA converter of approximately –23 to -24 dB, (see figure 6.6), instead of the

-20 dB sidelobe level of figure 5.9b. But it results in a longer profile unfortunately.

$$a = 0.36 \cdot \overline{D_0} + 0.57 - e^{\left(2.2 - 2.5 \cdot \sqrt{\overline{D_0}}\right)} \tag{6.3}$$

where $\overline{D_0}$ is the normalised inner diameter.

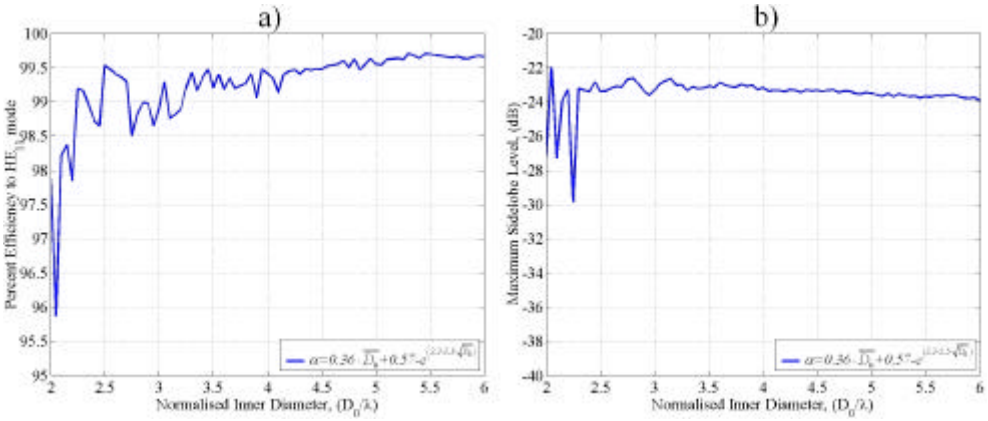

Figure 6.6. a) Efficiency of this symmetrical corrugated GPHA to a HE_{11} hybrid mode
b) Maximum sidelobe level for this symmetrical corrugated GPHA

After the definition of the equation for the symmetrical corrugated GPHA, we can describe completely as in the previous case, the design method for this combination symmetric GPHA + GPHA.

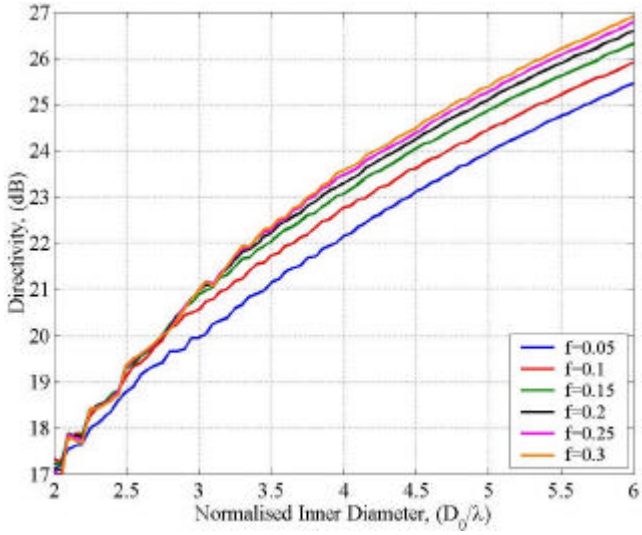

Figure 6.7 Directivity design curves for the combination sym. GPHA + GPHA

To start the design, we need to select from figure 6.7 the needed directivity of our design which will give a value for $\overline{D_0}$.

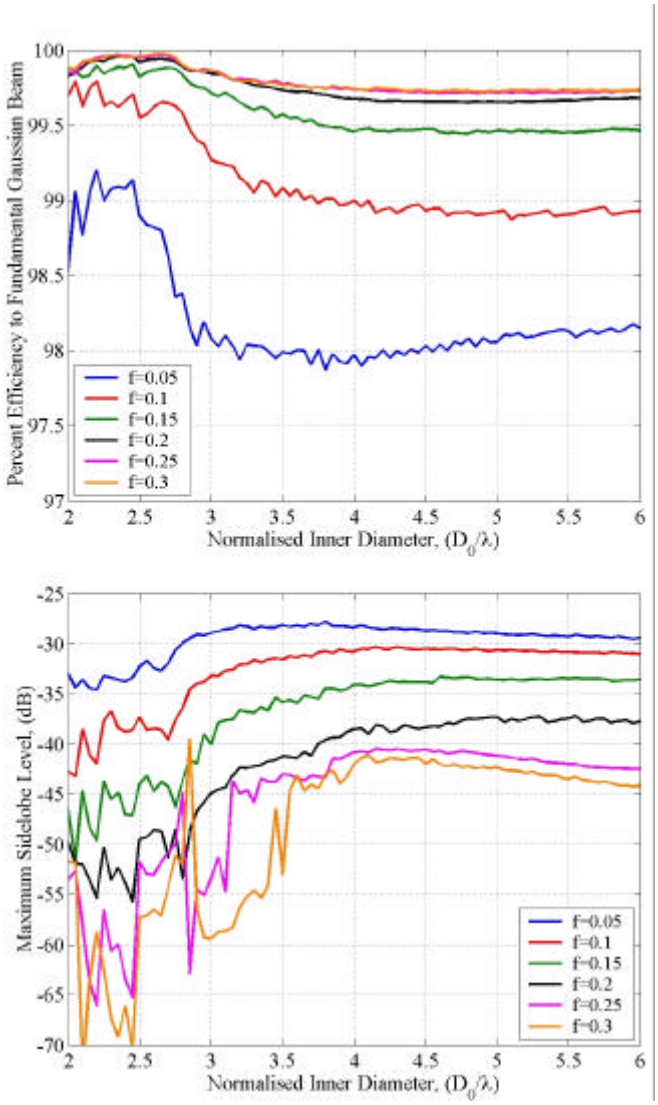

Figure 6.8 a) Efficiency to a fundamental gaussian beam for the combination symmetrical GPHA + GPHA
b) Maximum sidelobe level for the combination symmetrical GPHA + GPHA

The value of $\overline{D_0}$ is affected by the sidelobe level we want to achieve in the design. Then we must consider figure 6.8b in order to select exactly

the length of the second section corrugated GPHA for the desired side-lobe level. Figure 6.9 can help us to select the most compact profile that fulfils all of our requirements. The design procedure is exactly the same as in the last two sections, but with the use of new figures.

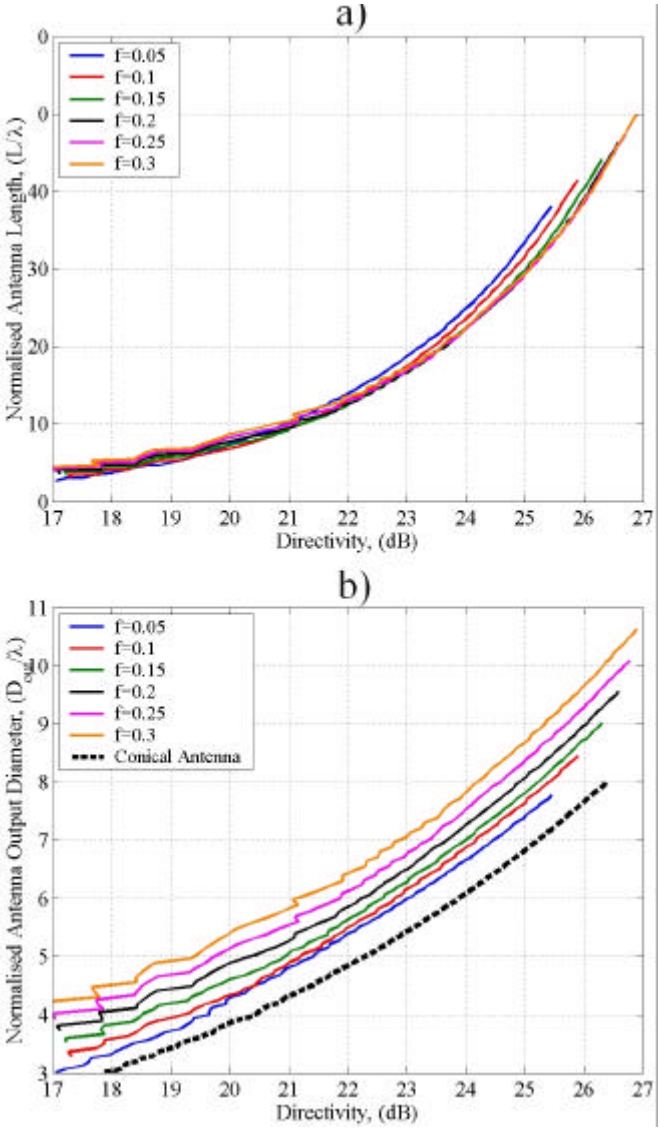

Figure 6.9 a) Normalised antenna length against directivity for the combination Symmetrical GPHA + GPHA

b) Normalised antenna output diameter against directivity for the combination symmetrical GPHA + GPHA (conical corrugated horn antenna output diameter is also depicted for a better comparison)

6.3.1 Design of a 22 dB combination symmetrical GPHA + GPHA

Again, as a practical example of how to design a complete corrugated antenna, and also to compare it with the conical corrugated horn antenna designed in chapter 3; we are going to design a *22 dB* directivity combination of a GPHA output section with a symmetrical corrugated GPHA mode converter as input.

With the aid of figures 6.7, 6.8b and 6.9 and using an input diameter of 0.78·λ, we can summarize the following table:

Normalised inner diameter,($\overline{D_0}$)	**GPHA factor of length, (f)**	**Sidelobe level, (dB)**	**Normalised antenna length, (l)**	**Normalised antenna output diameter, (l)**
3.94	0.05	-28.2 dB	13.85·λ	5.39·λ
3.65	0.1	-31.1 dB	12.93·λ	5.50·λ
3.48	0.15	-35.6 dB	12.48·λ	5.64·λ
3.41	0.2	-41.6 dB	12.53·λ	5.86·λ
3.37	0.25	-43.5 dB	13.07·λ	6.12·λ
3.37	0.3	-54.9 dB	13.57·λ	6.43·λ

Table 6.2. 22 dB directivity combination symmetrical GPHA + GPHA design parameters (symmetrical corrugated GPHA input converter)

With the information of table 6.2 we should decide what design to do. Again, to compare it with the antenna designed in chapter 3 and with the antenna designed in the first section of this chapter, we have decided to fix the maximum sidelobe level to *–35 dB*.

In this case, we can extract from the table the following parameters for the design: $\overline{D_0} = 3.48$ and $f=0.15$. The α parameter (equation 6.3) for the symmetrical corrugated GPHA converter input should be

$a=0.36\cdot 3.48+0.57\text{-}e^{\left(2.2\text{-}2.5\cdot\sqrt{3.48}\right)}=1.74$. Thus, the symmetrical corrugated GPHA converter will result in a length of $7.34\cdot l$, with an input diameter at the throat of $0.78\cdot l$. The second corrugated GPHA part will result in a length of $\lambda\cdot 3.48\cdot\sqrt{0.15\cdot\left(1+3.48^2\right)}=4.88\cdot ?$ (equation 4.3), and with an $\alpha=0.635$ (equation 6.1).

The corrugation parameters we are going to use another time for this antenna design will be: corrugation period ($p=l/5$), corrugation tooth width ($w=p/3$), corrugation depth ($d=l/4$), first corrugation depth $l/2$ linearly tapered to $l/4$ in a length of $1.73\cdot l$.

The total length of this antenna will be of $12.48\cdot l$ calculated by means of equation 6.2. The output diameter is $5.64\cdot l$. In figure 6.10 the resultant antenna is depicted as well as its resultant far field radiation pattern.

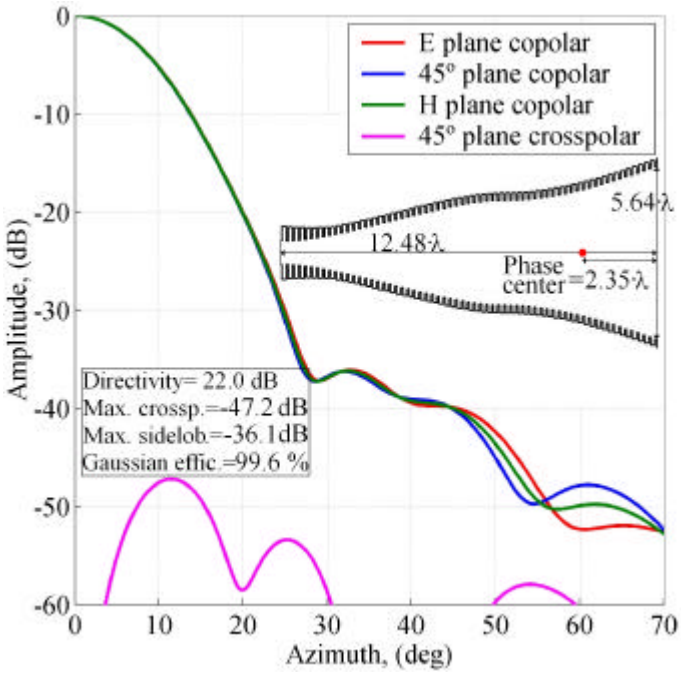

Figure 6.10. Combination symmetrical GPHA + GPHA of 22 dB directivity and -35 dB sidelobe level

This antenna design is $5.3 \cdot l$ shorter than the conical corrugated design of chapter 3 and presents *10 dB* lower sidelobe level but its output diameter is $0.78 \cdot l$ wider. It is also $0.8 \cdot l$ shorter than the one with conical corrugated converter input and presents a $0.08 \cdot l$ narrower output diameter.

The phase centre for this combination symmetrical GPHA + GPHA design is also placed inside the horn antenna $2.35 \cdot l$ (a 19% inside from the output aperture, in this example). So it is not as inside the horn antenna as in the corrugated GPHA with conical corrugated input converter (27% inside).

6.4 Comparison between different combinations

Once we know how to design a corrugated GPHA we need to know which method to select depending upon our requirements. In fact, what we would pursue is to design the most compact antenna profile that meets all of our requirements.

In the following pages, figures 6.11, 6.12 and 6.13 will help for sure a lot to select the optimum design. All the figures are based in the formulas described before in the chapter and depend on the length of the second section corrugated GPHA.

Usually, the most compact profile will be the combination symmetrical GPHA + GPHA, but in some cases, another input profiles must be chosen. Length, output diameter, sidelobe level and bandwidth (will be covered more extensively in the following sections), will be the requirements to achieve and will lead to the prefect design for sure.

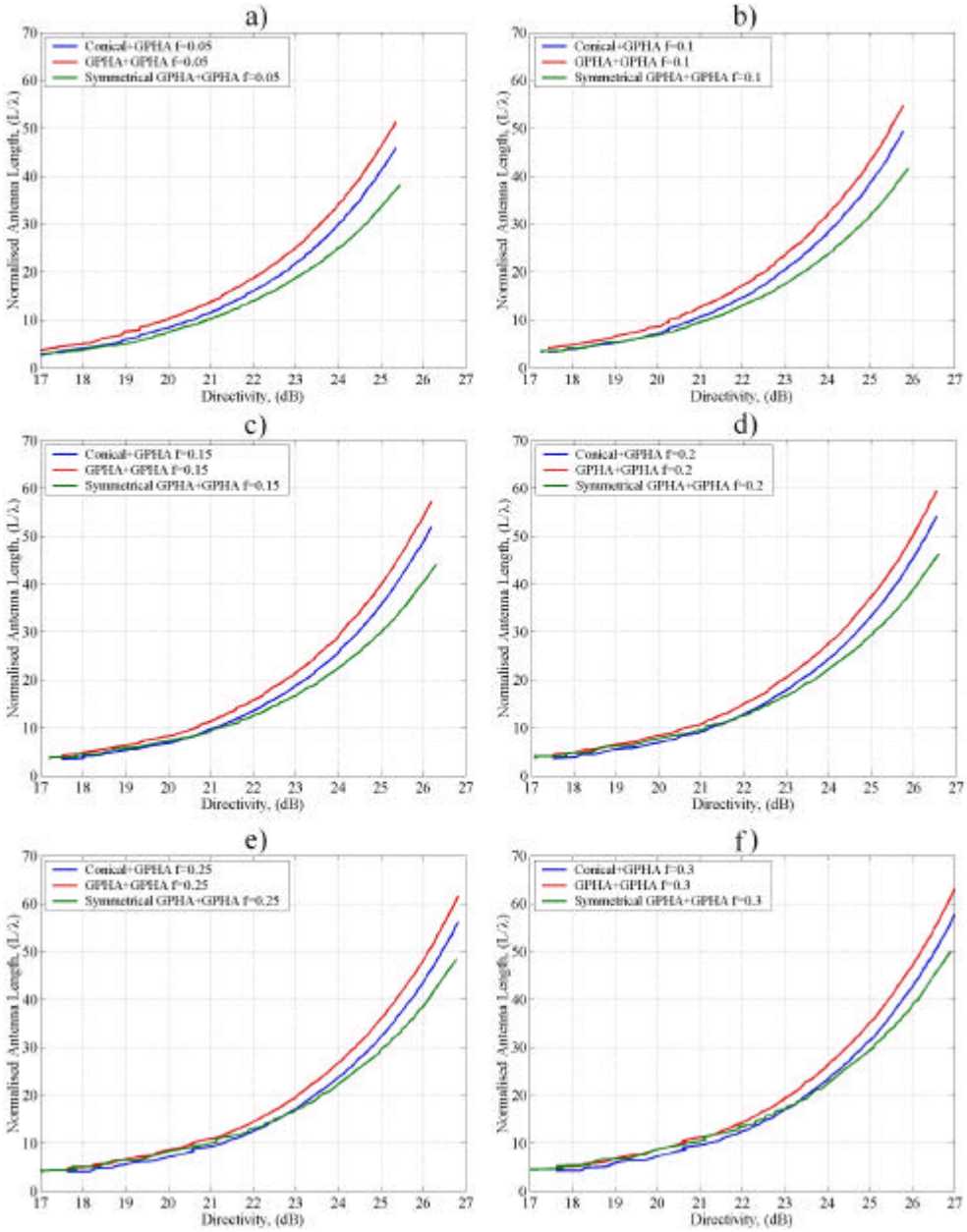

Figure 6.11. Length comparison of the three different models
a) f=0.05 b) f=0.1
c) f=0.15 d) f=0.2
e) f=0.25 f) f=0.3

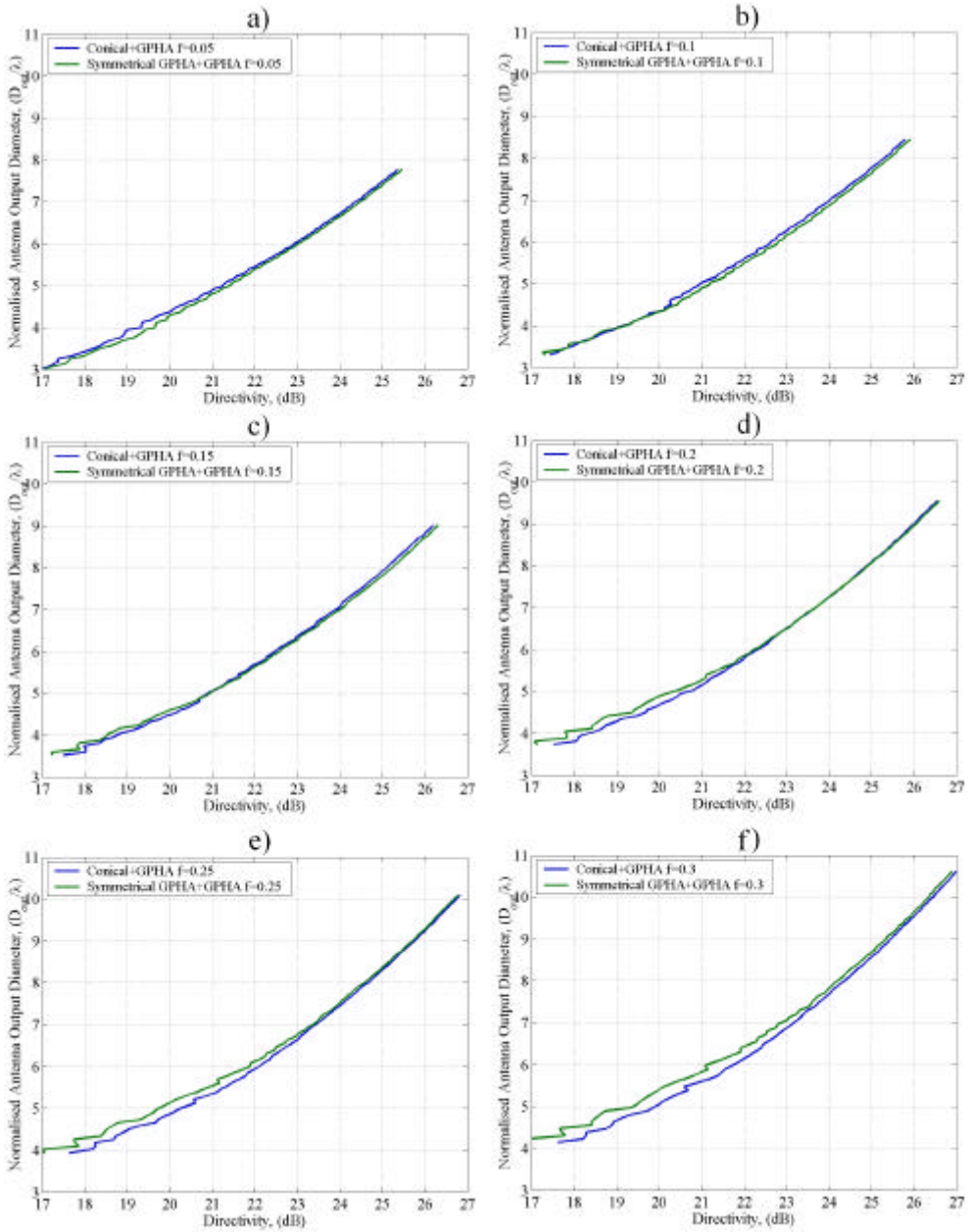

Figure 6.12. Output diameter comparison of three different models
a) f=0.05 b) f=0.1
c) f=0.15 d) f=0.2
e) f=0.25 f) f=0.3

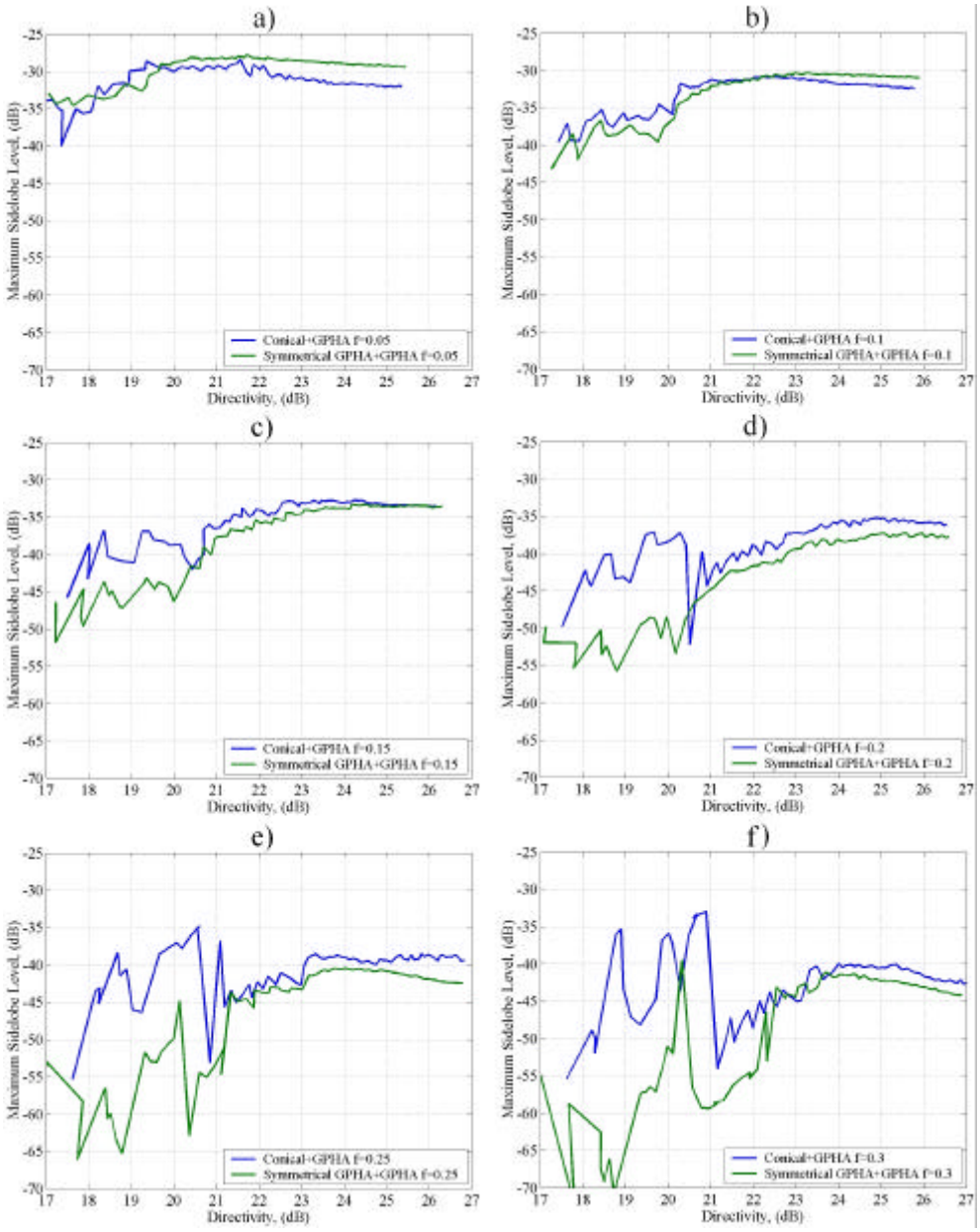

Figure 6.13. Max. sidelobe level comparison of three different models
a) f=0.05 b) f=0.1
c) f=0.15 d) f=0.2
e) f=0.25 f) f=0.3

6.5 Other possibilities to excite a corrugated GPHA

During the development of this chapter, we have proved that it is not strictly necessary to use a perfect TE_{11} to HE_{11} mode converter at the input of a corrugated GPHA. In fact, the really important idea is to provide at the input of the second GPHA section a field that has as lower sidelobes as possible, with equal beamwidths and low crosspolar level. The best feeding field of a corrugated GPHA would be just a high purity gaussian beam.

This property of corrugated GPHA's supposes some degree of freedom to develop the design of the input section. In fact, we can make use of another profiles that give a nice radiation pattern and cascade at their aperture some section of a corrugated GPHA. These new designs will usually provide shorter solutions. In the following paragraphs, two different models are presented, all designs of the 22 dB directivity with –35 dB sidelobe level will be considered.

6.5.1 Design of a 22 dB combination CSIRO [2] + GPHA

The people from CSIRO describe in [2] a complete antenna with a corrugated GPHA as final section and a new short input profile. Their short profile combines some properties from conical corrugated horn antennas and other from symmetrical corrugated GPHA's.

In figure 6.14 we can see that their profile can be divided in three main parts. It assumes a quick and smooth change in the slope at the beginning, (less than 10% of the total length), a conical profile to get quickly the needed diameter (more than 65% of the total length), and a smoothed end to connect to the corrugated GPHA second section (less than 25% of the total length). It presents two main differences with the symmetrical GPHA profile, at the input part the slope changes quicker, (nearly as in a conical

corrugated horn antenna), and at the final part doesn't finishes with a flat slope, it just closes a little the profile.

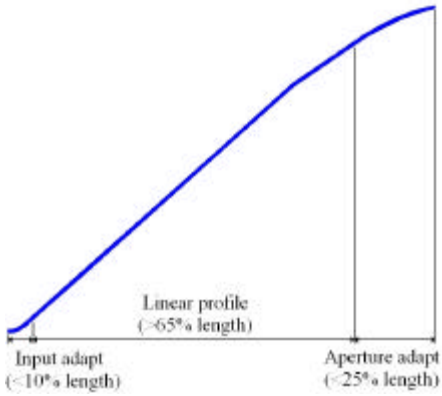

Figure 6.14. CSIRO profile for the input section of a complete corrugated GPHA

With this idea of a new corrugated input, the 22 dB directivity horn antenna with –35 dB sidelobe level has been designed. In fact, the first part of the combination symmetrical GPHA + GPHA of section 6.3.1 has been directly substituted by a 6·λ long CSIRO profile with an output diameter of 3.48·λ and an input diameter of 0.78·λ. To design the CSIRO corrugated profile, a polynomial has been defined to follow the curve. The parameters of the second section corrugated GPHA have remained the same.

In figure 6.15 a reduction in length of 1.4·λ with respect to the antenna of section 6.3.1 can be appreciated. This antenna also has the phase center a little bit more inside (see figure 6.15) than the one in section 6.3.1, (a 21% inside from the output aperture).

So, this is another possibility to design a shorter antenna using a new corrugated profile section at the input part. The result is a more compact antenna than the ones describe before. But the design method is not completely described for this one, so the designer must play a little with the parameters to obtain the final design.

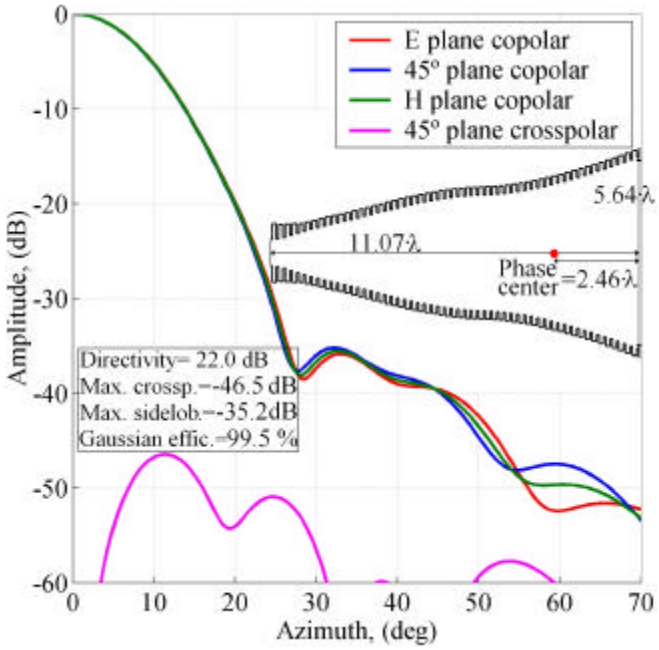

Figure 6.15. Combination CSIRO + GPHA with 22 dB directivity and –35 dB sidelobe level

6.5.2 Design of a 22 dB combination Choked + GPHA

The most compact profile at the moment for a corrugated GPHA is the one that uses at its input a choked waveguide corrugated profile [3, 4].

In fact, with this design method we obtain several advantages over the other corrugated profiles, (see figure 6.16). The combination choked + GPHA is the most compact antenna available in the actual technology. It provides really excellent radiation patterns with extremely low sidelobes in incredible compact profiles. Also the choked part has an easier manufacture process avoiding the complicated λ/2 deep first corrugations of the other corrugated profiles.

As a disadvantage, we must say that the maximum obtainable bandwidth at the moment of these corrugated horn profiles is around 15%.

These choked corrugated GPHA's are under research at the moment to improve bandwidth.

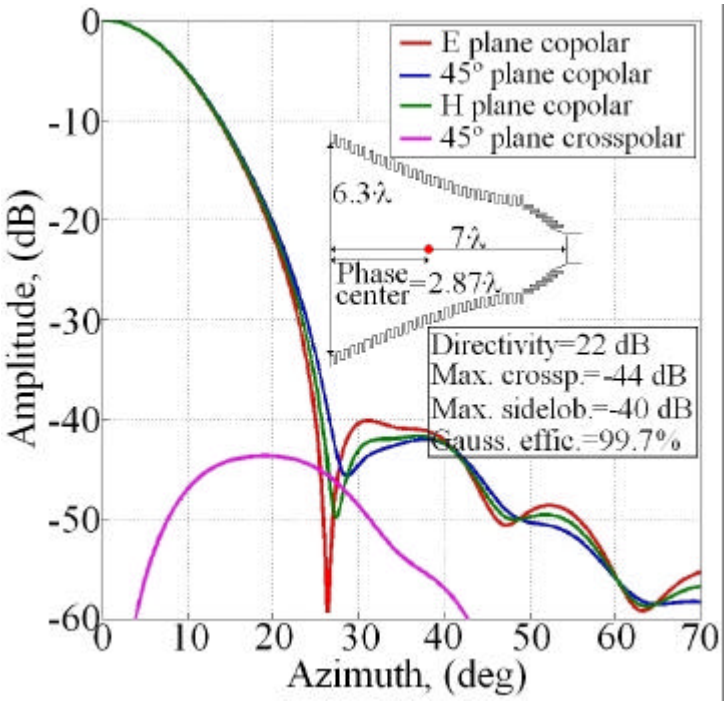

Figure 6.16. Complete corrugated GPHA with a choked corrugated waveguide input for 22 dB directivity and –40 dB sidelobe level

The antenna presented in figure 6.16 has a choked part of a ridiculous 1.26·λ length. The normalised inner diameter is of $\overline{D_0}=2.6$. The corrugated GPHA final section has a length factor of $f=0.633$ and an output diameter of $6.29\cdot l$ with an $\alpha=0.701$.

The total length of the complete antenna is only $7\cdot l$, a really incredible compact profile and with *5 dB* lower sidelobe level than the rest of the designs of this chapter. The choked part is really short, but it doesn't provide a really nice output field, so the corrugated GPHA final section must be longer than in the other profiles. But as the inner diameter is quite small, the length of the second part is not to large.

This type of antennas are under research at the moment. It is very promising the massive use of this horns, the first design is at the moment being commercialised by the UK company Flann Microwave Ltd, (www.flann.com).

6.6 On the bandwidth of the different complete GPHA profiles

If the reader has followed completely this chapter, at this point knows how to design directly many types of corrugated horn antennas using Gaussian profiles. To develop the best possible design, we usually will choose the most compact one, but we should know what is the reachable bandwidth for each case, because usually as shorter is the profile as narrower is its effective bandwidth.

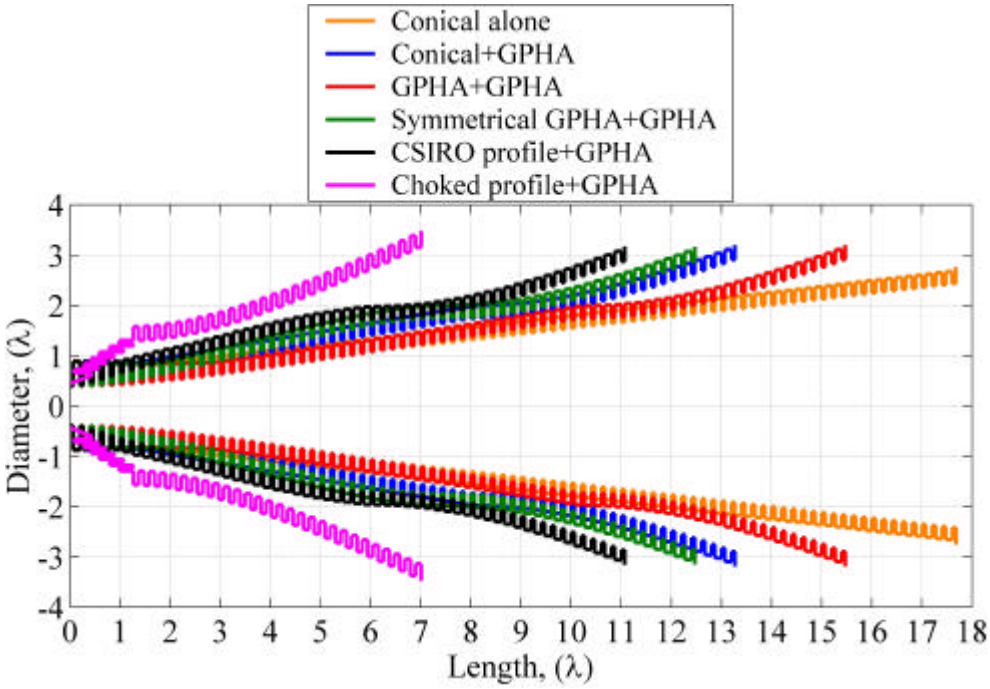

Figure 6.17. Size comparison for the designed 22 dB directivity antennas

This bandwidth exercise is going to be made for the five *22 dB* corrugated antennas designed in this chapter, the conical corrugated horn antenna design of chapter 3 will be added in the figures to facilitate the comparison.

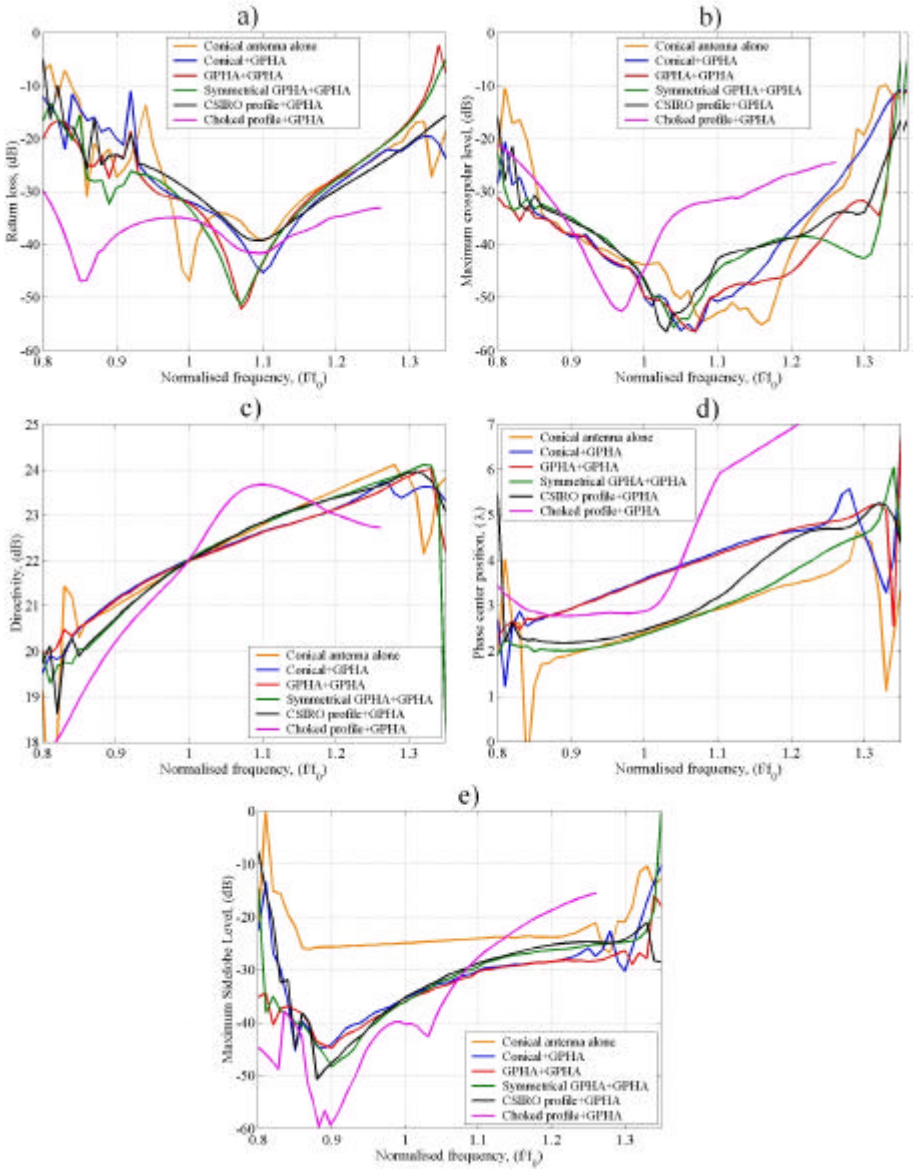

Figure 6.18. Bandwidth comparison between the different complete GPHA models
a) Return loss *b) Maximum crosspolar level*
c) Directivity *d) Normalised phase center position*
e) Maximum sidelobe level

Figure 6.17 shows an antenna size comparison picture, including the pure conical corrugated horn designed in chapter 3. The choked profile GPHA is incredibly short and its wider output diameter is determined by the *–40 dB* sidelobe level obtained for it, (see figure 6.16).

From figure 6.18, (this figure relates the bandwidth of every profile we have designed), we can extract several conclusions:

- The return loss bandwidth is very nice for the choked + GPHA, (always below *–30 dB*). For the rest of horn antennas is similar but slightly better for the GPHA + GPHA and the symmetrical GPHA + GPHA. The reason for this is the smoother throat section in these antennas.
- Regarding to crosspolar level (with *l/4* corrugation depth), the bandwidth is similar in all the designs, except for the choked + GPHA that presents a poorer bandwidth (around *10%* bandwidth for *–40 dB* crosspolar level). A slightly wider crosspolar level bandwidth for the GPHA + GPHA, the symmetrical GPHA +GPHA and the CSIRO + GPHA can be observed. In general, with corrugated antennas the crosspolar level bandwidth can be improved with the information given in the following section of this chapter.
- Figures 6.18c and 6.18d can be explained altogether because they are strongly related. In figure 6.18c we can see the directivity bandwidth curve for each design. It can be appreciated three different slopes.
    - The lowest slope is found for the conical + GPHA and GPHA + GPHA. Both of them provide a high efficiency HE_{11} at the inner diameter. The phase centre of both (figure 6.18d) present also a certain slope, this means that as higher the frequency is as more inside the phase centre of the horn antenna is placed. In fact, a phase centre variation going inside the antenna provides a

narrower diameter where the antenna effectively radiates. This effect compensates a lot the slope of the directivity, but the phase centre moves quite a lot also.

- Symmetrical GPHA + GPHA and CSIRO + GPHA present a steeper slope in directivity. The reason for this behaviour depends strongly on the lower purity of the HE_{11} mode at the inner diameter. However, if we check the bandwidth curve of the phase centre we see that both are flatter than the others. This means that in fact this both designs are radiating from a single point phase centre in most of the frequency band. The diameter of the horn at phase centre remains the same, then the radiation pattern controlled by this effective diameter changes the directivity quicker with frequency.
- The choked + GPHA presents the steepest change in directivity as well as the flattest phase centre position but in the narrowest bandwidth.

- Maximum sidelobe level bandwidth always follows a slope that provides lower sidelobe level for lower frequencies and higher sidelobe level for higher frequencies in the band. This must be taken into account if we need to maintain the sidelobe level, for example, below *-35 dB* along all the usable bandwidth of the antenna. The choked GPHA has also a poorer sidelobe level bandwidth.

So, summarizing we can conclude the following:

- The return loss bandwidth for corrugated GPHA's can be one of the most important problems to achieve bandwidths above 30%. This is clearly not the case of the choked + GPHA profile, because it doesn't present return loss problems in a huge bandwidth despite it has poorer

bandwidths in the rest of the radiation pattern parameters. A research on this type of GPHA's is being carried at present to improve the results.

- A compromise must be reached between maximum allowable change in directivity along the usable bandwidth and maximum allowable movement of the phase centre.
- Maximum sidelobe level must be chosen for a given profile to design taken into account its bandwidth. The worst case sidelobe level will always be the highest frequency in the band.

6.7 On the corrugation depth

During the development of the present manuscript, only a few information has been given about corrugation depth. The corrugation depth along the antenna was fixed to $l/4$ in chapter 2 and no more considerations about this critical design parameter have been taken into account.

This parameter controls the amount of crosspolar fields at a certain frequency and its value affects the return loss. Nevertheless a small change in corrugation depth ($\pm 25\%$) will not change the copolar pattern, and its radiating properties (directivity, sidelobe level…).

The *balanced hybrid condition,* (this condition means a corrugation depth of $l/4$), was used in chapter 2 to theoretically obtain a null in the crosspolar component of the aperture fields. Practically, the real minimum crosspolar value happens always for a corrugation depth a little bit deeper than $l/4$ and it is affected by the diameter of the corrugated waveguide. In fact, for oversized aperture diameters, the minimum crosspolar corrugation depth is practically equal to $l/4$, but if the aperture diameter is not too oversized (between $2 \cdot l$ and $3 \cdot l$), the corrugation depth could be as much as

a *20%* deeper than the commonly used *l/4* value to obtain a minimum crosspolar level at the design frequency.

If we have a look to equation 2.1, it shows that the crosspolar term decreases as $k \cdot R$ increases (with *R* the output aperture radius of our horn antenna). So the larger the aperture diameter of the horn, the wider will be the bandwidth for a given crosspolar level, because the term *X-Y* in that equation will never vanish except theoretically at a single frequency.

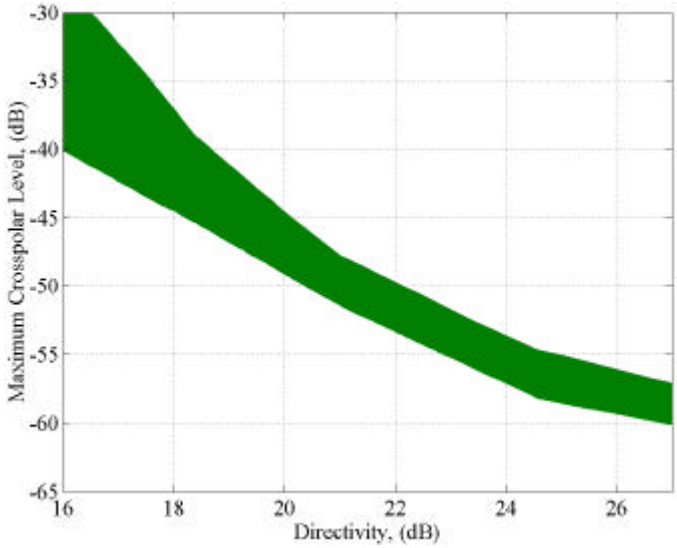

Figure 6.19. Directivity versus approximate obtainable maximum crosspolar level (constant corrugation depth at l/4)

The figure 6.19 shows the approximate obtainable crosspolar levels for a corrugated horn antenna with exactly *l/4* corrugation depth. The line is quite broad because the different possibilities of output diameter for a given directivity have been taken into account.

An important conclusion of the figure 6.19 is that it is easier to obtain a low crosspolar level antenna for a *22 dB* directivity antenna than for a *18 dB* directivity antenna. For example, to obtain a *–45 dB* crosspolar level in a *18 dB* directivity antenna is quite complicated, any of the considered

designs could satisfy that condition. Perhaps, with a corrugation depth slightly above *l/4* it will probably fulfil the requirement within a reduced bandwidth. On the other hand to obtain *–45 dB* crosspolar level with a *22 dB* directivity antenna (wider aperture diameter) should not be a problem.

6.8 Design tricks and rules

If everything has been reasonably understood until this point, the reader is now capable of designing a corrugated GPHA that best meets his specifications.

The obtainable antenna with the aid of this chapter 6 for sure will not be the optimal solution. However the best and final profile must start from that first approximation. In this section some design rules to help the designer to quickly obtain the final corrugated profile that best meets his specifications in a quite compact design will be explained.

First of all, the designer must know that there are two types of parameters, both nearly independent, that affect the design:

1. The profile shape will affect directivity and sidelobe level. In fact it will affect quite exclusively only to the copolar radiation pattern, (with the exception if the profile shape does not change smoothly).
2. The corrugation parameters affect crosspolar level and return loss, and not to copolar features.

These last properties allow the designer to practically separate the design in two parts; first of all the designer adapts exactly the copolar pattern, and after that lowers the crosspolar radiation and the return loss by means of the corrugation parameters.

6.8.1 Reducing the size of the complete corrugated GPHA

To make a more compact profile we must change the profile shape. After the design given by the empirical formulas of this chapter, a “rule of thumb” that works consists in shortening the input section corrugated GPHA, (if it is a conical corrugated section, making slightly bigger its profile angle; if it is a corrugated GPHA input, making slightly smaller the α parameter), but maintaining approximately the same inner diameter. The way this technique works is usually shortening the input section two corrugation periods and lengthening the second section GPHA one corrugation period. So the total shortening effect is one corrugation period per step. Usually this technique also assumes making the inner diameter slightly smaller and using an α parameter for the second GPHA section slightly bigger so that the output diameter doesn’t increase. Usually with this technique we can reduce the total length, three, four or perhaps more corrugation periods.

6.8.2 Reducing the crosspolar level and the return loss of any corrugated horn antenna

Once we have completely defined a corrugated horn antenna profile, to reduce the crosspolar level and the return loss of the profile, we must redesign the corrugations.

Usually we will have exactly a corrugation depth of $l/4$ along the profile and a matching device at the beginning of the horn starting with a corrugation depth of $l/2$ that diminishes in certain length linearly to $l/4$. This corrugation depth change at the throat has a length that is exactly the

distance where the inner diameter corrugation allows the TM_{11} mode to be in propagation, so a inner diameter of exactly $1.22 \cdot l$.

If we make the length of the transformer of corrugation depth between $l/2$ to $l/4$ a little bit longer than this theoretical value (*10-20%* longer), the return loss will be improved in bandwidth, but the crosspolar level will be poorer. And if we make it shorter, just the opposite will happen. Thus a compromise between return loss and crosspolar level in the whole frequency bandwidth must be reached.

If we make the first corrugation depth slightly deeper, probably the return loss will be improved and the crosspolar level not much affected, but this means more manufacture problems. In fact, usually to reach a $l/2$ first corrugation depth is impossible by means of a milling machine manufacture technique, so another solution should be found.

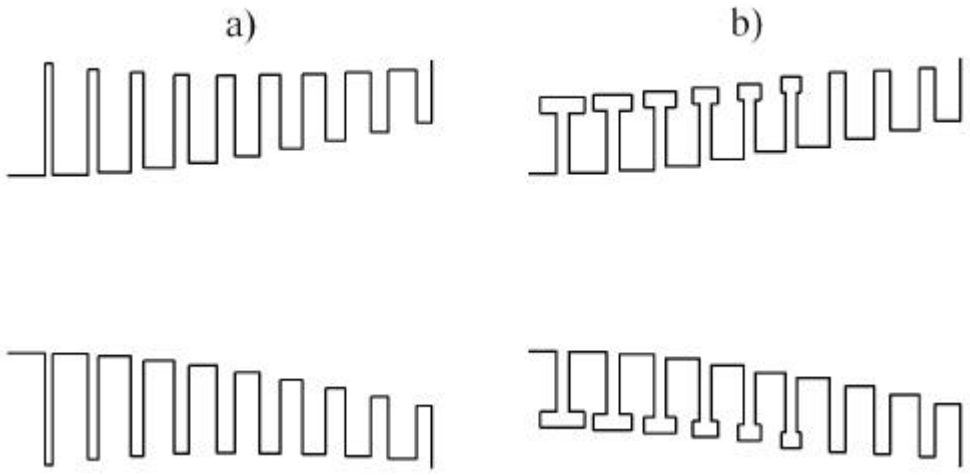

Figure 6.20. Different methods to improve the return loss bandwidth of a corrugated horn antenna
a) Variable corrugation tooth width at the throat
b) Ring loaded slots in the first corrugations at the throat

Corrugation period and corrugation tooth width usually doesn't affect too much to any radiation parameter (see appendix II), except at the throat region. For the rest of the antenna a corrugation period around $\lambda/5$ and a corrugation tooth with around *p/2* or slightly thinner (*p/3* where *p* is the corrugation period) are usually the best values and don't need to be changed. Usually corrugation widths must be chosen to minimise the manufacture problems, a variable corrugation period or a variable corrugation width complicates quite a lot the manufacturing process.

In figure 6.20 we present two ways to reduce the return loss of the antenna not affecting too much to the crosspolar radiation. Both methods complicate quite a lot the manufacture process, in fact the ring loaded slots are nearly impossible to implement unless the throat is made by means of stacking metallic pieces. This is one of the clear advantages of the choked profiled input GPHA which is under research at the moment because it reduces a lot the complexity in the manufacture process at the throat region, (probably the most difficult part to manufacture in a corrugated horn antenna).

Once we have defined the throat region that best meets our return loss and manufacture requirements, we must choose the optimum corrugation depth for the rest of the antenna (this depth is usually slightly above *l/4*) that best reduces the crosspolar level.

A technique that works quite well to reduce the crosspolar level is to use a tapered corrugation depth. This means that inside of the antenna the corrugation depth could be *10-15%* smaller than *l/4*, and as we approach to the aperture the corrugation depth increases above *l/4*. The reason for this technique is that at high frequencies of the band the outer part of the antenna

is not effectively seen by the radiated fields, so it is not affected by deep corrugation depths at the output aperture. However low frequencies of the usable bandwidth are affected by the whole antenna profile.

Fortunately, a tapered change in corrugation depth doesn't complicate the antenna manufacture process. This technique provides a quite flat crosspolar pattern (no deep crosspolar values), but it could be easy to achieve for example *-45 dB* crosspolar level in a *22 dB* directivity antenna in more than a *30%* bandwidth.

However, due to the fact of the continuously increased speed in computers, usually a good optimisation code reduces the optimum design time and complexity really a lot. It is usually the best tool to be used to implement the final design without the need of being continuously changing parameters in the design [1].

6.9 References

[1] R. García Esparza, "Optimización de los parámetros de antenas de bocina corrugadas de perfil gaussiano mediante Matlab" *Research to obtain the Spanish master degree on Telecommunications Engineering*, November 2001, Universidad Pública de Navarra, Pamplona, Spain

[2] S.G. Hay, S.J. Barker, C. Granet, A.R. Forsyth, T.S. Bird, M.A. Sprey and K.J. Greene, "Multibeam Earth Station Antenna for a European Teleport Application" *2001 IEEE AP-S International Symposium and URSI Radio Science Meeting*, 8-13 of July, Boston, United States.

[3] Teniente, J., Goñi, D., Gonzalo, R. and del Río, C. "Choked Gaussian Antenna: Extremely Low Sidelobe Compact Antenna Design", *IEEE*

Antennas and Wireless Propagation Letters, vol. 1, nr. 11, pp. 200-202, November 2002.

[4] Gonzalo, R., del Río, C., Goñi, D. and Teniente, J., "Antena de bocina que combina corrugaciones horizontales y verticales" *Spanish Patent Nr: P.2002 01264* Property of: Public University of Navarra, (UPNA), 24th of May 2002.

Chapter 7

Applications of corrugated GPHA

During the development of this Ph. D., many corrugated GPHA have been designed and some have been manufactured. In fact, the number of designed corrugated GPHA's is above one hundred and the number of manufactured ones above ten.

During the last six years we have been refining the design method until we have reached the design path we propose in the previous chapters of this thesis. Many antennas have been manufactured and measured obtaining really good results during this long developing time.

The first corrugated GPHA's we manufactured by means of electroforming and they were two millimeter wave horn antennas [1], one was a direct corrugated GPHA and the other a symmetrical corrugated GPHA. The measured results were very nice, validating our numerical design code, year 1996. At the same time, an antenna for the German company Reinhold Mühleisen (RM), was designed to work at 170 GHz and was integrated in a complete system for the Japan Atomic Research Institute.

In 1997 we designed, manufactured and measured a high directivity corrugated GPHA to emulate the radiation of the TJ-II gyrotron and test a quasi-optical transmission line at low power in the CIEMAT in Madrid [2,3].

In 1998, the design of the Hispasat 1C satellite horn antenna was performed. At the beginning of this year we managed to persuade the

engineers of CASA/EADS to use, for one of the three horns to be on board of Hispasat 1C satellite, a new technology based on corrugated GPHA's [4], this satellite was launched on February 2000. The nice performance of this antenna was the reason to be also selected to be on board of the new Hispasat 1D satellite launched in September 2002 with a slightly different frequency band.

The next antenna design to be manufactured had to be two years later. In the year 2000 we designed two sub-millimetre horn antennas of very high directivity and very low sidelobe level for the Rutherford Appleton Laboratory in England. They manufactured them by means of high precision electroforming and will be a part of ESA funded MARSCHALS airborne system.

In the year 2000 we were also involved in the design of the corrugated horn antennas for the Low Frequency Instrument (LFI) for the Planck satellite with the contacts with the people from the CNR in Bologna, Italy. In fact, all the horn antennas for the Planck satellite, (HFI and LFI) use corrugated GPHA's. The High Frequency Instrument (HFI) corrugated horns were developed by the people from the Queen Mary College in London, U.K. where the corrugated horn technology was firstly developed during the seventies [5,6]. The Planck mission is an ESA funded mission to look at microKelvin anisotropies in the 2.7^{o}K cosmic background radiation

Also year 2000 was the year of the international recognition of the good radiating properties of our GPHA designs by other authors [5,6,7]. People of the most important horn antenna research groups in the world began to use our corrugated GPHA designs for their own designs (Queen Mary College, CSIRO, Jet Propulsion Laboratory, CNR Bologna, etc.).

In the year 2001 we developed a set of corrugated GPHA's of very wide bandwidth [8] to be used in our anechoic chamber project. Then, a wide band measurement will be possible without changing the feed horn of the chamber.

Year 2002 was the year of the development of the new hybrid corrugated horn called the choked waveguide GPHA. This antenna provides a really nice radiation pattern in the most compact profile ever designed. It has entered the market with an important company as Flann Microwave Ltd., (http://www.flann.com/Sales/Feature_Article/feature_article.html) [9] This antenna is our last successful research, and an improvement to it is under development at the moment.

In this chapter of the thesis, all of these practical examples of complete corrugated GPHA's are going to be covered. We will understand the way how this important corrugated horn antennas has been carried on during the years of development of the present thesis.

7.1 Corrugated GPHA design for low power testing of the quasioptical transmission lines at TJ-II stellerator

During 1996, the need to test a quasioptical transmission line used to drive the very high power millimeter wave beam from the gyrotron generators to the TJ-II plasma at the CIEMAT in Madrid [2,3] gave us the opportunity to design one of the first corrugated GPHA for a practical application.

The gyrotron output (*53.2 GHz*) had a *95%* efficiency to a fundamental gaussian beam of *18 mm* beamwaist. So our design parameters

were to provide the most similar gaussian beam radiation pattern to that gaussian beam at *53.2 GHz*.

A fundamental gaussian beam of w_0*=18 mm* at *53.2 GHz* means a *29.6 dB* directivity radiation pattern with as low sidelobes as possible to obtain high efficiency. Such a high directivity for a corrugated horn antenna led to a huge profile.

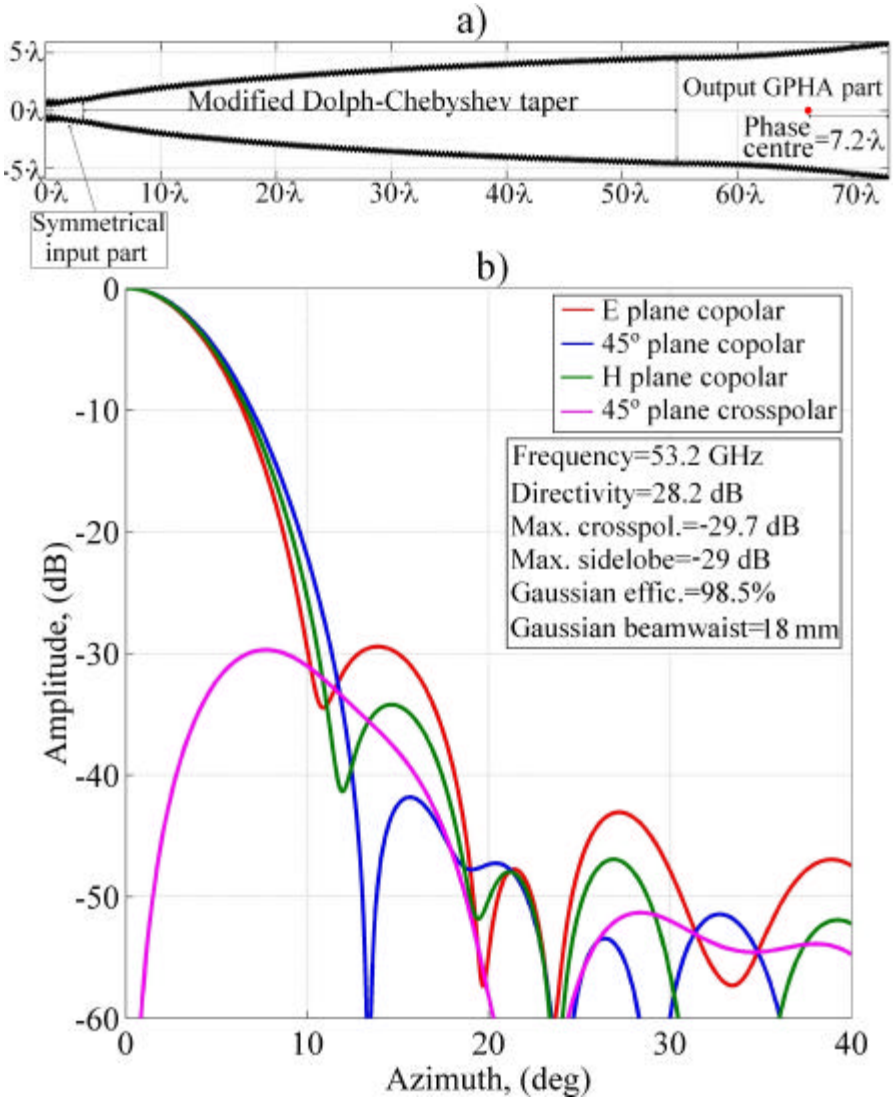

Figure 7.1 a) Antenna design to get a 18 mm fundamental gaussian beam b) Simulated far field radiation pattern for the antenna

In 1996, corrugated GPHA theory was in its infancy, so the design we made, was far away from the optimum, but it worked nicely to test the quasioptical waveguide. To develop the design we knew that the end part had to be a gaussian aperture corrugated horn with an α value around *0.6-0.7* and we also knew that the input diameter (D_0) of such a gaussian part had to be between $8 \cdot l$-$9 \cdot l$ to obtain the needed directivity to match efficiently a *18 mm* beamwaist fundamental gaussian beam. Our design problem came because in the year 1996 we didn't know yet how to obtain a nice HE_{11} mode in such a huge diameter in a short profile.

The design requirements were to obtain a *18 mm* beamwaist fundamental gaussian beam at *53.2 GHz* in the most compact and easiest to manufacture profile beginning from a smooth circular waveguide of *4.8 mm* diameter propagating the TE_{11} mode.

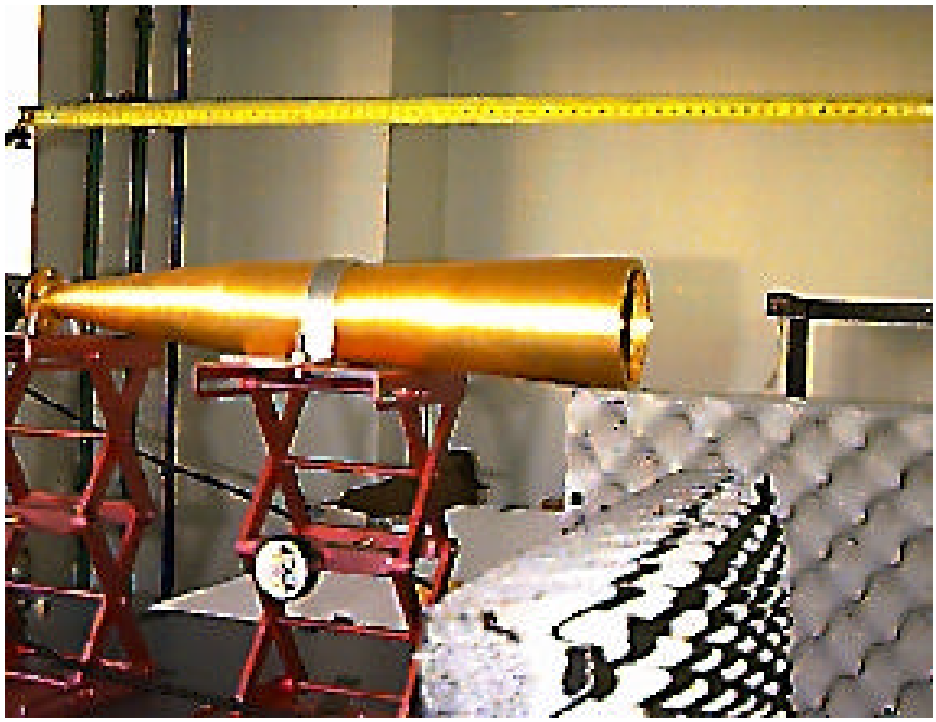

Figure 7.2 Manufactured antenna prepared to test the quasioptical transmission line at CIEMAT

The antenna was made by means of dividing it in three parts, (see figure 7.1a). The design frequency was *53.2 GHz* :

- The first part was a symmetrical GPHA TE_{11} to HE_{11} mode converter with an output diameter of only $1.67 \cdot l$ and an $\alpha = 1.61$.
- The second part was a modified Dolph-Chebyshev taper that maintained the HE_{11} mode from the $1.67 \cdot l$ output diameter of the first section to an $8.87 \cdot l$ output diameter. The length of this taper was huge, $52.17 \cdot l$ (see figure 7.1a).
- The third part was a corrugated GPHA with a $\overline{D_0} = 8.87$, $\alpha = 0.6$ and $f = 0.05$ resulting in an output diameter of $11.36 \cdot l$.

The corrugation parameters were; corrugation period $p = 2$ *mm*, corrugation tooth width $w = p/2 = 1$ *mm* and corrugation depth $d = l/4$. At the throat, a $l/2$ to $l/4$ impedance transformer of $1.53 \cdot l$ length was also used to adapt the TE_{11} mode at the input.

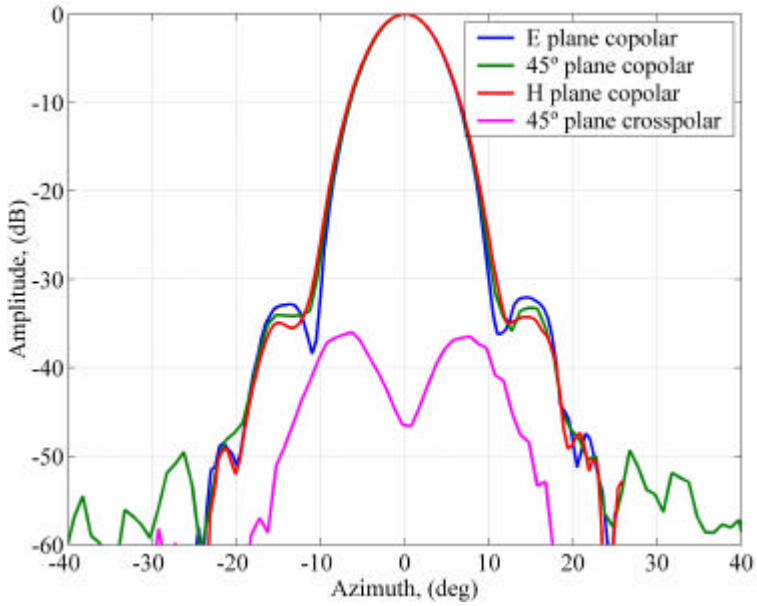

Figure 7.3 Measured radiation pattern of CIEMAT corrugated GPHA antenna at 53.2 GHz

The antenna was manufactured by Thomas Keating Ltd. by means of electroforming, (see figure 7.2) and measured in the ESA/ESTEC Compact Antenna Test Range (CATR). Measurement and simulations are in very good agreement, see figure 7.1 and 7.3.

This antenna was used to test the high power quasioptical waveguide of the TJ-II stellerator obtaining nice results previous to connect the high power gyrotron [2,3].

Now-a-days, a much more compact antenna (around $20 \cdot l$ shorter) could have been designed, with an efficiency to the *18 mm* beamwaist fundamental gaussian beam above *99%* and lower sidelobe and crosspolar levels maintaining approximately the same output diameter.

7.2 Corrugated GPHA design for Hispasat 1C satellite

At the end of year 1997, the antenna engineers from CASA/EADS space division proposed to our research group to collaborate in the design of the three corrugated horn antennas that were going to be on board of the Hispasat 1C satellite.

We had the specifications of the three antennas, but we put the effort in the design of two of them.

The specifications for the first antenna were the following (uplink and downlink for America antenna):

- Frequency range: from *11.9* to *12.2 GHz* and from *13.75* to *14 GHz*
- Illumination at *19* degrees below *-22 dB*
- Maximum crosspolar level below *-45 dB*
- Return loss below *-28 dB*

- Input diameter *23.4 mm*
- Corrugation period, *p=3.4* mm and corrugation tooth width, *w=0.9 mm*
- First corrugation depth below *11 mm*

The specifications for the second antenna were the following (downlink for Europe antenna):

- Frequency range: from *11.7* to *12.2 GHz*
- Illumination at *19* degrees below *-22 dB*
- Maximum crosspolar level below *-45 dB*
- Return loss below *-28 dB*
- Input diameter *23.4 mm*
- Corrugation period, *p=3.4* mm and corrugation tooth width, *w=0.9 mm*
- First corrugation depth below *11 mm*

The third antenna was used for the uplink to Europe and the frequency range was from *13* to *13.25 GHz* and from *13.75* to *14 GHz*.

The first two antennas had exactly the same specifications except that the frequency range began in *11.7 GHz* in the second one instead of *11.9 GHz* and that the first antenna had another band from *13.75* to *14 GHz*. So we decided to design an antenna that could cover both designs in the same profile extending the frequency range in our design from *11.7* to *12.2 GHz* and from *13.75* to *14 GHz*.

An illumination at *19 degrees* at exactly *–22 dB* means a directivity of *22.475 dB* exactly (see appendix III), if the antenna radiation pattern is similar to a fundamental gaussian beam. So if we must comply with this requirement, we should design the antenna to present a *22.5 dB* directivity at *11.7 GHz*.

But in this design, sidelobes can be as high as *–22 dB* in fact because no sidelobe level restriction has been required, so this restriction is superimposed by the illumination at *19 degrees* to be below *–22 dB*. This will mean that we will design the antenna to present at *14 GHz* exactly *-22 dB* sidelobe level to provide the most possible compact profile. To present a so high sidelobe level will mean that the needed directivity at *11.7 GHz* to provide the exact illumination will be lower than the theoretical value of *22.5 dB* because the high sidelobes will reduce the directivity although the main beam decay will mean a higher directivity to match the illumination.

With all this information, and because the complete bandwidth was quite large (around 18%), we decided to implement the best bandwidth design, a corrugated GPHA input as mode converter followed by a short corrugated GPHA output part (GPHA + GPHA).

After the optimisation of the profile, these were the resultant parameters:

- Design frequency: *11.7 GHz*.
- Input diameter: *23.4 mm*
- Corrugation parameters: *p=3.4 mm*, *w=0.9 mm* and *d=6.4 mm*
- First GPHA part:
  - α*=2.017*
  - Length=*88·p* (*299.2 mm*).
  - $\overline{D_0}$*=4.106*
  - Impedance transformer
    - Length=*60 mm*
    - 1st corrugation depth=*11 mm*
- Second GPHA part:
  - α*=0.686*

- Length=$22 \cdot p + w$ (*75.7 mm* or *f=0.0283*)
- $\overline{D_0} = 4.106$

So the total length of the antenna is *374.9 mm* ($14.6 \cdot l$) and the output diameter $4.54 \cdot l$ (*116.2 mm*). A picture of the antenna can be seen in figure 7.4.

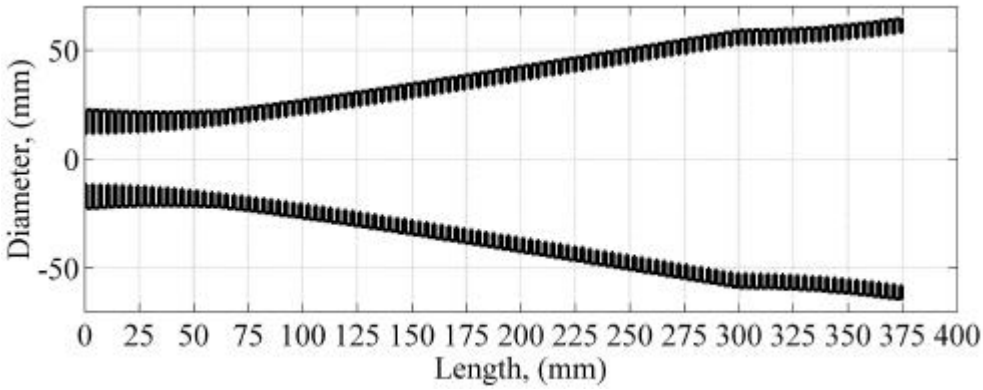

Figure 7.4 Proposed profile for Hispasat 1C satellite

The simulated far field of this proposed profile can be checked in figure 7.5. The profile was adjusted to present exactly maximum sidelobe level at *14 GHz* of *–22 dB* (not specified at the initial requirements), and the illumination at *19 degrees* at *11.7 GHz* is exactly *–22 dB*. Return loss is always below *-30 dB* and crosspolar level below *–45 dB*.

This horn was selected to be on board Hispasat 1C satellite to work in the downlink to Europe. Its frequency range was *11.7 GHz* to *12.2 GHz*. For sure it could have had a even more reduced its size because the initial design was prepared to take into account also the upper band (*13.75 GHz* to *14 GHz*), but EADS/CASA space division engineers selected it only for the downlink.

The horn was manufactured also by EADS/CASA space division, and measured in the far field range of the Polytechnic University of Madrid (UPM), see figure 7.6.

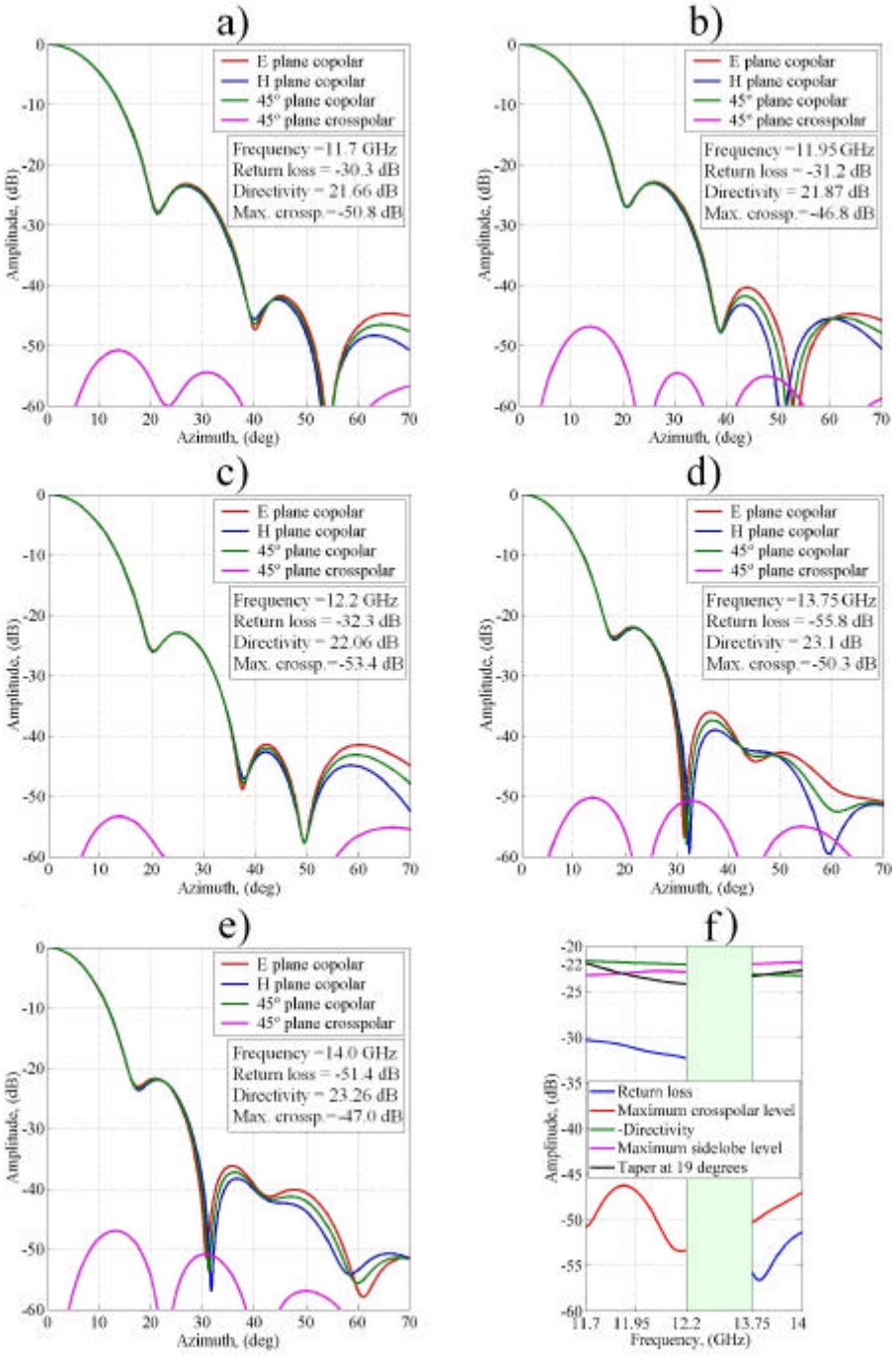

Figure 7.5 a) b) c) d) e) Simulated far field radiation pattern for proposed Hispasat 1C satellite profile antenna
f) Simulated far field parameters for proposed Hispasat 1C satellite profile antenna

Measured results are in really good agreement with simulated ones, (see figure 7.6), with measured crosspolar pattern always below *–40 dB* and copolar pattern exactly the same as the simulated one (see figure 7.5 to compare).

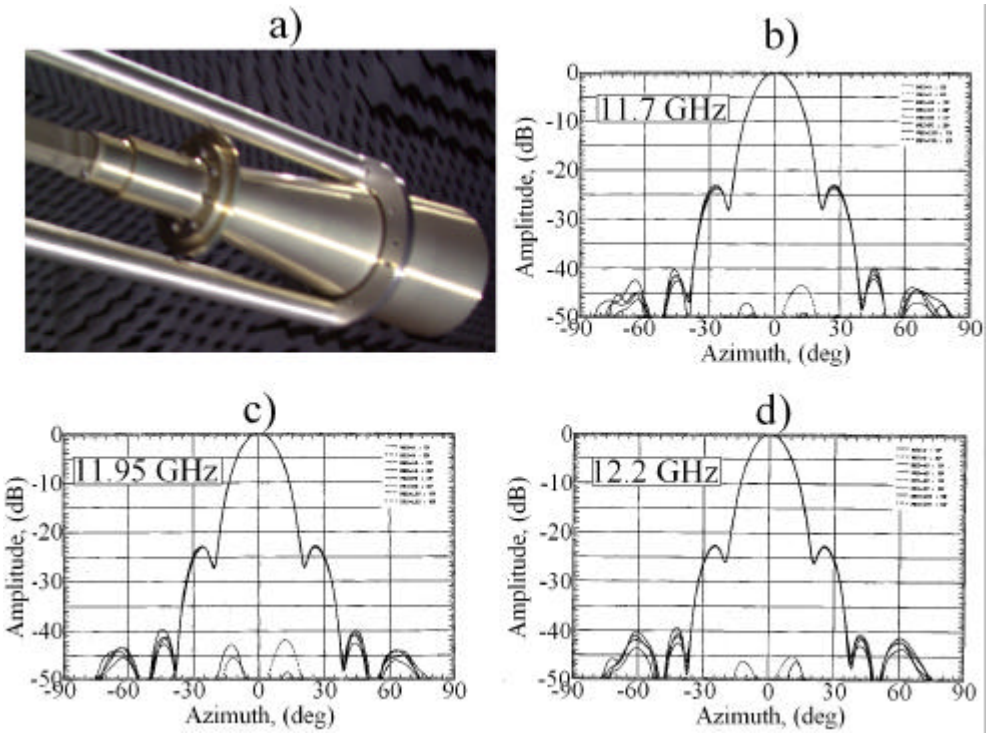

Figure 7.6 a) Manufactured antenna at UPM far field range
b) c) d) Far field radiation pattern measurements

Hispasat 1C was launched in February 2000 with this corrugated GPHA. The antenna behaviour was so nice that was selected exactly the same profile (not a scaled version) to be on board also of the new Hispasat 1D satellite that was launched in September 2002 to serve for the downlink to Europe but with a wider frequency band (from *11.45* to *12.75 GHz*).

7.3 Corrugated GPHA feedhorns for ESA funded MARSCHALS airborne system

In the year 2000, the engineers from the Millimetre Technology Group of the Rutherford Appleton Laboratory (RAL) in England asked us to design two sub-millimetre wave corrugated horn antennas for the ESA funded MARSCHALS airborne system. MARSCHALS is a three channel limb sounder for the European Space Agency (ESA) that will fly on an aircraft.

The engineers of the Millimetre Technology Group at RAL were specially concerned about the sidelobes generated by the feedhorns or the rest of the optics. The aim of the MARSCHALS project is the limb observation, and therefore any power introduced via a sidelobe pointing the earth should be consider as noise decreasing the performance of the whole system. They asked for *–35 dB* sidelobe level in both feedhorn designs, and this is just the perfect requirement for a corrugated GPHA.

The requirements for these corrugated horn antennas (called antenna in band C and antenna in band D), were the following:

Band	**Frequency Range**	**Centre Frequency**	**Beamwaist Radius**
C	*316.5 - 325.5 GHz*	*321.00 GHz*	*2.078 mm*
D	*342.2 - 348.8 GHz*	*345.50 GHz*	*2.003 mm*

Table 7.1 MARSCHALS feedhorns requirements

Other parameters common to both antennas were the following:

- Sidelobes: It was required sidelobes to be less than *-35dB* (with no "shoulders" on the main lobe). Obviously the lower the better.
- Peak crosspolar: below *-35dB* (again, the lower the better)
- Feed waveguide: Full height rectangular waveguide (*0.762 x 0.381 mm*)

- Horn Length (flange to aperture): Maximum *40 mm*.

Another requirement was that they wanted to manufacture the complete corrugated horns by means of high precision electroforming including the rectangular to circular transition to the rectangular feed waveguide of *0.762 x 0.381 mm* dimension. To reduce the manufacture complexity, the corrugation tooth width should be exactly half of the corrugation period and the constant along the whole antenna.

The bandwidth requirements were not too tight, *2.8%* for the C band antenna and 1.9% for the D band antenna, so we decided to use a corrugated antenna with a symmetrical gaussian profile followed by a pure gaussian output for the design.

The directivity, by means of translation of the beamwaist radius values was very high; *2.078 mm* beamwaist radius at *321 GHz* in C band antenna means an illumination at *16 degrees* of *–35 dB* and therefore a directivity of *26 dB*. As well, the *2.003 mm* beamwaist radius at *345.5 GHz* in C band antenna means an illumination at *15.5 degrees* of *–35 dB* and therefore a directivity of *26.3 dB*.

The transition from rectangular to circular waveguide was designed ending in a circular diameter of *0.762 mm*. This was used as the input waveguide diameter for both antennas.

After the optimisation of both profiles, these were the resultant parameters:

C band antenna

- Design frequency: *321 GHz*. Input diameter: *0.762 mm*
- Corrugation parameters: *p=0.2 mm*, *w=0.1 mm* and *d=0.24 mm*
- First symmetrical GPHA part:
  - α*=2.669*

- Length=*134·p* (*26.8 mm*).
- $\overline{D_0}$=*5.679*
- Impedance transformer
  - Length=*5 mm*.
  - 1st corrugation depth=*0.48 mm*

- Second GPHA part:
  - α=*0.73*
  - length=*67·p+w* (*13.5 mm)*
  - $\overline{D_0}$=*5.679*
  - *f=0.192* with suppression of the first *6* corrugation periods of this part, thus the resultant effective length is *12.3 mm*

The total length of the antenna is *39.1 mm* (*41.9·l*) and the output diameter *8.29·l* (*7.74 mm*). A picture of the antenna is shown in figure 7.7a.

D band antenna

- Design frequency: *345.5 GHz*. Input diameter: *0.762 mm*
- Corrugation parameters: *p=0.2 mm*, *w=0.1 mm* and *d=0.22 mm*
- First symmetrical GPHA part:
  - α=*2.62*
  - Length=*136·p* (*27.2 mm*).
  - $\overline{D_0}$=*5.972*
  - Impedance transformer
    - length=*5 mm*.
    - 1st corrugation depth=*0.44 mm*
- Second GPHA part:
  - α=*0.73*
  - length=*66·p+w* (*13.3 mm)*
  - $\overline{D_0}$=*5.972*
  - *f=0.18* with suppression of the first *7* corrugation periods of this part, thus the resultant effective length is *11.9 mm*

The total length of the antenna is *39.1 mm* (*45.1·l*) and the output diameter *8.53·l* (*7.398 mm*). A picture of the antenna is shown in figure 7.7b.

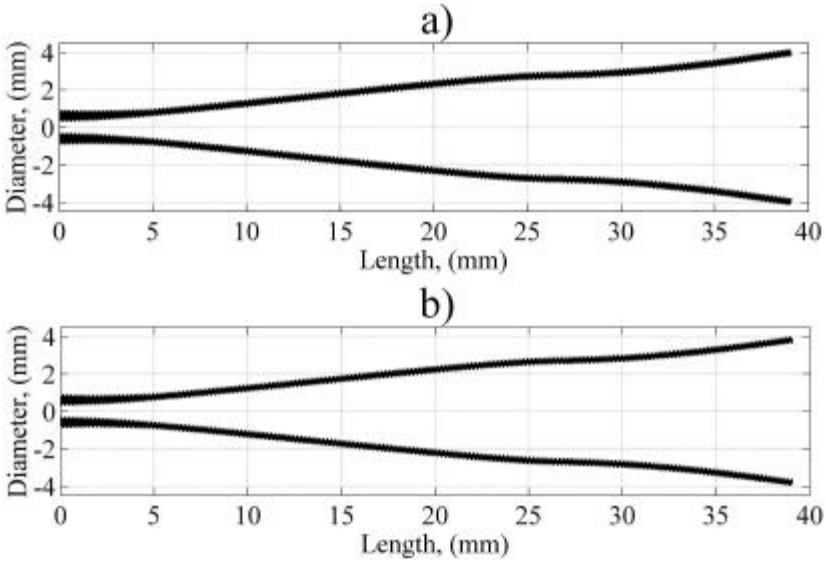

Figure 7.7 a) MARSCHALS feedhorn proposed profile for C band
b) MARSCHALS feedhorn proposed profile for D band

The rectangular to circular transition design was very simple and it was a direct cut of *15 degrees* angle of the circular input waveguide of each antenna in a *0.711 mm* length to result in the *0.762 x 0.381 mm* input rectangular waveguide, (see figure 7.8).

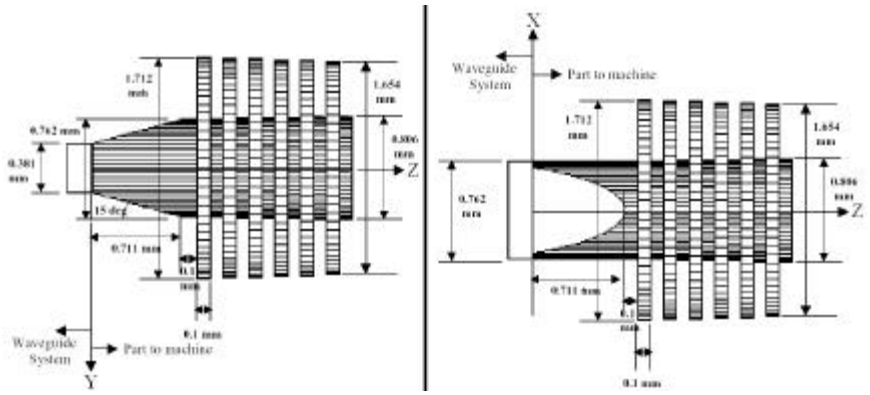

Figure 7.8 MARSCHALS feedhorns throat region with rectangular to circular transition

The antenna was manufactured by the workshop of the Millimetre Technology Group at RAL using a electroforming technique. The mandrel was made by a milling machine and a picture of it can be seen in figure 7.9. Observe in that figure the extremely high precision manufacturing remembering that the corrugation tooth width is only *0.1 mm*.

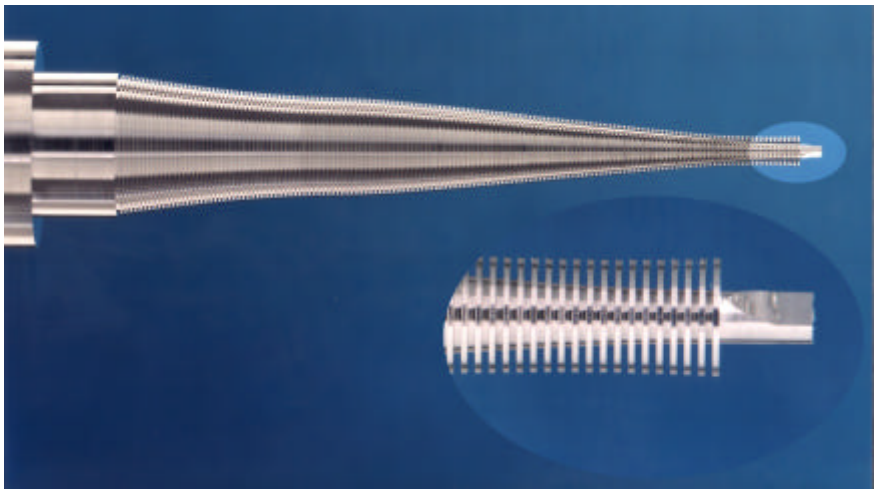

Figure 7.9 Mandrel of one of the MARSCHALS feedhorns

Frequency	**316.5 GHz**	**321 GHz**	**325.5 GHz**
Return loss	-38.939 dB	-42.102 dB	-46.567 dB
Directivity	25.717 dB	25.857 dB	25.988 dB
Phase centre posit. (relative to apert.)	-4.901 mm	-5.011 mm	-5.103 mm
Beamwaist radius, (w_0)	2.107 mm	2.115 mm	2.115 mm
Efficiency to w_0 Gaussian Beam	99.587 %	99.556 %	99.547 %
Efficiency to 2.078 mm beamwaist fundamental gaussian beam	99.521 %	99.492 %	99.465 %
Maximum crosspolar level	-56.302 dB	-53.542 dB	-49.221 dB
Maximum sidelobe level	-37.128 dB	-36.11 dB	-35.801 dB
16 deg edge taper (45 deg plane)	-31.1 dB	-32.3 dB	-34.1 dB

Table 7.2 MARSCHALS C Band feedhorn radiation behaviour

At present time we don't have yet the measurement of both antennas, but for sure will be really near to the simulations. Simulations of both antennas at central frequency can be found in figure 7.10 and tables 7.2 and 7.3 extract the main far field parameters.

Frequency	**342.2 GHz**	**345.5 GHz**	**348.8 GHz**
Return loss	-40.187 dB	-42.009 dB	-44.386 dB
Directivity	26.117 dB	26.206 dB	26.296 dB
Phase centre posit. (relative to apert.)	-4.659 mm	-4.77 mm	-4.882 mm
Beamwaist radius, (w_0)	2.057 mm	2.059 mm	2.062 mm
Efficiency to w_0 Gaussian Beam	99.482 %	99.446 %	99.424 %
Efficiency to 2.003 mm beamwaist fundamental gaussian beam	99.356 %	99.312 %	99.287 %
Maximum crosspolar level	-56.933 dB	-53.441 dB	-49.947 dB
Maximum sidelobe level	-35.394 dB	-34.835 dB	-34.566 dB
15.5 deg edge taper (45 deg plane)	-33.5 dB	-34.55 dB	-35.5 dB

Table 7.3 MARSCHALS D Band feedhorn radiation behaviour

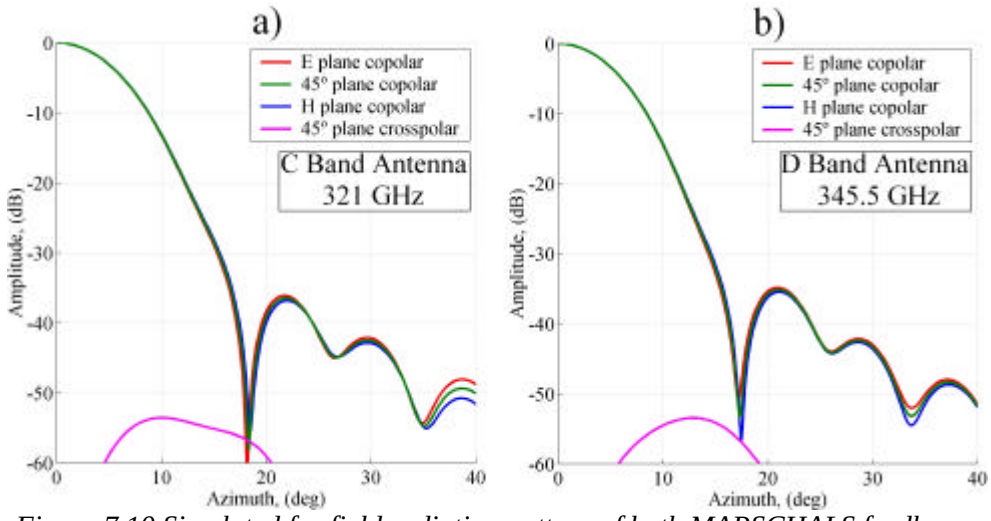

Figure 7.10 Simulated far field radiation pattern of both MARSCHALS feedhorns

Both antennas meet all the specifications widely (see figures 7.10 and 7.11). The shoulder that is slightly noticed in figure 7.10a and 7.10b for both antennas presents a very low importance. In fact, the difference between the no-shoulder slope gaussian decay and the maximum shoulder slope is in the worst case below *5 degree*.

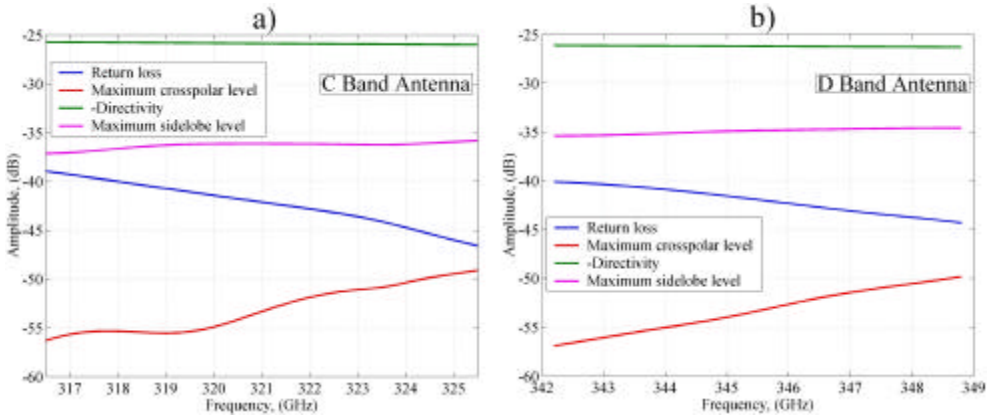

Figure 7.11Simulated far field behaviour of both MARSCHALS feedhorns

7.4 Ultra wide band corrugated GPHA design for the far field range measurement chamber at UPNA

In the year 2000 we were concerned about what would be the maximum bandwidth we could achieve with a corrugated GPHA. At that year, we were developing a project to build an antenna measurement chamber in our laboratory in the Public University of Navarra, (UPNA). A design to obtain the maximum achievable bandwidth was selected to overcome the annoying problem of the necessity to change the feedhorns each time it is necessary to cover a large frequency bandwidth antenna measurement.

The design was performed to accomplish an ultra-wide bandwidth (more than 40 %), with low side-lobe and cross-polar levels. The selected frequency bands were X and Ku. A *WR75* waveguide was selected in order

to cover the frequency range from *9* to *16 GHz*. A directivity around *21 dB* at the central frequency (*12-13 GHz)* was chosen, in order to illuminate the wider part of the far field range and allow measurement of bigger antennas.

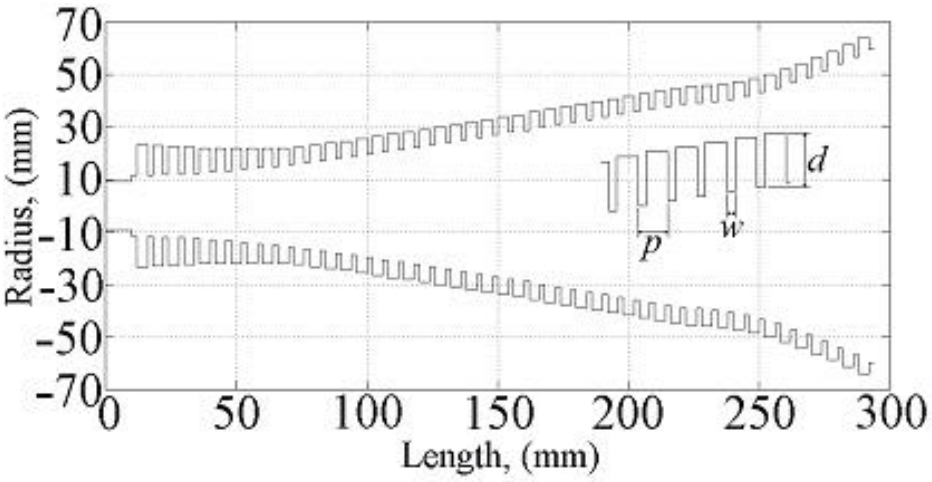

Figure 7.12 Ultra wide bandwidth corrugated GPHA profile

The optimised corrugated GPHA design, to cover the wide bandwidth requirement is formed by two corrugated GPHA stacked together. The design has the following parameters:

- Design frequency: *11.63 GHz*.
- Input diameter: *23.2 mm*
- Corrugation parameters: *p=6 mm*, *w=2 mm* and *d=6.45 mm*
- First GPHA part:
  - α*=2*
  - Length=*35·p* (*210 mm*).
  - $\overline{D_0}$*=3.02*
  - Impedance transformer
    - Length=*60.2 mm*
    - 1st corrugation depth=*12 mm*
- Second GPHA part:
  - α*=0.58*,

- length=$12 \cdot p + w$ (*74 mm* or *f=0.089*).
- $\overline{D_0}=3.02$

So the total length of the antenna is *284 mm* ($11 \cdot l$) and the output diameter $4.62 \cdot l$ (*119.2 mm*). A picture of the antenna can be seen in figure 7.12.

To allow connection of this corrugated GPHA to a *WR75* waveguide system, a Flann Microwave Ltd. rectangular to circular transition from *WR75* rectangular waveguide to *9.5 mm* circular waveguide radius was used. The connection of this transition to the corrugated GPHA input (*11.6 mm*) was not optimized at it shows a small step at the beginning of the corrugations, see figure 7.12.

This antenna was manufactured in aluminum by the company TMM Micromecánica (Oricain-Navarra). The antenna was measured in ESA/ESTEC Compact Antenna Test Range, and the results were really fine.

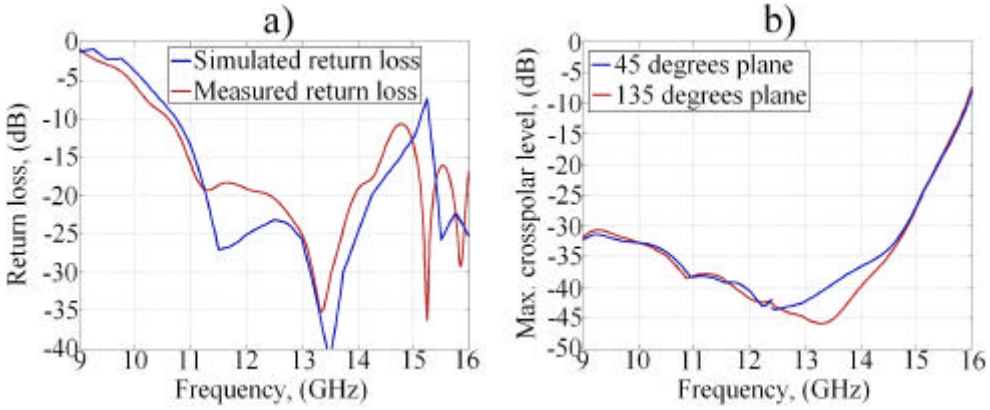

Figure 7.13 a) Simulated and measured return loss for the corrugated GPHA
b) Measured maximum crosspolar level for the corrugated GPHA

Measured input return loss (including the rectangular to circular converter and a coaxial to waveguide transition) values below *-18 dB* were obtained from *11 GHz* to *14 GHz*. These results are in good agreement with

the simulated ones obtained by using ANSOFT-HFSS finite element code (see figure 7.13a).

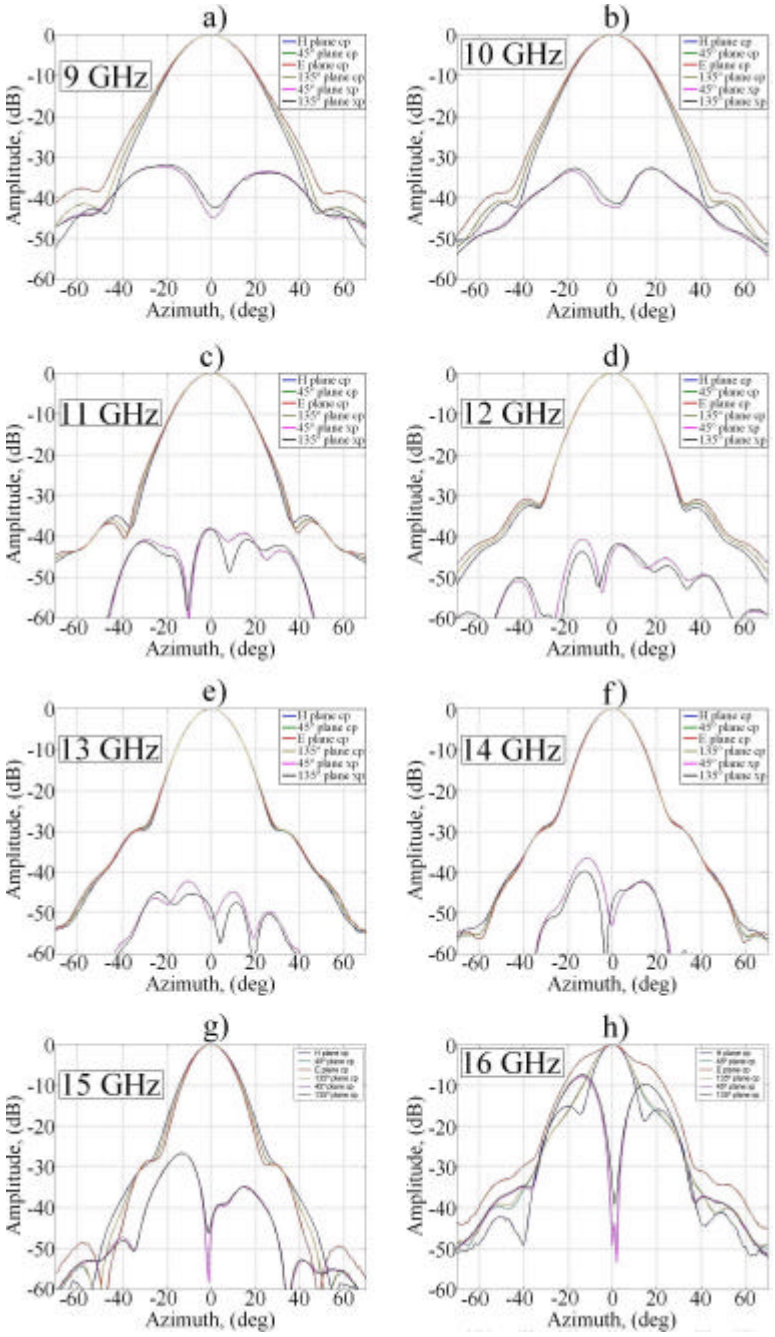

Figure 7.14 Measured far field radiation pattern for this ultra wide bandwidth corrugated GPHA

The antenna shows a measured maximum cross-polar level below *-30 dB* from *9* to *14.8 GHz*, (*49%* bandwidth), and below *–35 dB* from *10.6* to *14.4 GHz*, (more than *30 %* bandwidth), see figure 7.13b. Figure 5.7 depicts the radiation pattern in *1 GHz* steps for the whole band. High symmetry patterns with directivity values from 19 to 22 dB along the band have been obtained. Also it should be noted that the sidelobe levels are below *–28 dB* from *9* to *15 GHz*.

This corrugated GPHA will be perfect as a feedhorn for our future far field measurement chamber at UPNA. Return loss is not a critical parameter in a measurement chamber, and crosspolar levels are in fact only important at the center of the beamwidth (effective radiation area that receives the measured antenna in a far field chamber). Crosspolar levels for ± 5 *deg* are always below *–38 dB*, (see figure 7.14), for a *50%* bandwidth (*9* to *15 GHz*). Huge bandwidth measurements are then possible.

A complete set of antennas has been manufactured for the chamber, in fact the complete set are five identical corrugated GPHA's scaled for each band covering from *7 GHz* to *26.5 GHz*. The feedhorns overlap half of its bandwidth with the upper band feedhorn and the other half with the lower band feedhorn, so that we will have the possibility to select the perfect feedhorn for every antenna measurement in the chamber.

7.5 Choked corrugated GPHA. Extremely compact low sidelobe antenna design

Extremely low sidelobe horn antennas are often required for many current applications. This type of horn antennas are really important now-a-days to avoid interference with other communication systems. Because of

that, many research groups around the world are at present trying to redo the invention of the wheel [10,11]. Other groups just use our idea of corrugated GPHA at the output of any nice radiation pattern antenna that need to be improved in sidelobe level [6].

Recently, a compact corrugated horn antenna design proposed by Granet *et al*. [10] exhibiting low sidelobes for global earth coverage applications has been presented. In particular, this horn antenna design has sidelobes values of *-36 dB* and a total length of $5.6l$ and global earth coverage assumes a directivity around *21 dB* at central frequency. This antenna presents a really nice radiation pattern in a very compact size and doesn't make use of GPHA profiles, but it exhibits two principal disadvantages: a narrow bandwidth (less than *5%* for *–30 dB* sidelobe level, *–30 dB* crosspolar level and *–20 dB* return loss) and it is very sensitive to manufacturing tolerances in the throat region (mode generator) [11]. This antenna can be reclassified better as being a radiating resonator not an antenna because it works really nice for a 1% bandwidth.

Granet et al describe in [10] a corrugated horn antenna presented by our group [12]; they say that they designed a 17.4^{o} half-power beamwidth (this means *20.95 dB* directivity and global earth coverage from a geoestationary satellite, see appendix III) corrugated GPHA with $8.92 \cdot l$ length obtaining a *-33 dB* sidelobe level and a *-40dB* maximum crosspolar level. They assumed that this was the best antenna one can design with gaussian techniques. But as we have seen in this thesis, this is not completely true because with a Gaussian profile [13] sidelobe levels can be lowered much more and probably the length can be also improved. In fact, with the formulas of chapter 6, we can design directly a complete corrugated GPHA with sidelobe levels below *-40 dB* in a $9 \cdot l$ length and with a

bandwidth above *25%*. After an optimization for sure this length could be reduced at least one l.

But in fact, the antenna presented by Granet et al in [10] is really short and can be applied in those cases where bandwidth and manufacture precision are not a problem and the size restrictions are really important.

We were sure that an improvement in a new complete corrugated GPHA's should overcome the size disadvantage over the bowl-shaped antenna of [10,11] besides the corrugated GPHA should present a better bandwidth, a lower sidelobe level and a lower sensitivity to manufacturing tolerances. The main disadvantage of the complete corrugated GPHA's is the length that adds the TE_{11} to HE_{11} mode converter at its input, so the length improvement might come from changing completely this crucial component.

Furthermore, we knew that it was not so important to have a nice HE_{11} at the input of the second section GPHA, the really important parameter at the input of the second section GPHA is to have a low sidelobe field, which is the same as to have a field that has the power not too close to the metallic walls at the inner diameter, ($\overline{D_0}$).

Also, it is well known that a choked antenna offers one of the shortest antenna profiles with rather good radiation features [14,15].

With all this information, in the spring of year 2002 we implemented a new antenna concept which results in a sharp change into the current technology. It consists on attaching a short choked antenna to minimize the length at the initial part together with a second section corrugated GPHA to improve the performance. Really impressive radiation features are obtained for this new type of profiled corrugated GPHA, in fact a design was

included in chapter 6 and the choked waveguide TE_{11} to HE_{11} mode generator was briefly explained in chapter 5.

The first antenna design we developed with this new technology was manufactured and measured and in fact this profile has been further improved now-a-days. The UK company Flann Microwave, Ltd. includes it in their catalog at any frequency band.

The design was performed to accomplish a very short antenna (*length*$<6.5\cdot\lambda$) with very low sidelobes (lower than *-40 dB* at central frequency) and with low crosspolarization, and as much as possible bandwidth. The illumination is fixed to be *-3 dB* at *8.7 deg*rees half beamwidth (the angle subtended by the earth from a geoestationary satellite which means *20.95 dB* directivity) to make a comparison between this antenna and the antenna presented in [10].

After a complete study of the ways of attaching these two profiles, a rather short antenna, $6.2\cdot\lambda$ long and $5.23\cdot\lambda$ output diameter was designed with four choked rings as input part. The design parameters are the following:

- Central design frequency: *9.65 GHz*.
- Input diameter: *22.4 mm*
- Choked part:
  - *4* choked rings of *7 mm* depth.
  - Period of choke ring *5 mm*,
  - Choke ring width *2 mm*
- Vertical corrugation parameters: *p=7 mm*, *w=3 mm* and *d=8.8 mm*
- Second GPHA output part:
  - $\alpha=0.71$,
  - Length=$20\cdot p+w$ (*143 mm* or *f=0.489*).

- $\overline{D_0}=2.47$

So the total length of the antenna is *193 mm* (*6.2·l*) and the output diameter *5.23·l* (*162.5 mm*). A picture of the antenna can be seen in figure 7.15.

This antenna exhibited in simulation pure gaussian beam until *–43 dB* sidelobe level (11*%* bandwidth for *-40 dB* maximum sidelobe level).

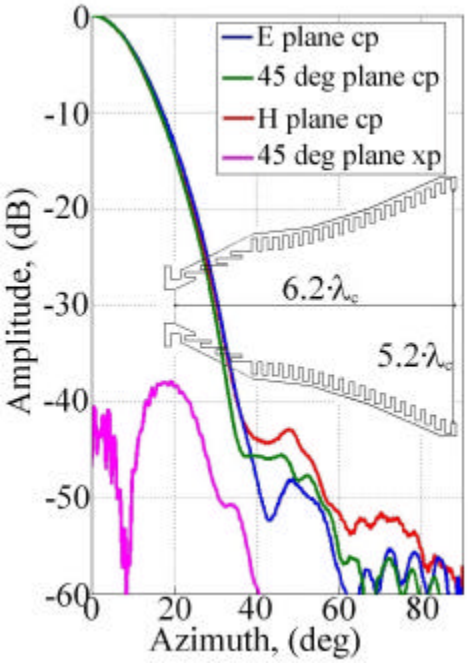

Figure 7.15. Measured radiation pattern at central frequency of choked corrugated GPHA

This antenna is a slightly longer than the bowl-shaped CSIRO (CSIRO stands for: Commonwealth Scientific & Industrial Research Organisation) antenna counterpart [10,11], but its radiation features and behavior are much better. Also the weight of this antenna will be similar to the bowl-shaped counterpart because this bowl-shaped presents a larger radius at the input part.

By the suppression of only the last two corrugation periods in the second corrugated GPHA section of this antenna which leads to $5.75 \cdot l$ length and $4.83 \cdot l$ output diameter; the simulated radiation features are still better than the bowl-shaped counterpart, and the size is the same.

The antenna was measured in a *17%* bandwidth with really good results. The measured return loss was below *–28 dB* for the whole *17%* bandwidth, (see figure 7.16a). The measured sidelobe level was extremely low, below *–30 dB* for the whole measured bandwidth and the measured crosspolarized level was also below *–30 dB* in a *16%* bandwidth, (fig 7.16a).

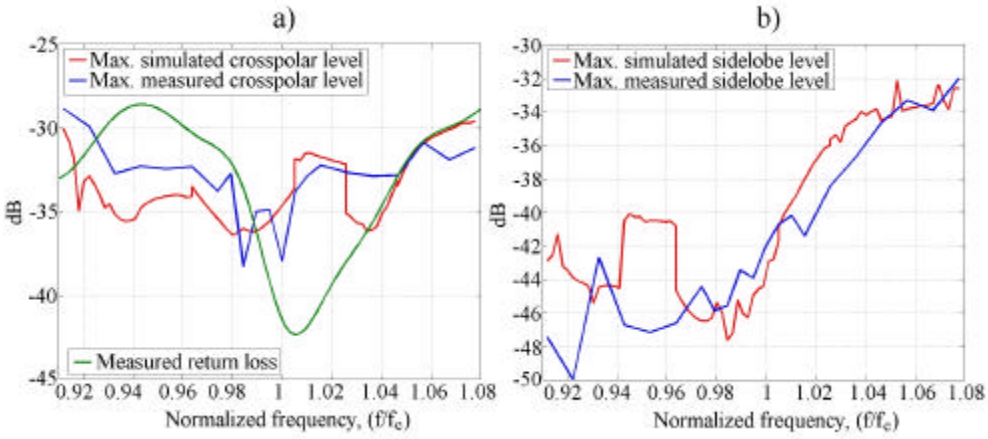

Figure 7.16. a) Measured and theoretical crosspolar levels of the choke-gaussian antenna as well as measured return loss
b) Measured and theoretical sidelobe level of the choke-gaussian antenna.

It is important to remark that in a *11%* bandwidth the measured sidelobe level was below *-40 dB*, see figures 7.15 and 7.16b [9].

In figure 7.15, the measured radiation pattern at central frequency is depicted. Also, in table 7.4, the main radiation characteristics of this antenna at central frequency are presented.

H plane taper @ 8.7 deg	45 deg plane taper @ 8.7 deg	E plane taper @ 8.7 deg	Maximum sidelobe level	Maximum crosspolar level	Directivity
-2.74 dB	**-2.82 dB**	**-2.9 dB**	**-43 dB**	**-38 dB**	**20.5 dB**

Table 7.4. Radiation pattern details of the choked corrugated GPHA at central frequency

It is also important to remark the high similarity between measured results and simulated ones. Simulated results were performed by means of the finite element electromagnetic simulator Ansoft-HFSS. At present we have upgraded to a new EM software tool called μWave Wizard which employs a mixture of analysis codes to improve speed and accuracy.

Figure 7.17 Manufactured choked GPHA antenna for 9.65 GHz (a 2 euro coin is photographed as well to compare)

From figure 7.16a, it can be seen that the crosspolar level is not really low in that first manufactured design. But the new software speed and easiness to change the design parameter allows us to improve the crosspolar level as well as the bandwidth so now we can manufacture for sure a choked

corrugated GPHA at any directivity with a crosspolar level comparable to the rest of corrugated horns. An improvement in bandwidth is being considered at the moment.

7.6 References

[1] Gonzalo, R., Martí-Canales, J., Teniente, J., del Río, C. and Sorolla, M., "Measurements of a New Gaussian Profile Corrugated Horn Antenna for Millimetre Wave Applications", *1998 IEEE AP-S International Symposium and URSI Radio Science Meeting*, 21-26 June, Atlanta, Georgia, United States

[2] Fernandez-Curto, A., Likin, K. M., Martín, R., Martí Canales, J., Teniente, J., Gonzalo, R., del Río, C. and Sorolla, M., "Corrugated Horn Antenna for Low-Power testing of the Quasioptical Transmission Lines at TJ-II Stellerator"**,** *AMTA'99 21st Annual Meeting and Symposium on Antenna Measurement Techniques Association*, October 1999, Monterrey Bay, California, United States

[3] Teniente, J., Gonzalo, R., del Río, C., Martí-Canales, J., Sorolla, M., Fernández-Curto, A., Likin, K. M. and Martín, R., "Corrugated Horn Antenna for Low-Power Testing of the Quasioptical Transmission lines at TJ-II Stellerator", *International Journal of Infrared and Millimetre Waves*, Vol. 20, No. 10, pp. 1757-1767, October 1999

[4] Teniente, J., Gonzalo, R., and del Río, C., "Gaussian Profiled Horn Antenna for Hispasat 1C Satellite", *International Journal of Infrared and Millimetre Waves*, Vol. 20, No. 10, pp. 1809-1815, October 1999

[5] R. Wylde , “Low loss THz Quasi-optics signal processing for cosmology remote sensing and material measurement”, *AP-2000 Conference*, Davos, Switzerland, April 2000

[6] B., Maffei, P. A. R. Ade, F. C. Gannaway, E. Wakui, R. J. Wylde, J. A. Murphy, R. Colgan, J. Dupuy, C. G. Parini, “Corrugated Gaussian back-to-back horns for cosmic microwave background continuum receivers”, *24th QMW Antenna Symposium*, 38-41, London, April 2000

[7] S.G. Hay, S.J. Barker, C. Granet, A.R. Forsyth, T.S. Bird, M.A. Sprey and K.J. Greene, “Multibeam Earth Station Antenna for a European Teleport Application” *2001 IEEE AP-S International Symposium and URSI Radio Science Meeting*, 8-13 of July, Boston, United States

[8] Teniente, J., Gonzalo, R., and del Río, C., “Ultra Wide Band Corrugated Gaussian Profiled Horn Antenna Design”, *IEEE Microwave and Wireless Components Letters*, Vol. 12, No. 1, pp. 20-21. January 2002

[9] Jorge Teniente, David Goñi, Ramón Gonzalo and Carlos del Río, “Choked Gaussian Antenna: Extremely Low Sidelobe Compact Antenna Design”, *IEEE Antennas and Wireless Propagation Letters*, Vol. 1, N. 11, pp. 200-202, November 2002

[10] C. Granet, T. S. Bird and G.L. James, “Compact Multimode Horn with Low Sidelobes for Global Earth Coverage”, *IEEE Transactions on Antennas and Propagation*, Vol. 48, No. 7, July 2000

[11] T. S. Bird, C. Granet and G.L. James, “Lightweight Compact Multi-mode Corrugated Horn with Low Sidelobes for Global-Earth Coverage”, *AP2000 Conference*, Davos, Switzerland, April 2000

[12] R. Gonzalo, J. Teniente and C. del Río, “Very Short and Efficient Feeder Design for Monomode Waveguide”, *Proceedings IEEE AP-S International Symp*osium, Montreal, Canada, July 1997

[13] C. del Río, R. Gonzalo, and M. Sorolla, “High purity beam excitation by optimal horn antenna,” in *Proceedings of the 1996 International Symposium on Antennas and Propagation*, vol. 4, pp. 1133-1136, Chiba, Japan, September 1996

[14] A.D. Olver, P.J.B. Clarricoats, A.A. Kishk and L. Shafai, “Microwave Horns and Feeds”, *IEE Electromagnetic waves series 39,* The Institution of Electrical Engineers, 1994

[15] A. W. Rudge, K. Milne, A.D. Olver and P. Knight, “The Handbook of Antenna Design”, *IEE Electromagnetic waves series 15 and 16.* The Institution of Electrical Engineers, 1982

Chapter 8

Conclusions and guidelines for future research

In this final chapter, the most relevant results derived from the research contained in this dissertation will be summarized. Subsequently, some recommendations for future research will be provided.

8.1 Conclusions

Corrugated Gaussian Profiled Horn Antennas (GPHA's) offer one of the best solutions for high performance horns where low sidelobes, wide bandwidth, low crosspolar levels, constant taper illumination and phase center stability are important design parameters.

In spite of conical corrugated horn antennas illuminate more efficiently the antenna aperture than corrugated GPHA's, the former are unable to offer sidelobes lower than *-30 dB* for directivities above *18 dB*.

This lower aperture illumination efficiency for the corrugated GPHA's doesn't lead to longer profiles; on the contrary, very often a shorter profile can be designed due to the better radiation features.

A design method to define completely a corrugated GPHA that meets all the required specifications in a quite compact profile has been explained during the last chapters. The design obtained by means of this method will not be the optimum one, but will be a nice initial solution to begin with.

Several antennas have been developed during the last 6 years with this technology, validating its computer simulations and achieving all the stringent requirements they were asked for.

As a practical examples, in 1.998 when this new technology was still in their infancy, an antenna design was made suitable for *Hispasat 1C satellite* and some years later was used also for *Hispasat 1D satellite*. This design was better than its conical corrugated counterpart related to physical and electromagnetic features. At the same time, the weight constrains, so important in satellite applications, were also improved. By using this new research technique, reduced sizes in length and output radius can be obtained with better radiation features.

At the beginning of the new millennium our research gave to the market a new design based on a Symmetric GPHA+ GPHA technology to accomplish ultra-wide bandwidth with low side-lobes (-30 dB in 40% bandwidth) and cross-polar levels (-30 dB in 49% bandwidth and –35 dB in 30% bandwidth). This new design was manufactured and measured to validate its results. A very good agreement between simulations and measurements was reported. These results made this type of antenna suitable for a wide variety of applications, i.e. as a feed for antenna measurement facilities or wide bandwidth satellite communications.

In 2002 a new type of corrugated horn resulting by the union of a choked waveguide antenna and a corrugated GPHA was developed. We called it the *choked corrugated GPHA*. This horn is impressively short and compact and presents really low sidelobes while it maintains good crosspolar levels and quite wide bandwidth. Simulated and measured results are also in good agreement. This antenna is being commercialized at the moment by the British company *Flann Microwave Ltd***.** Flann Microwave

engineers think that this antenna will be the future of communications links in a few years and they have put a lot of effort on its commercialization in the last few months. Nice qualities as simplicity of manufacture and low costs derived of its ruggedness, added to its really impressive radiation pattern in a really short and compact profile make of this type of antennas the antennas for the near future communication links. A reference to `http://www.flann.com` for more information about this antenna would be a nice conclusion on it (a non disclosure agreement stands between Flann Microwave Ltd. and the Antenna Group of the Public University of Navarra to avoid the massive copying of this antenna by other companies).

As a final conclusion we can say that corrugated GPHA's at the output of certain antennas are now-a-days the best choice for improving radiation patterns when extremely stringent requirements are required.

8.2 Guidelines for future research

A design method to completely define a corrugated GPHA has been explained in this thesis, however this design method has only been completely defined for three different input parts of the general corrugated GPHA (conical corrugated input, corrugated GPHA input and symmetrical corrugated GPHA input). It has been defined also another two possibilities, (the corrugated input developed by CSIRO and the choked waveguide input), but these both input parts have not been completely defined to be attached to the second section corrugated GPHA.

A design method for choked corrugated GPHA's must be defined after this thesis, so that the designer can prepare quickly a profile at any achievable directivity with low effort and nice quality. This is the main

guideline for future research of this type of Modern Corrugated Horn Antennas.

Appendix I

Characteristics of the Fundamental Gaussian mode

The gaussian mode family is of great interest in this thesis because the gaussian modes are the most commonly used modes to define the free space radiation. It is needed to make an approximation to solve the Maxwell equations to obtain the gaussian modes. This approximation is based on the paraxiality, and it will be always the case of horn antennas with moderate and high directivities. The paraxiality assumes the following:

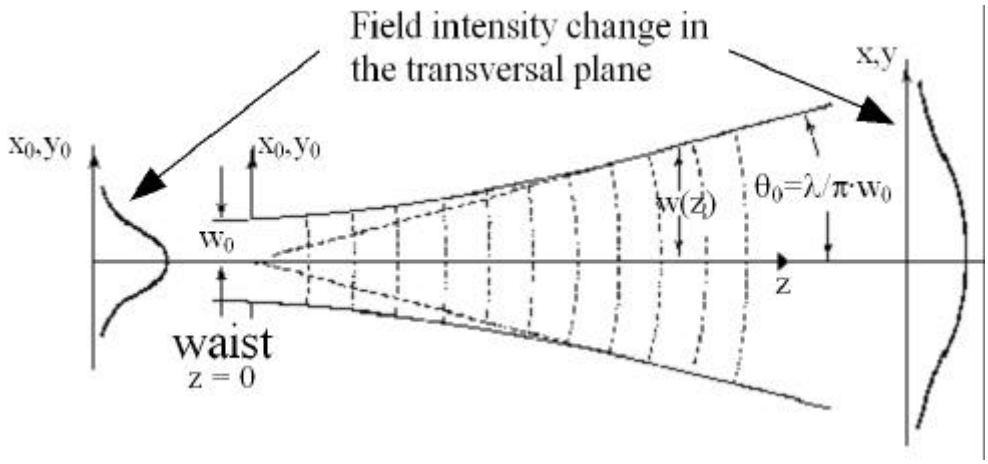

Figure A1.1. Propagation of a fundamental Gaussian beam mode

The electromagnetic radiation can be expressed as a beam spatially concentrated and with not much divergence. The free space propagating waves whose wavefronts direction forms little angles with respect to the propagation axis (*z* axis) can be called paraxial waves. This paraxial waves

must satisfy the Helmholtz paraxial equation. An important set of solutions of this equation is the gaussian beam mode family.

The free space propagation of the fundamental gaussian mode is depicted in figure A.1.1.

A1.1 General equations for the gaussian modes

A single component, Ψ, of an electromagnetic wave propagating in a uniform medium satisfies the Helmholtz (wave) equation,

$$\nabla^2\Psi + k^2 \cdot \Psi = 0 \qquad \text{(A1.1)}$$

where Ψ represents any component of $\boldsymbol{E}$ or $\boldsymbol{H}$. We have assumed a time variation at angular frequency w of the form $e^{j \cdot v \cdot t}$. The wave number k is equal to $2p/l$, so that $k = v \cdot \sqrt{e_r \cdot m_r}\,/c$, where e_r y m_r are the relative permitivity and permeability of the medium respectively. For a plane wave, the amplitudes of the electric and magnetic fields are constant; and their directions are mutually perpendicular, and perpendicular to the propagation vector. For a beam of radiation that is similar to a plane wave but for which we will allow some variation perpendicular to the axis of propagation, we can still assume that the electric and magnetic fields are (mutually perpendicular and) perpendicular to the direction of propagation. Letting the direction of propagation be in the positive z direction, we can write the distribution for any component of the electric and magnetic field (suppressing the time dependence) as:

$$E(x,y,z)=u(x,y,z) \cdot e^{(-j \cdot w \cdot z)} \qquad \text{(A1.2)}$$

where u is a complex scalar function that defines the non-plane wave part of the beam. In rectangular coordinates, the Helmholtz equation is defined as:

$$\frac{\partial E}{\partial x^2}+\frac{\partial E}{\partial y^2}+\frac{\partial E}{\partial z^2}+k^2E=0 \qquad \text{(A1.3)}$$

If we substitute our quasi-plane wave solution, we obtain:

$$\frac{\partial u}{\partial x^2}+\frac{\partial u}{\partial y^2}+\frac{\partial u}{\partial z^2}-2jk\frac{\partial u}{\partial z}=0 \qquad \text{(A1.4)}$$

which is sometimes called the reduced wave equation.

The paraxial approximation consists of assuming that the variation along the direction of propagation of the amplitude *u* (due to diffraction) will be small over a distance comparable to a wavelength, and that the axial variation will be small compared to the variation perpendicular to this direction. The first statement implies that (in magnitude):

$$\left[\frac{\Delta\left(\frac{\partial u}{\partial z}\right)}{\Delta z}\right]\cdot 1 << \frac{\partial u}{\partial z} \qquad \text{(A1.5)}$$

which enables us to conclude that the third term in the reduced wave equation (A1.4) is small compared to the fourth term. The second statement allows us to conclude that the third term is small compared to the first two. Consequently, we may drop the third term, obtaining finally the paraxial equation in rectangular coordinates:

$$\frac{\partial u}{\partial x^2}+\frac{\partial u}{\partial y^2}-2jk\cdot\frac{\partial u}{\partial z}=0 \qquad \text{(A1.6)}$$

Solutions to the paraxial equation are the Gaussian beam modes that form the basis for the analysis of the radiation of any of our horn antennas.

A1.2 Fundamental gaussian beam mode

A1.2.1 Propagation of the fundamental gaussian mode

The solution of paraxial Helmholtz equation (equation A1.6) for the fundamental mode and suppressing the normalization constants that doesn't affect the shape of the mode can be expressed as:

$$u(r,j,z)=\frac{w_0}{w(z)}\cdot e^{\frac{-r^2}{w^2(z)}}\cdot e^{-j\frac{kr^2}{2\cdot R(z)}}\cdot e^{-j(kz-z(z))} \qquad \text{(A1.7)}$$

Equation A1.6 is j dependant, but the this dependence is not found in the body of the equation. This means that the fundamental gaussian mode is j symmetrical.

In equation A1.7, we can identify the following terms:

- $r=\sqrt{x^2+y^2}$
- *w(z)* is the radial beamwidth where the normalised field has decayed *1/e* times, (*86%* of the power is concentrated in $\pm w(z)$). At *z=0*, *w(z)* has a minimum value known as beamwaist and identified by the term w_0:

$$w(z)=w_0\cdot\sqrt{1+\left(\frac{2\cdot z}{k\cdot w_0}\right)^2} \qquad \text{(A1.8)}$$

Equation A1.8 can be defined also with another variable called beam depth of Rayleigh distance, z_0. This variable defines the distance where the beamwidth is exactly $w(z)=\sqrt{2}\cdot w_0$:

$$z_0=\frac{k\cdot w_0^2}{2} \qquad \text{(A1.9)}$$

Equation A1.8 can be re-written as:

$$w(z) = w_0 \cdot \sqrt{1 + \left(\frac{z}{z_0}\right)^2} \qquad \text{(A1.10)}$$

In z_0, the field intensity has decayed in the axis –3 dB exactly.

For $z>>z_0$, the equation A1.10 can be re-written as:

$$w(z) \approx \frac{w_0}{z_0} \cdot z \qquad \text{(A1.11)}$$

Then, with equation A1.11, the divergence of the fundamental gaussian beam can be expressed as:

$$q_0 = arctan\, g\left(\frac{w_0}{z_0}\right) = arctan\, g\left(\frac{l}{p \cdot w_0}\right) \qquad \text{(A1.12)}$$

This value of q_0 will be the angle where the field has decayed *1/e* for $z>>z_0$, and a reduction in frequency or a reduction in the beamwaist value (w_0) will be translated as an increase of the beam propagation divergence. This is strongly related to the paraxial condition defined as $k \cdot w_0 \geq 6$ [1,2].

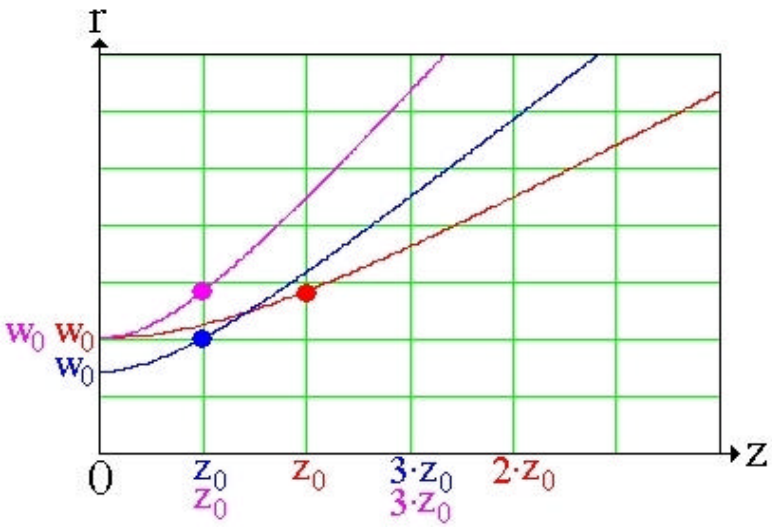

Figure A1.2. Beamwidth of a fundamental gaussian beam mode for different values of beamwaist and frequency

b) $w_{02} = \sqrt{2}/2 \cdot w_{01}$ *c)* $f_3 = 0.5 \cdot f_1$

- *R(z)* is defined as the wavefront radius of curvature. It is defined in the following equation:

$$R(z) = z \cdot \left(1 + \left(\frac{z_0}{z} \right)^2 \right) \qquad \text{(A1.13)}$$

In figure A1.3 it is depicted the variation of *R(z)*. It can be extracted from the figure that *R(z)* decreases from planar wave fronts at the beamwaist ($R(z) = \infty$) to its minimum value at z_0.

Figure A1.3. Fundamental gaussian beam wavefronts radius of curvature

- From equation A1.7 it is also defined *z(z)* as a little delay respect to the planar wavefronts. It is expressed in equation A1.14 as:

$$z(z) = arctan\, g\left(\frac{z}{z_0} \right) \qquad \text{(A1.14)}$$

Last equations define the propagation of a fundamental gaussian beam. Then, any fundamental gaussian beam can be completely defined by the beamwidth (*w(z)*) and the wavefront curvature radius (*R(z)*) in any place of the free space. Once we know those two parameters and with the use of equations A1.10 and A1.13 we can calculate the value for the beamwaist

(w_0) and its position in the *z* axis. With w_0 and its position we can easily define completely the fundamental gaussian beam.

A1.2.2 Field intensity and carried power of a fundamental gaussian beam mode

The field intensity of a fundamental gaussian beam mode is defined as the squared modulus of the scalar field, (equation A1.7). Its equation can be expressed as:

$$I(r,j,z) = I_0 \cdot \left(\frac{w_0}{w(z)} \right)^2 \cdot e^{-\frac{2 \cdot r^2}{w^2(z)}} \qquad \text{(A1.15)}$$

In figure A1.4, the fundamental gaussian field intensity in any place of the propagating axis *z* is depicted.

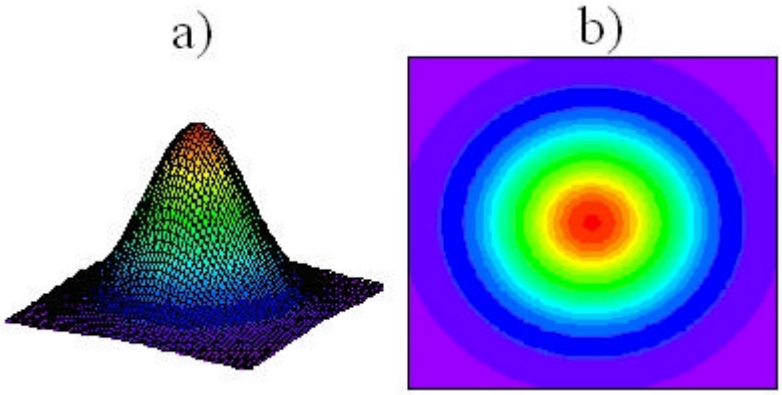

Figure A1.4. Fundamental gaussian beam field intensity in any point of the z axis
a) Lateral view b) Top view

A particularization of equation A1.15 in the axis ($r=0$), we obtain equation A1.16:

$$I(0,j,z) = I_0 \cdot \left(\frac{w_0}{w(z)} \right)^2 = \frac{I_0}{1 + \left(\frac{z}{z_0} \right)^2} \qquad \text{(A1.16)}$$

From equation A1.16, at $z=z_0$, the field intensity in the z axis is half of the initial value at the beamwaist (I_0).

In figure A1.5 is depicted the normalized field intensity, it can be appreciated how the beam propagating in z axis diminishes its field intensity and broadens itself.

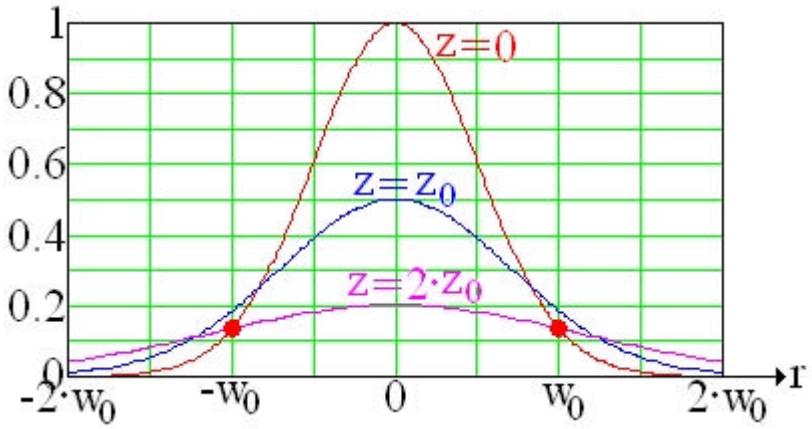

Figure A1.5. Fundamental gaussian beam normalized field intensity for three different points in the z axis

In figure A1.6 it is also depicted the normalized field intensity, but now the r axis is fixed at $r=0$. It can be observed that a $z=z_0$, the field intensity decay is half of its value at the beamwaist ($z=0$).

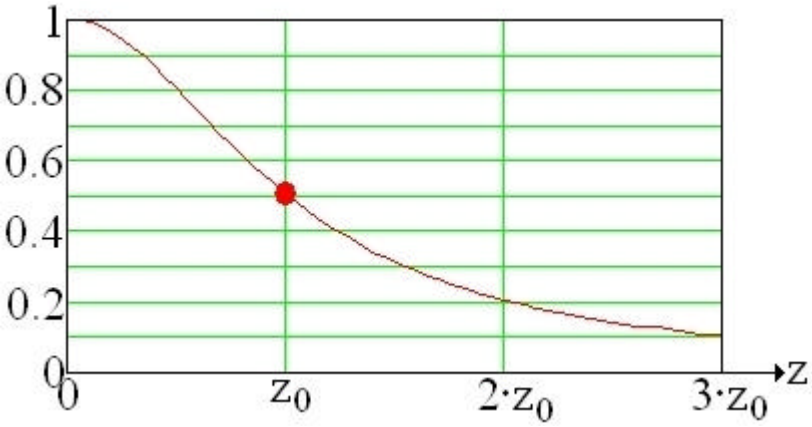

Figure A1.6. Fundamental gaussian beam normalized field intensity for over the axis r=0

In figure A1.7, a 3D view of figures A1.5 and A1.6 is depicted. This figure clarifies the way a fundamental gaussian beam propagates in free space.

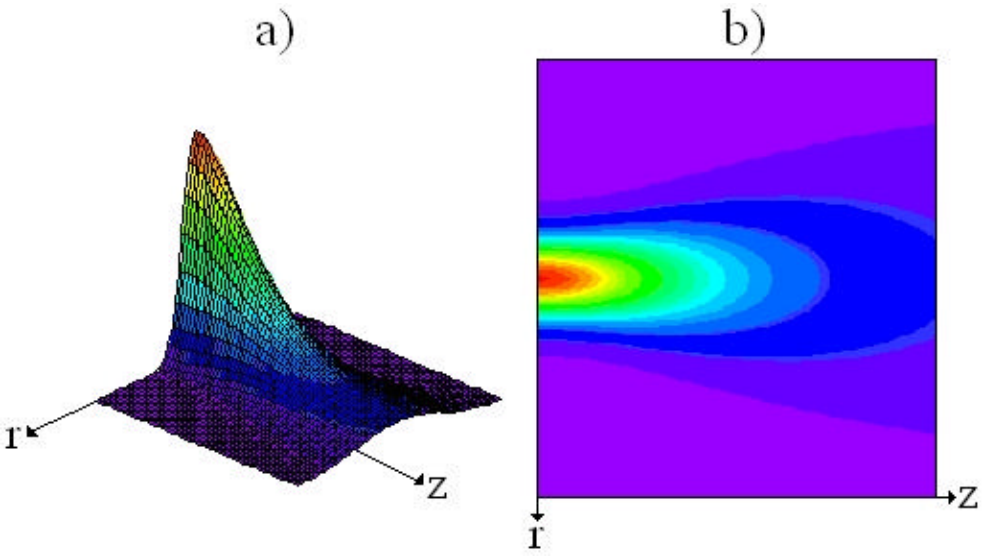

Figure A1.7. Three dimensional distribution of the fundamental gaussian beam normalized field intensity
a) Lateral view b) Top view

The power that carries a fundamental gaussian beam can be calculated by means of a field intensity integral over a surface, see equation A1.17:

$$P = \int_0^{2\cdot p} \int_0^{\infty} I(r, j, z) \cdot r \; dr \; dj \qquad \text{(A1.17)}$$

The fundamental gaussian beam has azimuthal symmetry, so the previous integral equation can be simplified, (see equation A1.18):

$$P = 2 \cdot p \cdot \int_0^{\infty} I(r, j, z) \cdot r \; dr \qquad \text{(A1.18)}$$

Integrating equation A1.18 for a certain *z*, the carried power of a fundamental gaussian beam results to be (equation A1.19):

$$P = \frac{1}{2} \cdot I_0 \cdot \left(p \cdot w_0^2 \right) \qquad \text{(A1.19)}$$

Then, the power carried by a fundamental gaussian beam is half of the intensity multiplied by the effective area of the beam defined by the radius w_0.

The relation between the power in a circle of radius r_0 in a transversal plane at a certain z position, and the total carried power by the beam can be calculated by means of equation A1.20:

$$\frac{1}{P}\cdot\int_0^{r_0} I(r,j,z)\cdot 2\cdot p\cdot r\ dr = 1-e^{-\frac{2\cdot r_0^2}{w^2(z)}} \qquad \text{(A1.20)}$$

Then, the power in a circle of radius $r_0=w(z)$ is approximately an *86.5%* of the total power, and in a radius of $r_0=1.5\cdot w(z)$ it is concentrated a *98.9%* of the total power carried by the beam.

A1.2.3 Phase fronts of a fundamental gaussian beam mode

The phase of a fundamental gaussian beam mode can be extracted from equation A1.7, (see equation A1.21):

$$arg(u(r,j,z)) = k\cdot z - z(z) + \frac{k\cdot r^2}{2\cdot R(z)} \qquad \text{(A1.21)}$$

We seek to obtain the expression for surfaces of constant phase, so equation A1.21 can be made equal to a constant $2\cdot p\cdot q$ and then we obtain the following equation:

$$2\cdot p\cdot q = k\cdot z - z(z) + \frac{k\cdot r^2}{2\cdot R(z)} \qquad \text{(A1.22)}$$

Equation A1.22 provides the 3D constant phase surfaces with a phase of a value $2\cdot p\cdot q$.

In the following paragraphs, the approximated behaviour of the phase fronts evolution is explained, [2]:

- When $z \to 0$, equation A1.22 can be simplified as:

$$2 \cdot p \cdot q = \frac{k \cdot r^2}{2 \cdot z_0^2} \cdot z \qquad \text{(A1.23)}$$

where the approximation $R(z) \approx z_0^2 / z$ has been considered.

Equation A1.23 provides an asymptotic behaviour when $r \to \infty$ defining a planar phase front.

- When $z \to \infty$, equation A1.22 can be simplified assuming $R(z) \approx z$ and $z(z) \approx p/2$ resulting in:

$$2 \cdot p \cdot q = k \cdot z - \frac{p}{2} + \frac{k \cdot r^2}{2 \cdot z} \qquad \text{(A1.24)}$$

Equation A1.24 is the equation of an ellipse with a minor diameter of $2 \cdot z_c$ and a mayor diameter of $2 \cdot \sqrt{2} \cdot z_c$. The diameters crosspoint is $(r,z)=(0,z_c)$. The formula of this ellipse is then defined in equation A1.25:

$$\left(\frac{r}{\sqrt{2}} \right)^2 + \left(z - z_c \right)^2 = z_c^2 \qquad \text{(A1.25)}$$

where z_c is:

$$z_c = \frac{l \cdot \left(q + \frac{1}{4} \right)}{2} \qquad \text{(A1.26)}$$

The last approximations are depicted in figure A1.8 with a real picture of the phase fronts. The approximation can be validated by means of such figure.

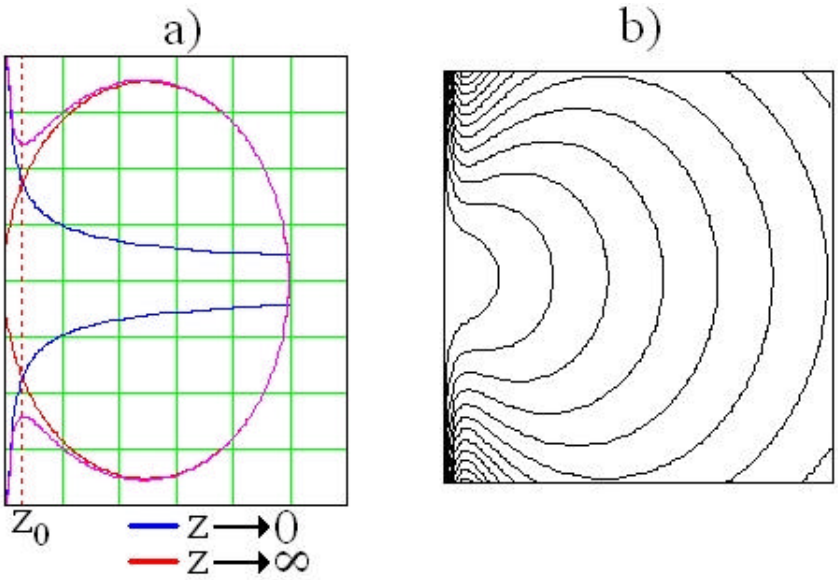

Figure A1.8. Phase front representation of the fundamental gaussian beam
a) Approximated phase fronts
b) Real phase fronts

The phase fronts are also depicted in figure A1.9 within the propagation of the fundamental gaussian beam mode restricted to the region that carries the *86.5%* of the power ($r<w(z)$). Figure A1.9 shows that very near the beamwaist the phase fronts are nearly planar and for far away the beamwaist the phase fronts can be approximated by spheres.

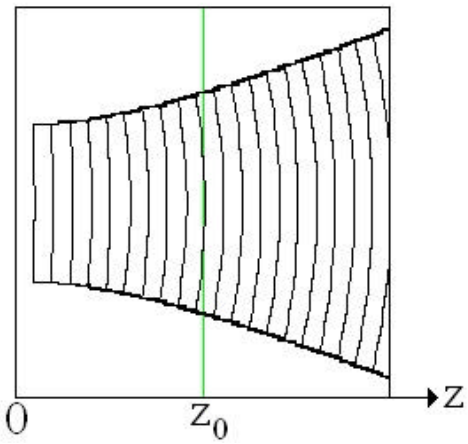

Figure A1.9. Phase front representation of the fundamental gaussian beam restricted to $r<w(z)$

A1.3 References

[1] del Río, C., Gonzalo, R. and Sorolla, M., "Paraxiality Considerations of Higher Order Gaussian Modes", *International Conference on Infrared and Millimeter Waves. Year* 1996. AT11, Conf. Proceedings, ISBN: 3-00-000800-4

[2] del Río, C., "Diseño de Guías de Onda Cuasi-Ópticas para Modos Gaussianos de Orden Superior", Ph. D dissertation, Electric and Electronic Engineering Department, Public University of Navarra. Year 1996.

Appendix II

Resonance spikes in corrugated horn antennas

A theoretical study reinforced with practical measurements about the origin of the return loss spikes in corrugated horn antennas is covered in this appendix. These spikes are directly related to the periodic structure of the corrugations and can be evaluated in simulation and sometimes in measurements. In this appendix we try to explain their effects, their origin and also several techniques to avoid them.

A2.1 Origin of the resonance spikes

Every corrugated horn antenna presents at a certain frequency band some resonance spikes. To characterize these spikes we will use the conical corrugated horn antenna model for X band of figure A2.1. This antenna presented this type of resonance spikes in the middle of its bandwidth (*11.6* to *12.2 GHz*), see figure A2.2. Its corrugation parameters are *p=3.4 mm*, *w=0.9 mm* and *d=5.9 mm*. It presents also an impedance transformer between *l/2* to *l/4* corrugation depth at the throat (see figure A2.1).

Corrugated horn antennas, due to the periodic structure of its corrugations (with ideally completely straight walls) can be considered as the concatenation of a series of small resonators.

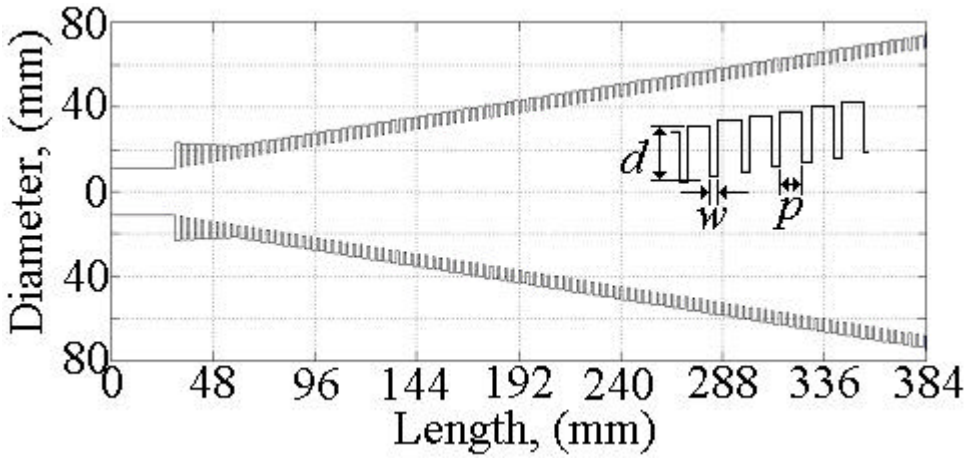

Figure A2.1. Conical corrugated horn antenna profile

This resonators will produce certain reflections at certain frequencies due to the collision of the electromagnetic field against this corrugations, (see figure A2.2). The most likely place to receive such a collision is just where the impedance transformer finishes and this happens due to two principal reasons:

- Corrugation depth is $l/4$
- The diameter of the horn is reduced, so there is a quite big amount of electromagnetic fields very near the corrugations.

A resonance implies a high diffraction of the electromagnetic field travelling inside the corrugated horn (a big field intensity inside the corrugation). This electromagnetic field diffraction at the throat is strongly related with the input diameter of the horn antenna, if the input diameter is small, (below $0.7 \cdot l$), the diffraction will be big. Usually we select an input diameter of $0.78 \cdot l$, but the operating band of an antenna produces at low frequencies to have the electromagnetic field at the input diameter of the horn antenna slightly tight. If the relation between the corrugation period, (p), the corrugation tooth width, (w) and the wavelength of every mode in

the corrugated region (l_g) are an exact multiple of $l_g/2$, then we will have a lot of possibilities of having a resonance inside our corrugated horn antenna.

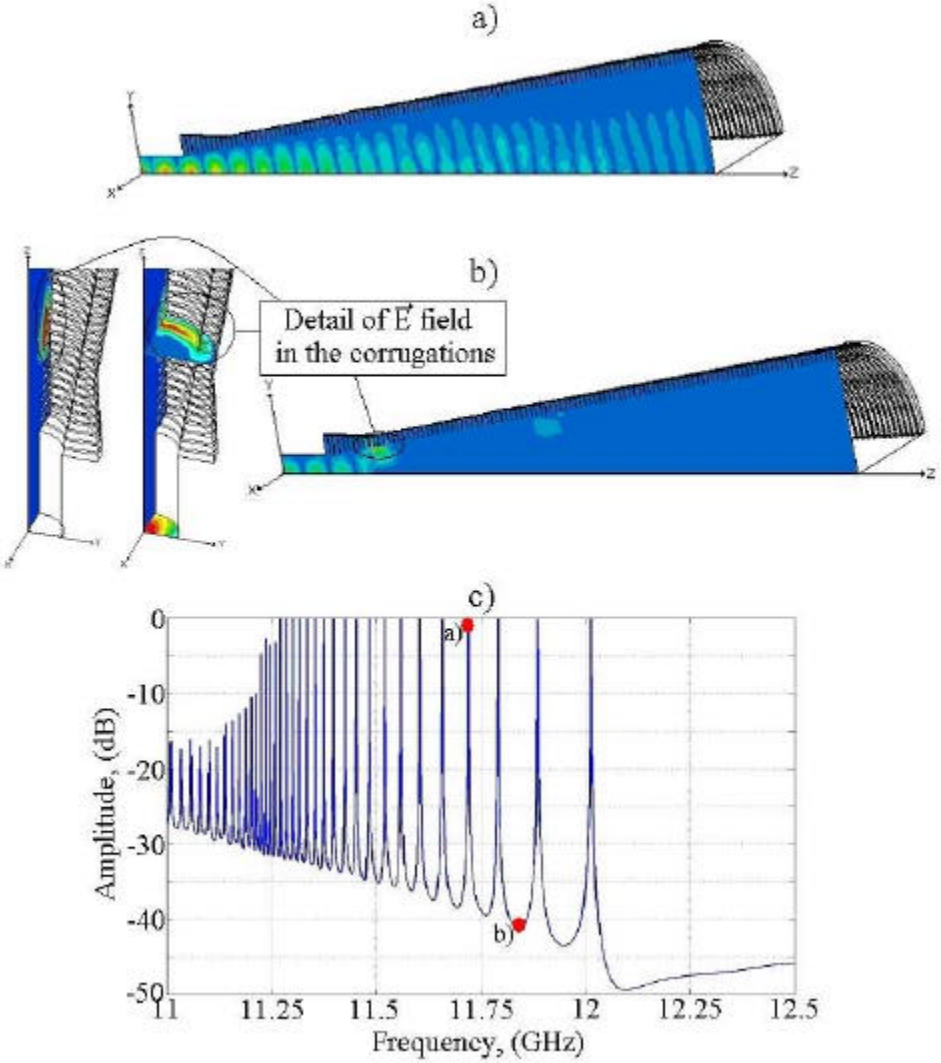

Figure A2.2. Electric field intensity inside the conical corrugated horn antenna at two frequencies
a) Without resonance b) With resonance
c) Return loss detail of the antenna

A2.2 How to eliminate the resonance spikes

To suppress the resonance spikes in a corrugated horn antenna there are several methods:

- An increase in the corrugation period of the antenna lowers the resonance spikes to lower frequencies. Figure A2.3 shows the effect of using a corrugation period of 4.5 mm instead of 3.4 mm for the antenna. No resonance spikes and the radiation parameters remain unchanged, now $p \approx l/5$.

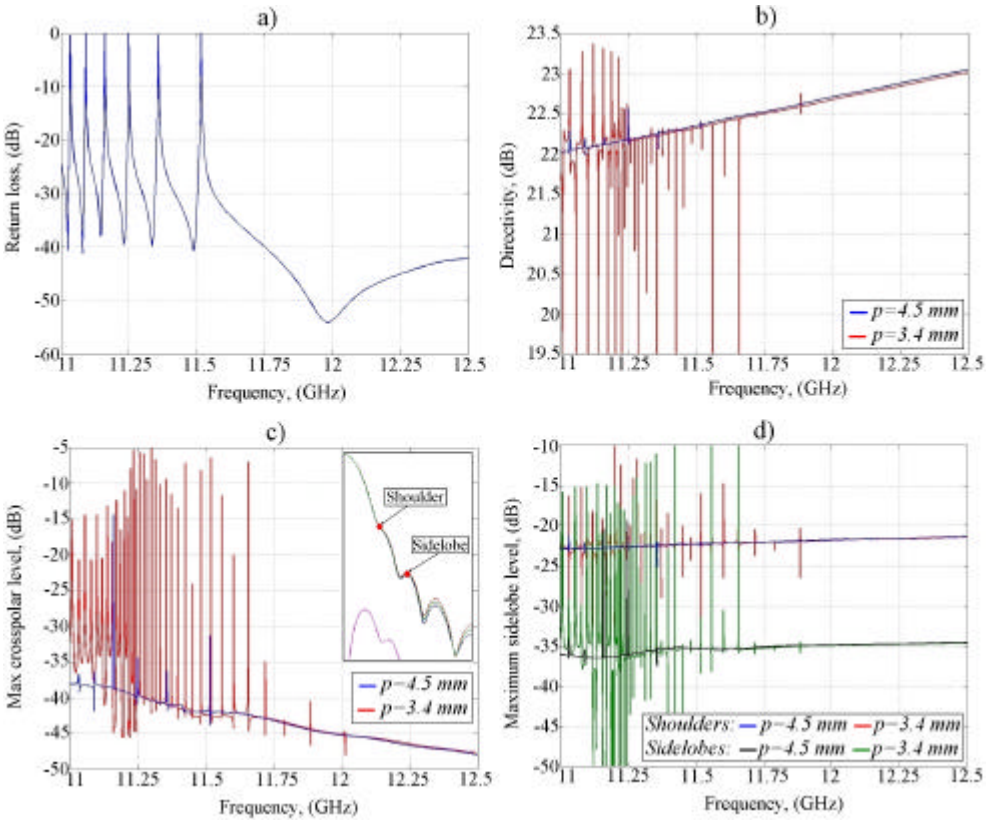

Figure A2.3. a) Return loss, p=4.5 mm and w=1.5 mm
b) Directivity comparison
c) Maximum crosspolar level comparison
d) Sidelobe and shoulder level comparison

- A change in the corrugation depth for the antenna will change the resonating frequency of each little resonator. Using a corrugation depth of *6.6 mm* instead of the *5.9 mm* of the last figures the resonance spikes move to lower frequencies and in the radiating properties, only the

crosspolar pattern changes, in this case changes to better response, (see figure A2.4).

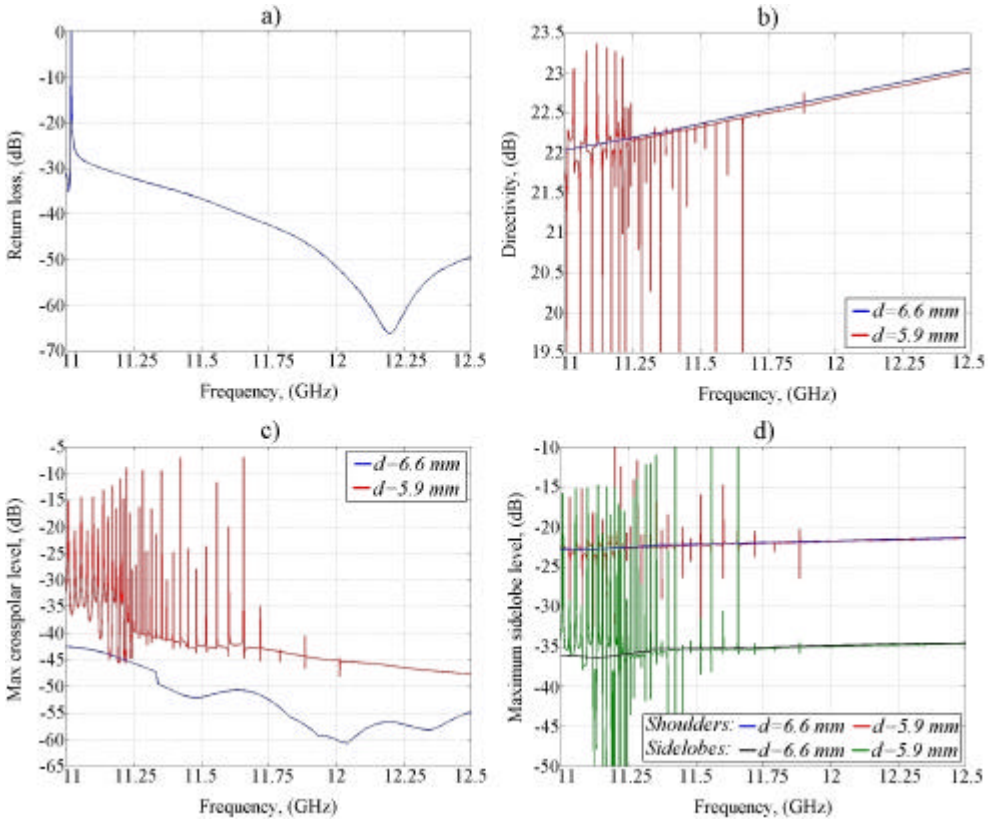

Figure A2.4. a) Return loss, d=6.6 mm
b) Directivity comparison
c) Maximum crosspolar level comparison
d) Sidelobe and shoulder level comparison

- Another way of reducing the resonance spikes is affecting to the purity of the resonators (corrugations). In a manufactured antenna, the corrugation walls will never be completely straight. Because of that the resonance spikes will have a finite quality factor (Q). A slight slope in the corrugations manufacture process will be welcome in case annoying spikes result impossible to remove in the simulation process, (see figure A2.5).

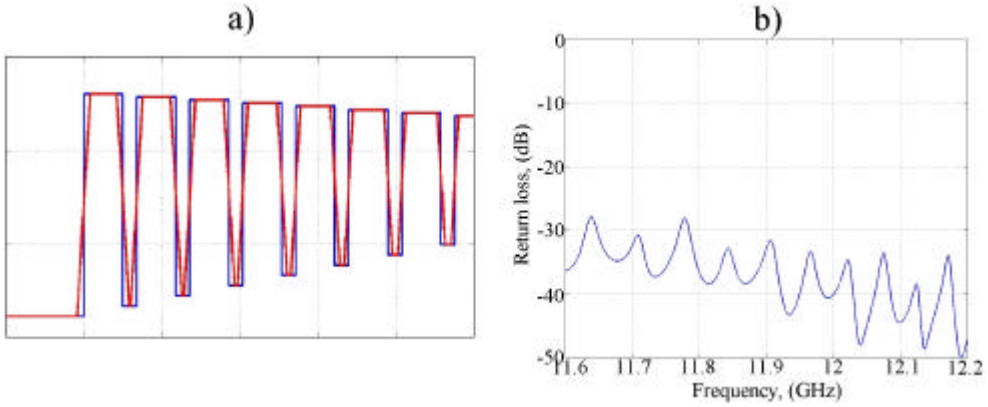

Figure A2.5. a) Detail of an exaggerated slope of the corrugations
b) Return loss for the antenna with a corrugation slope of 0.2 degrees

A2.3 References

[1] Arun K. Bhattacharyya, "High-Q resonances due to surface waves and their effects on the performances of corrugated horns", *IEEE Transactions on Antennas and Propagation, vol. 49, n. 4, pp. 555-566,* April 2001

[2] Teniente-Vallinas, J., Gonzalo-García, R. and del-Río-Bocio, C., "Ultra-Wide Band Corrugated Gaussian Profiled Horn Antenna Design", *2001 IEEE AP-S International Symposium and USNC/URSI National Radio Science Meeting*, 8-13 of July, Boston, Massachusetts, United States of America

[3] Teniente-Vallinas, J., Gonzalo-García, R. and del-Río-Bocio, "Estudio de Resonancias Parásitas en Antenas Corrugadas", *XVI Symposium de la Unión Científica Internacional de Radio (URSI'01)*. Villaviciosa de Odón, (Madrid), September 2001

Appendix III

Relation between Beamwidth and Directivity

In this appendix, the relation between beamwidth and directivity, assuming a perfect fundamental gaussian beam radiation, is given.

For corrugated GPHA's, the radiated field is very similar to a fundamental gaussian beam. Because of that nice radiation property, we can make a nearly perfect comparison between the radiated fields that we can obtain with the design methods proposed in this thesis and a fundamental gaussian beam.

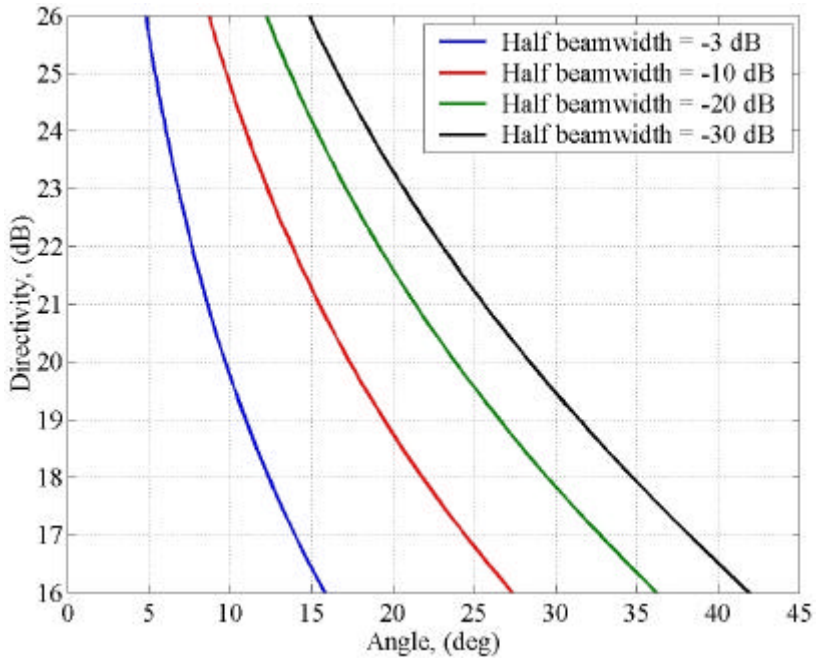

Figure A3.1 Half beamwidth to directivity comparison curves

To aid the designers that work on beamwidth values to define the radiation pattern of a corrugated GPHA, in the following figures this directivity to different beamwidth values can be found. In figure A3.1 a comparison between 4 different half beamwidths is given. Figure A3.2 gives a clearer plot for each of the four beamwidths of figure A3.1.

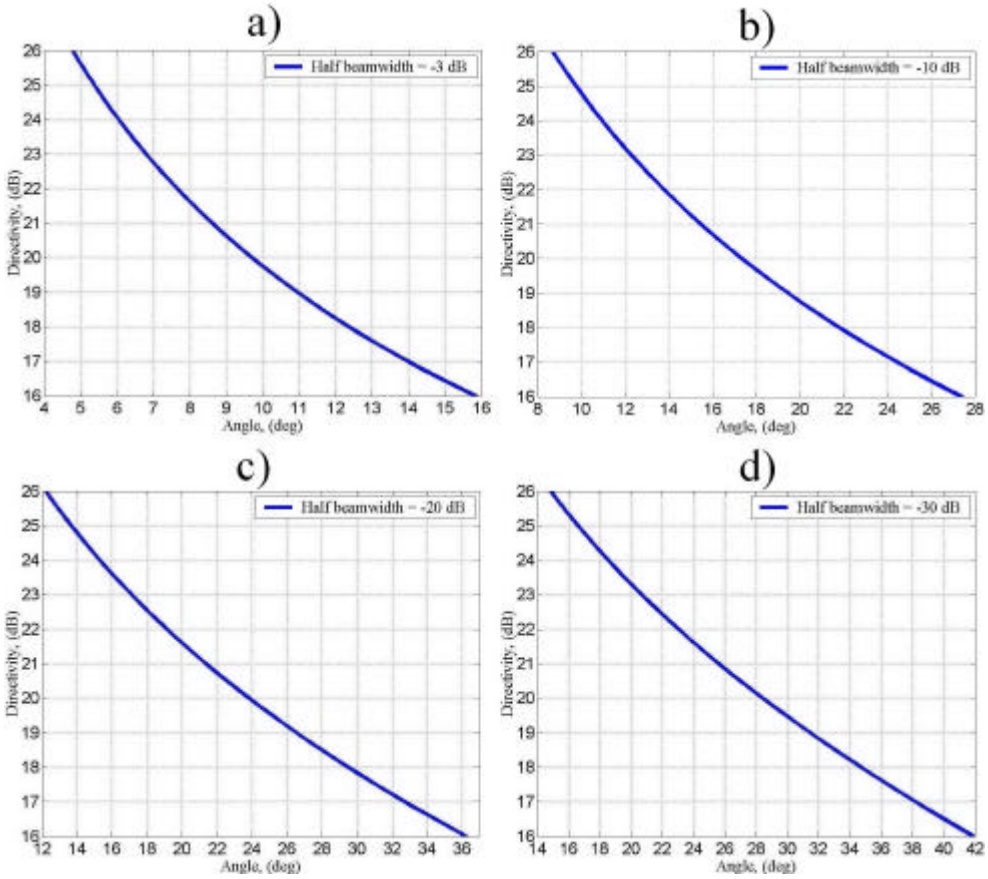

Figure A3.2 Half beamwidth to directivity comparison (detailed plots)
a) Half beamwidth –3 dB
b) Half beamwidth –10 dB
c) Half beamwidth –20 dB
d) Half beamwidth –30 dB

List of Publications

Related to the Thesis

Patents

1. Gonzalo, R., del Río, C., Goñi, D. and Teniente, J. *"Antena de bocina que combina corrugaciones horizontales y verticales"* Number: P.2002 01264. Priority country: Spain. Priority date: 24-05-2002 PCT initiated: 17-05-2003 Property of: Public University of Navarra (U.P.N.A.)

Journals

1. Teniente, J., Goñi, D., Gonzalo, R. and del Río, C. "Choked Gaussian Antenna: Extremely Low Sidelobe Compact Antenna Design", *IEEE Antennas and Wireless Propagation Letters*, Vol. 1, N. 11, pp. 200-202, November 2002

2. Gonzalo, R., Teniente, J., del Río, C. "Improved Radiation Pattern Performance of Gaussian Profiled Horn Antennas", *IEEE Transactions on Antennas and Propagation*, Vol. 50, N. 11, pp. 1505-1513, November 2002

3. Teniente, J., Gonzalo, R., del Río, C. "Ultra Wide Band Corrugated Gaussian Profiled Horn Antenna Design", *IEEE Microwave and Wireless Components Letters*, Vol. 12, No. 1, pp. 20-21. January 2002

4. Teniente, J., Gonzalo, R., del Río, C. "Gaussian Profiled Horn Antenna for Hispasat 1C Satellite"**,** *International Journal of Infrared and millimeter Waves*, Vol. 20, No. 10, pp. 1809-1815, October 1999

5. Teniente, J., Gonzalo, R., del Río, C., Martí-Canales, J., Sorolla, M., Fernández, A., Likin, K. M. and Martín, R. "Corrugated Horn Antenna for Low-Power Testing of the Quasioptical Transmission lines at TJ-II Stellerator", *International Journal of Infrared and millimeter Waves*, Vol. 20, No. 10, pp. 1757-1767, October 1999

International conferences

1. Teniente, J., Gonzalo, R., del Río, C. "Modern Corrugated Horn Antenna Design for Extremely Low Sidelobe Level " *Poster presentation at the 26th ESA Antenna Technology Workshop on Satellite Antenna Modelling and Design Tools*, 12-14 November 2003, ESA/ESTEC, Noordwijk, Holland

2. Teniente, J., Ortiz, N., Gonzalo, R., del Río, C. "Choked-Gaussian Corrugated Horn Antenna Design Small Global Coverage Horn Antenna for TT&C with Extremely Low Sidelobe Level" Poster presentation at the 26th ESA Antenna Technology Workshop on Satellite Antenna Modelling and Design Tools, 12-14 November 2003, ESA/ESTEC, Noordwijk, Holland

3. Teniente, J., Gonzalo, R., del Río, C. "Conical versus gaussian profiled corrugated horn antennas", *2002 IEEE AP-S International Symposium and USNC/URSI National Radio Science Meeting*, 16-21 of June, San Antonio, Texas, United States of America

4. Teniente, J., Gonzalo, R., del Río, C. "Ultra-Wide Band Corrugated Gaussian Profiled Horn Antenna Design", *2001 IEEE AP-S International Symposium and USNC/URSI National Radio Science*

Meeting, 8-13 ofe July, Boston, Massachusetts, United States of America

5. Teniente, J., Gonzalo, R., del Río, C. "Gaussian Profiled Horn Antennas"**,** *ISRAMT'99 7th International Symposium on Recent Advances in Microwave Technology*. Malaga, Spain December 1999.

6. Fernandez Curto, A., Likin, K. M., Martín, R., Martí Canales, J., Teniente, J., Gonzalo, R., del Río, C. and Sorolla, M. "Corrugated Horn Antenna for Low-Power testing of the Quasioptical Transmission Lines at TJ-II Stellerator"**,** *AMTA'99 21st Annual Meeting and Symposium on Antenna Measurement Techniques Association.* Monterey Bay, California, United States of America. October 1999

7. Teniente, J., Gonzalo, R., Sorolla, M. and del Río, C. "Generation of the HE_{11} mode in Rectangular Waveguide Using Gaussian Techniques", *1999 IEEE AP-S International Symposium and URSI Radio Science Meeting*, 11-15 of July, Orlando, Florida, United States of America

8. Gonzalo, R., Martí-Canales, J., Teniente, J., del Río, C. and Sorolla, M. "Measurements of a New Gaussian Profile Corrugated Horn Antenna for Millimeter Wave Applications", *1998 IEEE AP-S International Symposium and URSI Radio Science Meeting*, 21-26 of June, Atlanta, Georgia, United States of America

9. del Río, C., Teniente, J., Gonzalo, R., and Sorolla, M. "On the Determination of the Phase Center of Gaussian Horn Antennas", *2nd ESA Workshop on Millimetre Wave Technology and Applications*, 27-29 of May 1998, Millilab, Espoo, Finland

10. Teniente, J., Gonzalo, R. and del Río, C. “A novel and Efficient Corrugated Feeder for Reflector Antennas”, *1997 IEEE AP-S International Symposium and URSI Radio Science Meeting*, 14-18 of July, Montreal, Canada

11. Gonzalo, R., Teniente, J. and del Río, C., “Very Short and Efficient Feeder Design from Monomode Waveguide”, *1997 IEEE AP-S International Symposium and URSI Radio Science Meeting*, 14-18 of July, Montreal, Canada

12. Gonzalo, R., Teniente, J., del Río, C. and Sorolla, M. “New Approach to the Design of Corrugated Horn Antennas”, *20th ESTEC Antenna Workshop on Millimetre Wave Antenna Technology and Antenna Measurements*, 18-20 of June 1997, Noordwijk, Holland

13. Gonzalo, R., del Río, C., Teniente, J. and Sorolla, M “Optimal horn antenna design to excite high purity gaussian beam using overmoded waveguides”, *XXI Int. Conf. on Infrared and Millimeter Waves*. Berlin, Germany, July 1996

National conferences

1. Ortiz, N., Teniente, J., Gonzalo, R. and del Río, C., “Diseño de una antena dual gaussiana de doble profundidad de corrugación” *XVIII Symposium de la Unión Científica Internacional de Radio (URSI’03)*. La Coruña, Spain, September 2003

2. Teniente, J., Gonzalo, R. and del Río, C., “Comparación Entre Antenas Cónicas Corrugadas y Antenas Gaussianas Corrugadas” *XVII Symposium de la Unión Científica Internacional de Radio (URSI’02)*. Alcalá de Henares, Madrid, Spain, September 2002

3. Goñi, D., Teniente, J., Gonzalo, R. and del Río, C., “Diseño y Medida de una Antena Choke-Gaussiana” *XVII Symposium de la Unión Científica Internacional de Radio (URSI’02)*. Alcalá de Henares, Madrid, Spain, September 2002

4. Teniente, J., Gonzalo, R. and del Río, C., “Antena Corrugada con Perfil Gaussiano de Gran Ancho de Banda” *XVI Symposium de la Unión Científica Internacional de Radio (URSI’01)*. Villaviciosa de Odón, Madrid, Spain, September 2001

5. Teniente, J., Gonzalo, R. and del Río, C., “Estudio de Resonancias Parásitas en Antenas Corrugadas” *XVI Symposium de la Unión Científica Internacional de Radio (URSI’01)*. Villaviciosa de Odón, Madrid, Spain, September 2001.

6. Teniente, J., Gonzalo, R. and del Río, C., “Alimentadores Gaussianos en Guía de Onda Rectangular” *XIV Symposium de la Unión Científica Internacional de Radio (URSI’99)*. Santiago de Compostela, Spain, September 1999

7. Fernandez, A., Likin, K. M., Teniente, J., Turullols, P., Gonzalo, R., del Río, C., Sorolla, M. and Martín, R. “Líneas de Transmisión Cuasi-ópticas en el Stellerator TJ-II” Poster presentation *XIII Symposium de la Unión Científica Internacional de Radio (URSI’98)*. Pamplona, Spain, September 1998

8. Teniente, J., Turullols, P., del Río, C. and Sorolla, M. “Fórmulas de Referencia Normalizadas para Propagación y Radiación en Guía Rectangular” Poster presentation *XIII Symposium de la Unión Científica Internacional de Radio (URSI’98)*. Pamplona, September 1998

9. Gonzalo, R. and del Río, C., Teniente, J. and Sorolla, M. “Diseño óptimo de antenas de bocina multimodo para excitar un haz gaussiano fundamental de alta pureza” *XI Symposium de la Unión Científica Internacional de Radio (URSI’96)*. Madrid, Spain, September 1996

10. Gonzalo, R. and del Río, C., Teniente, J. and Sorolla, M. “Generación del modo HE_{11} a partir de una guía circular lisa monomodo” *XI Symposium de la Unión Científica Internacional de Radio (URSI’96)*. Madrid, Spain, September 1996

Epilogue

El hombre no tejió la trama de la vida;
él sólo es un hilo
Lo que hace con la trama se lo hace a sí mismo